also preserved VEGF receptor 2 (Flk-1) phosphorylation (Ang II 0.19±0.02 *vs.* Ang II+EPO 0.69±0.14, P<0.05), but there was no effect on endothelial nitric oxide synthase (eNOS) expression (Ang II 0.093±0.01 *vs.* Ang II+EPO 0.059±0.02, pNS). Akt is pivotal in angiogenesis and in promoting cell survival. In our study, Akt phosphorylation was improved by EPO in GEN injured by Ang II (Ang II 0.645±0.01 *vs.* Ang II+EPO 0.884±0.10, P<0.05).

Conclusions: Our data suggest that EPO has direct effects on GEN to promote angiogenesis and protect against Ang II-induced apoptosis, possibly related to Akt phosphorylation and synergistic interactions with VEGF.

1384 Proliferative m-TOR Pathway Is Associated with Injury Tolerance and Repairing in Rat Kidneys

PL Zhang, W Li, RE Brown. William Beaumont Hospital, Royal Oak, MI; University of Texas Health Sciences Center, Houston, TX.

Background: Renal injury is known to trigger upregulation of many intracellular signal proteins, but role of mammalian target of rapamycin (m-TOR) prolifeative pathway in injured kidneys remains unknown. In this study, protein expression of phosphorylated (p)-mTOR and its down-stream signal p-p70S6K in renal tubules and glomeruli of rat kidneys after renal ischemia-reperfusion injury was evaluated.

Design: Three groups of male adult rats all had right nephrectomy on the day of surgical produre (n = 7 in each group). The left kidney was untouched in group 1. In group 2, the left renal artery was clamped for 20 minutes, followed by 48 hours of reperfusion. A third group of rats received a bolus intraperitoneal injection of nephrotoxic tunicamycin (0.1 mg/kg) one day before the surgery and then underwent the same surgical procedure as in group 2. Serum creatinine was measured in each rat. The rat kidneys were fixed and stained for phosphorylated (p)-mTOR and its down-stream signal p-p70S6K by immunohistochemical method.

Results: Serum creatinine (mg/dl) was significantly higher in group 3 rats (3.82 ± 0.80) than in group 2 rats (0.70 ± 0.07) and group 1 rats (0.37 ± 0.02). Under normal condition, the glomeruli and distal nephron tubules had prominent cytoplasmic expression of p-mTOR and remarkable nuclear expression of p-p70S6K, whereas all segments of proximal tubules had low expression of both markers. In group 2 and group 3 rats, the expression of both markers in glomeruli, S1 segment of proximal tubules and distal nephron tubules was not affected, subjected to the ischemia-reperfusion injury (regardless of tunicamycin treatment). In group 2, both p-mTOR and p-p70S6K were upregualted dominantly in the S3 segment of proximal tubules, following by S2 segment of proximal tubules. These changes were more prominent in group 3, with an additive nephrotoxicity of tunicamycin and corresponding to the morphologic features of acute tubular injury along the vulnerable renal tubules.

Conclusions: Our data suggest that high baseline expression of p-m-TOR and p-p70S6K in glomeruli and distal nephron tubules may be associated injury resistance. The m-TOR proliferative pathway was activated in the injury-vulnerable segment of renal tubules, implying an important role of this proliferative pathway in the repairing process of renal tubules.

1385 Altered Balance of Thymosin β4 and Ac-SDKP Exacerbates Tubulointerstitial Fibrosis

Y Zuo, SA Potthoff, TJ Brolin, T Myohanen, N-E Rhaleb, OA Carretero, H-C Yang, L-J Ma, AB Fogo. Vanderbilt University, Nashville, TN; University of Kuopio, Kuopio, Finland; Henry Ford Hospital, Detroit, MI.

Background: Our previous study showed that the G-actin sequestering protein thymosin β4 (Tβ4) is remarkably upregulated in the unilateral ureteral obstruction (UUO) model of tubulointerstitial fibrosis. Tβ4 is postulated to be profibrotic but is also degraded by prolyl oligopeptidase (POP) to the anti-fibrotic Ac-SDKP peptide. In this study we investigate whether POP inhibition with or without exogenous Tβ4 affects the early stage of tubulointerstitial fibrosis.

Design: Adult male C57BL/6 wild type mice underwent UUO and were divided into four groups and sacrificed on day 5. Groups were as follows: control UUO without treatment, or with POP inhibitor (S17092, 40mg/kg per day, by gavage), Tβ4 (150μg/d, i.p.), or combination treatment (POP inhibitor plus Tβ4).

Results: Tubulointerstitial injury score was dramatically higher in POP inhibitor and combination treatment groups than untreated UUO (POP inhibitor, 2.87±0.09; combination, 2.94±0.23; control UUO, 2.22±0.19, both p<0.05 vs control). POP activity was significantly lower in POP inhibitor and combination groups (POP inhibitor, 2.06±0.26; combination, 5.73±1.59; control UUO, 26.62±2.74 pmol/min*mg tissue, both p<0.05 vs control). Compared to untreated UUO control group, neither injury score nor POP activity was different in Tβ4 group (2.19±0.13 and 21.19±1.61 pmol/min*mg tissue, respectively). There was no difference in Tβ4 expression among all four groups by western blot analysis (POP inhibitor, 1.15±0.17; combination, 0.84±0.09; control UUO, 1.02±0.05; Tβ4, 0.83±0.06). However, the balance of Tβ4 vs Ac-SDKP level in both serum and tissue could be shifted.

Conclusions: Our study suggests that POP inhibitor with or without Tβ4 may cause tubulointerstitial fibrosis by inhibiting degradation of Tβ4 and thus also Ac-SDKP formation. We propose that the balance of Tβ4 and Ac-SDKP may play a pivotal role in determining renal interstitial fibrosis.

Liver & Pancreas

1386 Precancerous Bile Duct Pathology in Sporadic Hilar Cholangiocarcinoma

SC Abraham, S Leung, CB Rosen, TT Wu. MD Anderson Cancer Center, Houston; Mayo Clinic, Rochester.

Background: Most cholangiocarcinomas (CCAs) arise in the hilum, an anatomic region that often renders them surgically unresectable. This has hindered the study of presumed precursor lesions (metaplasia and dysplasia) in noncancerous bile ducts of the hilum and intrahepatic parenchyma.

Design: We studied 29 patients with sporadic hilar CCA who underwent neoadjuvant chemoradiation followed by liver transplantation from 1994-2007. After reevaluating the preserved gross liver explants, we took multiple (11) casettes of large hilar and intrahepatic bile ducts. Ducts were scored for the following histologic features: metaplasia (intestinal, pyloric, and mucinous/foveolar), dysplasia (low or high grade, number of dysplastic ducts, and hilar or intrahepatic location), and cancerization (malignant biliary epithelium near invasive CCA). These results were compared with two previously published control groups: 1) 28 patients with PSC-associated hilar CCA who received chemoradiation and liver transplant, and 2) 65 noncirrhotic liver transplants without CCA in patients >21 yr.

Results: Twenty-eight (97%) patients were Caucasian and 1 (3%) Asian; none had known predisposing conditions for CCA (choledochal cysts, hepatolithiasis, etc). Residual CCA was detected in 22 (76%) and ductal cancerization in 3 (10%). They had low rates of intestinal metaplasia (10%) but high rates of pyloric metaplasia (90%), mucinous metaplasia (93%) and bile duct dysplasia (55%). Of 16 cases with dysplasia, 10 involved both hilar and intrahepatic ducts and 6 involved intrahepatic ducts only. Comparison with PSC-associated CCA and non-CCA liver explants is shown below.

Bile Duct Pathology in Hilar CCA

	Age	Gender	Biliary Metaplasia			Biliary Dysplasia	
			Intestinal	Pyloric	Mucinous	Any	High-grade
Sporadic hilar CCA (n=29)	52 yr (22-64)	62% M	10%	90%	93%	55%	17%
PSC with hilar CCA (n=28)	47 yr (p=0.09)	71% M (p=1)	39% (p=0.015)	75% (p=0.2)	89% (p=0.7)	82% (p=0.045)	57% (p=0.003)
Noncirrhotic without CCA (n=65)	47 yr (p=0.08)	63% M (p=1)	8% (p=0.7)	9% (p<0.001)	72% (p=0.03)	15% (p<0.001)	0% (p=0.002)

*P values are in comparison to the sporadic CCA group

Conclusions: The presence of intestinal metaplasia and the presence and extent of bile duct dysplasia are significantly lower in sporadic vs. PSC-associated hilar CCA, suggesting a "field effect" in PSC. Pyloric metaplasia and dysplasia of noncancerous bile ducts best distinguish CCA from non-CCA cases.

1387 Serum and Tissue FGL2 as a Surrogate for Treg Cells Activity in Patients with Chronic Viral Hepatitis C (HCV)

OA Adeyi, N Selzner, I Shalev, Y Zhu, GA Levy. University of Toronto/UHN, Toronto, ON, Canada.

Background: CD4+/CD25+/FoxP3+ T cells (Tregs) a subset of T cells have been implicated in the suppression of specific T cell-mediated immune responses to HCV. Tregs activity appears to correlate with more aggressive disease in HCV infected patients, suggesting that identification of these cells in serum and tissue could be an important prognostic marker. Hitherto FoxP3 was thought to be the most specific marker for Tregs, but recent data has cast doubts on their specificity. Data genearted in our lab our from mice studies supports the hypothesis that Fibrinogen-like protein (FGL2)/fibroleukin is an important effector molecule of Tregs. We have therefore tested the hypothesis that measurement of FGL2 as surrogate marker for Tregs activity in serum and liver tissue has prognostic value in predicting disease severity and response to antiviral therapy.

Design: We measured serum levels of human FGL2 using a highly sensitive and reproducible ELISA method in healthy individuals (controls) and post-transplant HCV-patients. The latter were grouped according to HCV genotype and response to antiviral therapy, to determine whether levels of FGL2 can be a useful prognostic marker of response to IFN therapy. FGL2 and FGL2/FoxP3 double staining was performed on randomly selected liver explants of these HCV patients.

Results: Serum levels of FGL2 were significantly higher in HCV patients (13.1±4.7ng/ml) than control (5.8±1.3 ng/ml p=0.007). HCV genotype 1 infected patients had higher levels of FGL2 (13.11+2.4ng/ml) than genotype 2/3 patients (6.1+1.4ng/ml) (p=0.04). Serum FGL2 levels were lower in patients who responded to anti-viral therapy than non-responders (3.5+1 ng/ml p =0.001) and was similar to non infected controls. FgL2 immunostaining demonstrated more positive cells among portal and lobular infiltrates in HCV patients with genotype 1 >> other genotypes. FoxP3/FGL2 co-staining showed that the majority of FoxP3+cells were not FGL2 positive, supporting the views that not all FoxP3+ cells are Tregs.

Conclusions: In HCV patients high Serum FGL2 levels, as surrogate for Tregs activity, mirror histopathologic findings and both correlate with known risk factors for progression (HCV genotype 1 and poor response to IFN). Serum and/or histologic demonstration of FGL2 could provide useful prognostic information in the management of HCV-infected patients. We have an ongoing prospective study to investigate the predictive value of serum and tissue FGL2 in HCV infection.

1388 Histologic Features of Non-Alcoholic Fatty Liver Disease in Young Adults

DS Allende, LM Yerian. Cleveland Clinic, Cleveland, OH.

Background: The clinical and pathological findings of non-alcoholic fatty liver disease (NAFLD) have been well-characterized in adults, and more recently a unique histologic pattern of NAFLD ("Type 2") has been described in pediatric patients. Most of the adult

NAFLD studies to date are dominated by middle-aged to older adult patients, while the histologic findings in young adults (18-35 years old) have not been well-characterized, and it is unknown whether the Type 2 pattern of NAFLD described in pediatric patients may also occur in young adults.
Design: 121 liver biopsies from 121 patients between 18 and 35 years old were reviewed (1988-2008). The search criteria included a diagnosis of "steatosis" or "steatohepatitis." Alcohol use was excluded. Each biopsy (H&E, trichrome) was scored using the NAFLD activity score (Kleiner D et al., 2005), and additional features of hepatic injury were recorded.
Results: 30/121 patients showed only minimal fat (<5%) and were not scored. The remaining 91 cases were classified as steatosis (62), steatohepatitis (21), or borderline steatohepatitis (8). Using the NAFLD activity score, mild and moderate steatosis were the most frequent findings (45 and 32 cases, respectively). Most cases showed a zone 3 (45 cases) or azonal (31 cases) distribution of steatosis; no cases exhibited a zone 1 distribution of steatosis. Lobular inflammation was present in <2 foci/20x field in 45 cases, followed by 2-4 foci in 28 cases. Most cases contained none to minimal portal inflammation (68 cases). Portal-based disease (inflammation and/or fibrosis confined to the portal areas) was seen in 4/91 cases. In seven additional cases, inflammation was predominantly but not exclusively seen in portal tracts. Other features, such as ballooning, acidophil bodies, Mallory hyaline, pigmented macrophages and glycogenated nuclei were prominent only in a minority of cases. 38/91 cases showed evidence of zone 3 fibrosis only (Stage 1), 10 cases showed periportal and zone 3 fibrosis (Stage 2), 6 cases showed bridging fibrosis (Stage 3) and 3 cases exhibited cirrhosis (Stage 4 disease).
Conclusions: Most cases showed mild to moderate steatosis in a zone 3 or azonal distribution. Lobular inflammation was mild, and portal inflammation, absent to minimal in most cases. Slightly over 20% of cases showed stage 2 to 4 fibrosis. Although the majority of cases revealed the histologic pattern seen in adult NAFLD, a small number of cases exhibited predominantly or exclusively portal-based inflammation and/or portal fibrosis, suggesting the existence of the "Type 2" pattern of NAFLD in young adults.

1389 Insulin Growth Factor-Binding Protein 2 Overexpression Correlates with Disease Specific Survival in Biliary Tract Adenocarcinoma

F Bao, A Yopp, WR Jarnagin, LH Blumgart, RP DeMatteo, M D'Angelica, DS Klimstra. Memorial Sloan-Kettering Cancer Center, New York, NY.
Background: The insulin-like growth factor (IGF) signaling pathway is involved in the tumorigenesis of some human malignancies. The mitogenic and anti-apoptotic activities of IGFs are regulated by six IGF binding proteins (IGFBP-1 to IGFBP-6), among which IGFBP-2 is the most commonly overexpressed in malignancies such as breast, prostate, ovarian carcinomas and glioblastomas. But their roles in biliary tract adenocarcinoma have not been investigated.
Design: A tissue microarray (TMA) was constructed from paraffin-embedded specimens of 128 patients with resected biliary adenocarcinomas, including 55 hilar cholangiocarcinomas, 23 peripheral cholangiocarcinomas, 32 gallbladder adenocarcinomas and 18 distal common bile duct adenocarcinomas. Immunohistochemical analysis using antibodies against IGF-2, IGFBP-2 and a downstream effector molecule, pancreatic endoplasmic reticulum kinase (PERK) was performed.
Results: Cytoplasmic staining for IGF-2, IGFBP-2 and PERK was detected in 19%, 36% and 8% of biliary tract adenocarcinomas, respectively. The percentages of expression of each marker in the four tumor types are listed in table 1.

Table1. Expression of IGF-2, IGFBP-2 and PERK in the four tumor types

antibody/tumor type	hilar	peripheral	gallbladder	distal
IGF-2	26%	4%	17%	21%
IGFBP-2	39%	27%	31%	50%
PERK	10%	9%	7%	36%

Kaplan-Meier survival analysis showed the expression of IGFBP-2 was associated with disease-specific survival time (DSS) ($p<0.001$). The expression of IGF-2 was not correlated with prognosis ($p=0.476$). The expression of PERK showed a trend towards prolonged DSS, ($p=0.144$). After stratifying the data based on the tumor site, the strong correlation with prognosis remained for the hilar and peripheral cholangiocarcinomas ($p = 0.006$ and 0.014, respectively).
Conclusions: IGFBP-2 overexpression correlates with disease specific survival in biliary tract adenocarcinoma, specifically in hilar and peripheral cholangiocarcinomas. It has been shown that IGFBP-2 expression is negatively regulated by PTEN and positively regulated by PI3K and Akt activation. Evaluation of the upstream and downstream target molecules of PI3K-Akt-mTOR pathway, namely PTEN, pAkt, p16 and p27, in a larger patient cohort of patients would be of interest and, along with our current data, may form the basis for treatment of patients with mTOR-targeted therapy.

1390 Analysis of Novel Immunohistochemical Markers and Genetic Pathways in Mixed Carcinomas of the Pancreas

F Bao, M Arcila, J Garcia, E Stelow, R Hruban, DS Klimstra. Memorial Sloan-Kettering Cancer Center, New York, NY; University of Virginia Health System, Charlottesville, VA; Johns Hopkins University, Baltimore, MD.
Background: Mixed pancreatic carcinomas have significant elements of more than one line of differentiation. Because of their rarity, mixed carcinomas raise many problems in diagnosis, management and therapy. The pathogenesis of these tumors is poorly understood.
Design: We collected 21 cases of mixed carcinomas of the pancreas, including 13 acinar-ductal carcinomas, 6 acinar-endocrine carcinomas and 2 ductal-endocrine carcinomas. Most of the mixed carcinomas (19 of 21, 91%) expressed markers of acinar differentiation in >25% of the tumor cells. Immunohistochemical analysis using novel pancreatic epithelial markers (maspin and mesothelin) and stromal marker (fascin) as well as CK19, p53, DPC4 and b-catenin was performed on paraffin-embedded tissues. KRAS mutations were analyzed by direct sequencing.
Results: Twenty out of 21 mixed carcinomas (95%) expressed CK19 in 40-100% of the tumor cells. Focal expression of maspin and mesothelin (10-40%) was infrequently observed in mixed carcinomas (4/21 and 2/21, respectively). More than half of mixed carcinomas (11/21) showed focal expression of fascin (5-15%). Interestingly, two of 6 mixed acinar-endocrine carcinomas (33%) had strong cytoplasmic fascin and nuclear b-catenin expression in more than 30% of the tumor cells. This finding supports a correlation between b-catenin abnormality and fascin expression. KRAS mutations were identified in 1 ductal-endocrine and 2 acinar-ductal carcinomas, one of which also showed p53 expression by immunohistochemistry. The loss of DPC4 was found in 1 mixed acinar-ductal and 1 ductal-endocrine carcinoma. Detailed immunohistochemical results are listed in the table.

Tumor/marker	CK19	maspin	mesothelin	fascin	b-catenin	p53	loss of DPC4
Acinar-ductal	13/13	3/13	1/13	7/13	0/13	1/13	1/13
Acinar-endocrine	5/6	0/6	0/6	2/6	2/6	0/6	0/6
Ductal-endocrine	2/2	1/2	1/6	2/2	0/2	0/2	1/2

Conclusions: The fact that mixed carcinomas of the pancreas universally expressed CK19 but infrequently expressed the terminally differentiated ductal markers (maspin and mesothelin) indicates that they resemble "protodifferentiated" epithelial cells with features of ductal cells. Our study shows that, in contrast with conventional ductal adenocarcinoma, KRAS, p53, and DPC4 are rarely involved in the pathogenesis of the mixed tumors that predominantly express acinar differentiation.

1391 Patterns of Histological Alteration and Their Clinical Significance in Colorectal Liver Metastases Following Preoperative Chemotherapy

F Bao, J Park, D Klimstra, P Mastrodomenico, N Katabi, E Vakiani, L Tang, M D'Angelica, J Shia. Memorial Sloan-Kettering Cancer Center, NY.
Background: An increasing number of patients with colorectal liver metastases (CRLM) undergoing surgical resection are being treated with preoperative chemotherapy regimens combining 5-fluorouracil, oxaliplatin, and/or irinotecan, with a resultant improved survival. This "neoadjuvant" approach presents a unique type of liver resection specimen in which the metastatic carcinoma is altered by the preoperative chemotherapy. The histopathological patterns and their clinical significance in such specimens have not been well characterized.
Design: Detailed histological characteristics, including fibrosis, necrosis, mucin pools, and viable tumor cells, were qualitatively and semi-quantitatively analyzed in 94 CRLM resection specimens that received 5-fluorouracil, oxaliplatin, and/or irinotecan-based preoperative chemotherapy. The histological findings were then correlated with the patient's clinical features and survival.
Results: In these CRLM specimens, the dominant histological pattern of non-viable tumor component in the lesion was necrosis (34% with >50% necrosis), followed by fibrosis (11% with >50% fibrosis) and acellular mucin (4% with >50% mucin pools). Tumors with extensive fibrosis tended to have no or only small amount of necrosis. The viable carcinoma had the conventional gland-forming colorectal carcinoma histology in the majority of the cases. Cellular alterations with features of neuroendocrine differentiation as seen in irradiated rectal carcinomas were observed in some cases with advanced CR. Over all, 6 (6%) had no residual viable tumor, and 18 (19%) had <30% viable tumor. With a median follow-up of 35.7 months, residual viable tumor <30%, and fibrosis >25% significantly correlated with a better overall survival ($p=0.002$ and 0.04 respectively), whereas necrosis alone did not ($p=0.8$).
Conclusions: This study provides a detailed morphological description of post-chemotherapy colorectal liver metastasis. These tumors show a histological pattern similar to the pattern seen in post-chemoradiation rectal carcinomas in some aspects (such as tumor fibrosis and neuroendocrine differentiation), but not in others (more necrosis in liver metastasis). The correlation of tumor fibrosis, but not necrosis, with patients' outcome suggests that tumor fibrosis is a more reliable histologic indicator for good tumor response to preoperative chemotherapy, and can potentially serve as a prognostic factor, in such colorectal liver metastasis patients.

1392 Metaplasia in the Gallbladder: Populational Differences in the Incidence of Intestinal Metaplasia Supports Its Association with Carcinoma

O Basturk, O Tapia, JC Roa, E Bellolio, C Delgado, S Bandyopadhyay, I Coban, D Thirabanjasak, JM Sarmiento, H Losada, NV Adsay. NYU, NY; Frontera U., Temuco, Chile; WSU, Detroit; Emory U., Atlanta; Emory U., Atlanta.
Background: There is conflicting data regarding the incidence/clinical significance of metaplasia in the gallbladder (GB) carcinogenesis.
Design: Metaplasia was investigated in 600 benign cholecystectomies from 3 different risk groups: **A)** High Risk (HR): 300 chronic cholecystitis (CC) cases from Chile where the GB carcinoma (CA) incidence is very high; **B)** Low/Minimal Risk (L/MR): 160 CC and 60 morbid obesity cases from N. America; **C)** No Risk (NR): 80 GBs removed as a part of pancreatoduodenectomy for pancreatic diseases. An average of 8.7 cm of GB tissue/case was examined; cases with autolysis were excluded. Metaplasia score: **0; 1:** *<1 mm, 1 focus*; **2:** *1-5 mm or >1 foci*; **3:** *>1 foci, at least 2 of which >5 mm but <70% of mucosa*; **4:** *>70% of mucosa*. The incidence of metaplasia was also correlated with the degree of chronic inflammation, sclerosis, rokitansky aschoff sinuses (RAS) and cholesterolosis.
Results: **Intestinal metaplasia (IM):** Overall 10.1% of the cases had IM. There was a progressive increase in the incidence and quantity of IM from NR to L/MR to HR groups ($p=0.001$). Most IM was represented as goblet cells while the participation of absorptive cells/brush-border appeared to be very minimal. **Pyloric metaplasia (PM):** The overall incidence of PM was very high (44.1%) and in 3% of the cases, there was diffuse transformation of the mucosa into pyloric type glands. PM did not increase in incidence with CA risk (Its incidence was higher in the L/MR group *vs* HR or NR;

p=0.003). No association was identified between the incidence of IM or PM and the degree of chronic inflammation, sclerosis, RAS and cholesterolosis.

	High Risk Group	Low/Minimal Risk Group	No Risk Group	
IM	n=43 (14.3%)	n=17 (7.7%)	n=1 (1.2%)	p=0.001
PM	n=126 (42%)	n=115 (52.2%)	n=24 (30%)	p=0.003

Conclusions: There is a significant progressive increase in the incidence of IM in the GB, increasing with the risk of CA, supporting its association with CA. PM, on the other hand, appears to be more ubiquitous, not associated with CA risk. The incidence of either metaplasias does not correlate with the degree of chronic changes, suggesting that they may be a direct result of the chemical milieu rather than being a secondary product of inflammation.

1393 Retractile Pancreatoduodenopathy with Neural Hypertrophy

PA Bejarano, MT Garcia, LP Herrera. University of Miami School of Medicine/Jackson Memorial Hospital, Miami, FL.

Background: Most Whipple procedures are performed to treat a malignant process. However, a fraction of them reveal benign non-neoplastic conditions. One such case is the so-called paraduodenal pancreatitis characterized by chronic inflammation, myofibroblastic proliferation, dilated ducts, and cysts. It is associated with heavy alcohol intake. In this study we identified an unusual histopathological process involving the wall of the duodenum and the head of the pancreas that appears to be different from what is known as paraduodenal pancreatitis.

Design: The histological slides of 420 consecutive Whipple procedure specimens were reviewed. Of these, 35 showed benign non-neoplastic conditions, and among these, four were selected because of their unique features.

Results: There were two women and two men who ranged in age from 41 to 71 years (mean: 56 y). Imaging studies showed a duodenal mass with pancreatic involvement. Gross examination of the specimens revealed irregular areas of white-tan fibrosis measuring 2.0 cm (range 1.5 to 2.5 cm) and involving the duodenal wall. Microscopically, the most remarkable feature was the presence of sub-duodenal and periductal thickened trunks of peripheral nerves dissecting and crossing the connective tissue and the pancreatic acini. These individual neural structures had a diameter of up to 1.7 mm and in areas they formed aggregates of up to 2.3 mm. They ran in a radial and centrifugal fashion from the duodenum into the pancreas. The arteries and arterioles in the area were markedly thickened, showing fibrointimal proliferation. In one case, recanalized thrombi were present. The interface between the duodenum and the pancreas was effaced by fibrosis with pancreatic tissue pulled into the overlying duodenal muscularis mucosa. No inflammation of the pancreas was present in 3 of the cases. Inflammation around the bile duct found in the fourth case was associated with the presence of a duct catheter. There was no necrosis, myofibroblastic proliferation, cysts, calculi, eosinophils, or Brunner's gland hyperplasia.

Conclusions: The structural anomaly of nerve hypertrophy, fibrosis, thickened blood vessels, minimal to absent inflammation, and retraction of the pancreas into the duodenum all resulting in the formation of mass is found in 0.1% of all pancreatoduodenectomies. While it may correspond to a variant of paraduodenal pancreatitis, a hamartomatous process or an acquired phenomenon related to ischemia may be considered. It enters in the differential diagnosis of causes of duodenal/pancreatic masses.

1394 Assessment of the p27/Skp2/Cks1 Axis in Pancreatic Ductal Adenocarcinoma and Ampullary Adenocarcinoma

AM Bellizzi, M Bloomston, SM Bellizzi, OH Iwenofu, WL Frankel. Ohio State University, Columbus, OH.

Background: p27, a tumor suppressor, is a cyclin dependent kinase inhibitor governing cell cycle progression. Skp2 and Cks1 are components of an E3-ubiquitin ligase responsible for p27's ubiquitylation and subsequent proteosomal degradation. These proteins direct p27 recognition and binding, conferring specificity to the E3-complex. Loss of p27 and overexpression of Skp2 and Cks1 have been described in various tumors. We investigated this pathway because these proteins have rarely been studied in pancreatic ductal adenocarcinoma (PDA), and, to our knowledge, they have not been studied in ampullary adenocarcinoma (AMP).

Design: Tissue microarrays were constructed from cases of PDA (67), AMP (40), and non-neoplastic ducts (NML, 35); duplicate cores were taken from each case. Immunohistochemistry for p27, Skp2, and Cks1 was performed. p27 and Skp2 were scored as follows: p27 (positive:≥10% nuclear staining), Skp2 (positive:≥5% nuclear staining). Cks1 was evaluated for intensity (0, 1+, 2+) and quantity (%) of nuclear staining and a score (product of intensity and quantity) was calculated. Fisher's exact test (p27 and Skp2) and Mann Whitney U test (Cks1) were used for pairwise comparisons. Log-rank analysis (p27 and Skp2) and Cox proportional hazards model (Cks1) were used for survival analysis.

Results: Loss of p27 expression was noted in just over half of PDAs and AMPs, while Skp2 and Cks1 were frequently overexpressed (see table). Comparisons between PDA vs. NML and AMP vs. NML were highly statistically significant for all 3 proteins (p≤0.001). While Skp2 and Cks1 expression correlated with survival in PDA (p=0.02, 0.03), they did not in AMP. p27 failed to correlate with survival in PDA or AMP.

Expression of p27, Skp2, and Cks1

	PDA	NML	AMP
p27	28/65 (43%)	29/33 (88%)	18/40 (45%)
Skp2	31/66 (47%)	0/35 (0%)	26/37 (70%)
Cks1	46.7 ± 45.4	5.7 ± 11.5	81.3 ± 61.8

for p27 and Skp2 data represents number of positive/total cases; Cks1 reported as score ± sd

Conclusions: p27 expression is commonly decreased, while Skp2 and Cks1 expression is frequently increased in PDA and AMP. Skp2 and Cks1 correlate with survival in PDA and not in AMP. Lack of correlation in AMP may reflect the relatively indolent nature of these tumors. Given their frequent overexpression in PDA and AMP and their limited target specificities, Skp2 and Cks1 represent potential targets for small molecule therapy. They also may be potential prognostic indicators.

1395 Frequent Activation of the mTOR Pathway in Pancreatic Ductal Adenocarcinoma

AM Bellizzi, OH Iwenofu, XP Zhou, M Bloomston, WL Frankel. Ohio State University, Columbus, OH.

Background: Mammalian target of rapamycin (mTOR) is a serine-threonine kinase critical to cell growth and proliferation. Activation of the PI3K/Akt/mTOR pathway has been described in various tumors. Previous studies have demonstrated loss of PTEN function (a tumor suppressor interacting with the pathway) and Akt amplification (a kinase directly upstream of mTOR) in a fraction of pancreatic ductal adenocarcinomas (PDAs). We utilized immunohistochemistry for PTEN, p-Akt, and p-S6rp (a major downstream effector of mTOR) to assess the status of the mTOR pathway in a group of PDAs.

Design: Tissue microarrays were constructed from 49 tumors; duplicate cores were taken from each. Slides were stained with antibodies to PTEN, p-Akt, and p-S6rp. Cases were scored as follows: PTEN (intact: ≥5% staining, lost), p-Akt (positive: ≥5% staining, negative), p-S6rp (0, 1+: modest intensity ≥5%, 2+: strong intensity ≥5%). Ducts in normal pancreas (NL, 12 cases) and chronic pancreatitis (CP, 27 cases) served as controls.

Results: A large number of the PDAs demonstrated loss of PTEN (41% of cases), while p-Akt was generally negative (84%). The majority of cases stained for p-S6rp (75%, 1+ in 33, 2+ in 3). PTEN was uniformly intact in NL and CP; p-Akt expression was frequent. While p-S6rp immunoreactivity was only noted in 1 NL control (8%), 1+ positivity was seen in 62% of CP. Results are summarized in the table.

mTOR Pathway Protein Expression

	PTEN	p-Akt	p-S6rp
PDA	intact: 29	positive: 8	0: 12
	lost: 20	negative: 41	1+: 33
			2+: 3
NL	intact: 10	positive: 12	0: 11
	lost: 0	negative: 0	1+: 1
			2+: 0
CP	intact: 27	positive: 18	0: 10
	lost: 0	negative: 9	1+: 16
			2+ 0

Data refers to number of cases

Conclusions: mTOR pathway activation, as evidenced by p-S6rp immunoreactivity, is frequent in PDA. In most cases this appears to be independent of p-Akt status. Interestingly, p-S6rp expression was also noted in most cases of chronic pancreatitis, highlighting the possible importance of this pathway in both neoplastic and inflammatory processes. Given evidence of pathway activation and the existence of specific anti-mTOR therapeutics, mTOR may represent a logical target for directed biologic therapy.

1396 Genetic Mutations Associated with Cigarette Smoking in Pancreatic Cancer

A Blackford, G Parmigiani, T Kensler, CL Wolfgang, S Jones, X Zhang, DW Parsons, JC Lin, RJ Leary, J Eshleman, M Goggins, EM Jaffee, CA Iacobuzio-Donahue, SE Kern, A Maitra, JL Cameron, K Olino, RD Schulick, J Winter, B Vogelstein, VE Velculescu, KW Kinzler, RH Hruban. The Johns Hopkins Medical Institutions, Baltimore, MD.

Background: Cigarette smoking doubles the risk of pancreatic cancer and it has been estimated that smoking accounts for 20 to 25% of pancreatic cancers. The recent sequencing of the pancreatic cancer genome (Jones et al Science 2008) provides an unprecedented opportunity to identify the genetic mutations associated with smoking.

Design: We previously sequenced over 750,000,000 base pairs of DNA from 23,219 transcripts, representing 20,661 protein-coding genes in a series of 24 pancreatic cancers. The number and types of non-synonymous somatic mutations in the cancers obtained from individuals who ever smoked cigarettes (n=11) were compared to the number and types of non-synonymous somatic mutations in the cancers obtained from individuals who never smoked cigarettes (n=13). Mutations were also correlated with other clinical parameters.

Results: More mutations were identified in the carcinomas obtained from ever smokers than in the carcinomas obtained from never smokers, in high-grade carcinomas than moderate grade carcinomas, in carcinomas obtained from patients ≥70 years of age than those obtained from patients <70, and in carcinomas obtained from men than women.

Mutations Per Tumor

	N	Mean (SD)	Adjusted p value*
Non-smoker	13	41.4(11.5)	0.07
Smoker	11	56.8(30.9)	
Age <70	16	45.1(14.7)	0.30
Age 70+	8	55.2(35.3)	
Black	3	44.3(9.9)	0.75
White	21	49(24.8)	
Female	10	42.2(9.6)	0.22
Male	14	52.9(29.1)	
Moderate Grade	8	43.6(11.4)	0.66
Poor Grade	15	51.1(28.4)	

* p-values for age, race, gender, and grade are adjusted for smoking

When adjusted for gender and age, carcinomas obtained from smokers harbored significantly more mutations than carcinomas from never smokers.

Relative Risks♣

	IRR	95% CI	p value
Smoking	1.36	(1.01, 1.84)	0.04
Age	1.30	(0.95, 1.78)	0.11
Gender	1.21	(0.90, 1.64)	0.21

All variables were included in the same model♣

Conclusions: Pancreatic carcinomas obtained from cigarette smokers harbor significantly more mutations than do carcinomas obtained from never smokers, adjusting for gender and age. The types and patterns of these mutations provide insight into the mechanisms by which cigarette smoking causes pancreatic cancer.

1397 PDX-1, CDX-2, TTF-1 and CK7: A Reliable Immunohistochemical Panel for Pancreatic Neuroendocrine Neoplasms

ES Chan, J Alexander, PE Swanson, MM Yeh. University of Washington Medical Center, Seattle, WA.

Background: Neuroendocrine neoplasms (NENs) can occur in virtually all sites of the body. Since NENs arising in different organs share similar morphologic features, attempt to distinguish metastatic vs primary NENs based on morphologic grounds alone is difficult. Pancreatic duodenal homeobox 1 (PDX-1) is a Hox type transcription factor essential for both exocrine and endocrine pancreas differentiation and maintenance of beta-cell function. We investigated PDX-1 as an immunohistochemical marker in primary pancreatic NENs.

Design: 79 primary NENs (25 pancreas, 29 lung, 25 gastrointestinal tract) were studied. Clinical and radiologic data were reviewed to ensure the validity of the stated primary sites. Immunohistochemistry for PDX-1, CDX-2, TTF-1, CK7 and CK20 was performed and results were based on consensus review of two authors blinded to the primary sites.

Results: PDX-1 reactivity was predominantly cytoplasmic, with occasional nuclear labeling. PDX-1 was seen in 19 of 25 (76%) pancreatic NENs; in contrast, only 3 of 29 (10%) pulmonary NENs and 1 of 25 (4%) gastrointestinal NENs were positive. PDX-1 was therefore 93% specific and 76% sensitive for pancreatic NENs (Youden s index = 0.69). TTF-1 was expressed only in pulmonary NENs; all other NENs were negative for TTF-1 (Youden s index = 0.52). CK7 was also very specific (90%) and sensitive (66%) for pulmonary NENs (Youden s index = 0.56). CDX-2 was seen in 21 of 25 (84%) cases of gastrointestinal NENs and only in 1 of 25 (4%) cases of pancreatic NENs. Thus, CDX-2 was 98% specific and 84% sensitive for gastrointestinal NENs (Youden s index = 0.82).

Immunohistochemical profiles of NENs arising in different sites

Site	PDX-1	CDX-2	TTF-1	CK7	CK20
Pancreas	19/25 (76%)	1/25 (4%)	0/25 (0%)	3/25 (12%)	3/25 (12%)
Lung	3/29 (10%)	0/29 (0%)	15/29 (52%)	19/29 (66%)	1/29 (3%)
Gastrointestinal tract	1/25 (4%)	21/25 (84%)	0/25 (0%)	2/25 (8%)	4/25 (16%)

Conclusions: PDX-1 is highly specific with very good overall diagnostic accuracy for pancreatic NENs. An immunohistochemical panel including PDX-1, CDX-2, TTF-1, CK7 and CK20 may be useful in distinguishing NENs of pancreatic origin from other primaries.

1398 Cystic Biliary Hamartoma of the Liver: 17 Examples of a Clinicopathologically Distinct Entity

I Coban, D Altinel, D Martin, B Kalb, J Sarmiento, NV Adsay. Emory Uni., Atlanta.

Background: A hitherto unrecognized type of cystic lesion in the liver which appears to be the cystic/complicated version of bile duct hamartoma is described.

Design: Clinicopathologic features of 17 cases with a distinctive MRI appearance and corresponding pathologic findings were analyzed. Only the patients that underwent hepatic resection for this suspected lesion were included into the study.

Results: 12 female, 4 male. Mean age, 62 (40-84). Mean size, 11 cm (2-30). MRI: Distinctive and specific pattern characterized by a lobulated, well-marginated cyst demonstrating a very thin line of peripheral rim enhancement. MRI also showed multiple small bile duct hamartomas in the uninvolved hepatic parenchyma in 13/17. Gross: Cyst walls, well defined fibrotic band (0.1-0.8 cm). Cyst lining, smooth and devoid of any excresences or discrete lesions; however, substantial hemorrhage in 8, and purlent contents in 1 (with previous history of intervention). Fibrous septations, creating a pattern of multilocularity in 11. Microscopy: The cyst walls, composed predominantly of fibrous tissue containing biliary ductules and low to moderate inflammation. In 8, microscopic conglomerate of dilated ducts on the cyst walls with all the characteristics of bile duct hamartomas (von-Meyenburg complexes) including contour irregularities, attenuated epithelium, and 2 with bile in the lumen, many giving the impression of transforming into the main cyst. In 9, macroscopic daughter cysts with features of von- Meyenburg complexes. Cyst lining, often attenuated, and where preserved, low cuboidal with minimal cytoplasm, and exhibiting the typical appearance of bland biliary epithelial cells. Other findings variably present: hemorrhage in 8, calcification in 6, and vascular malformation in 3 (suggestive of a developmental ductal plate abnormality). Other lesions: bile duct hamartomas in 13 and hemangioma in 1. Uninvolved liver: steatosis in 6, cirrhosis in 1, and the remaining 10 unremarkable.

Conclusions: Described here is a previously uncharacterized type of cystic lesion in the liver with distinctive clinicopathologic features. The MRI findings and morphologic appearance are that of a mega-cystic version of bile duct hamartomas, and they are also frequently associated with smaller hamartomas in adjacent liver. Therefore, we propose the term cystic biliary hamartoma for this entity.

1399 Paraduodenal Pancreatitis Is One of the Main Causes of Pseudotumor in the Pancreas and Periampullary Region: Features of a Distinct Entity Becoming Clearer

I Coban, O Basturk, D Martin, B Kalb, J Sarmiento, D Kooby, C Staley, NV Adsay. Emory Uni., Atlanta; NYU, NY.

Background: Paraduodenal pancreatitis (PDP) was recently proposed as a unifying term for a distinctive subset of pancreatitis previously reported under *cystic dystrophy of heterotopic pancreas, groove pancreatitis* and those associated with *paraduodenal wall cyst*. There has not been any systematic study of this entity.

Design: Clinicopathologic findings of 31 PDP cases among 700 pancreatic head resections were reviewed.

Results: Overall incidence: 4%. All, clinically misdiagnosed as carcinoma. Increasingly common cause of pseudotumor (among the last 100 resections, 7 PDP *vs* 2 LPSP). M/F= 21/10. Mean age, 50. H/O smoking and alcohol in 19/21. MRI (evaluated retrospectively in 12): Distinctive inflammation and abnormal enhancement of duodenal wall and a unique tubulocystic pattern along the expected course of *accessory duct/ minor papilla*. Macroscopy: Mucosal-covered nodularities in the *accessory ampullary region*; narrowed lumen; on cut sections, thickened mucosa, trabeculation of the wall; homogenous firm-white pseudotumor extending to and in some, extensively replacing the pancreas especially in the *groove region* (groove pancreatitis), and variably sized cysts, some up to several cms (paraduodenal wall cyst). Microscopy: Brunner gland hyperplasia in the mucosa; on the wall, exuberant myoid proliferation intermixed with scattered round pancreatic lobules (myoadenomatosis), variably cystic ducts, some with partial duct-epithelial lining (cystic dystrophy of heterotopic pancreas) as well as ruptured ducts associated with hypercellular reactive tissue and stromal deposition of acinar secretions associated with inflammatory/fibroblastic reaction rich in eosinophils, foreign-body giant cells and eosinophilic abcesses.Stones in 17.

Conclusions: PDP is often mistaken as carcinoma clinically, and with advancing technology that allows recognition of less problematic mimickers, it constitutes an increasingly high percentage of pseudotumors. It is seen in the middle-aged with H/O of alcohol and smoking. Collaboration of macroscopic and MRI findings confirm that the process is centered in the accessory duct /minor papilla. It appears that PDP results from an alcoholic/obstructive injury inflicted upon a functioning but vulnerable accessory duct. Recognition of the distinctive features of this entity should allow accurate diagnosis both pre- and post-operatively.

1400 Immunohistochemical Validation of Proteomic Analysis in Pancreatic Ductal Dysplasia (PanIN)

JF Coleman, R Chen, TA Brentnall, MP Bronner. Cleveland Clinic Foundation, Cleveland, OH; University of Washington, Seattle, WA.

Background: Pancreatic ductal adenocarcinoma is an insidious disease, often diagnosed at a late stage and with an almost uniformly and rapidly fatal prognosis. Methods of early detection hold promise for improved outcomes, but more reliable biomarkers of early tumorigenesis are needed. Interrogation of the pancreatic ductal neoplasia proteome offers a promising approach for biomarker discovery.

Design: Using an isotope-coded affinity tagging (ICAT) proteomics strategy, the differential expression of peptides between dysplastic ductal tissue and normal pancreatic tissue was determined. Annexin V and laminin were selected for morphologic validation. Tissue microarrays and standard immunohistochemistry were used to semiquantitatively characterize these markers in 73 surgically-resected pancreatic adenocarcinomas and 40 non-neoplastic pancreatic controls. Carcinoma, dysplasia, normal ducts, and their surrounding stroma were graded for the intensity of immunohistochemical staining (0-3), as well as the approximate percentage of positive cells (25%, 50%, 75%, 100%). A cumulative score for each tissue was calculated as the mean of the product of the intensity and percentage grades. The score distributions of adenocarcinoma, high-grade dysplasia (PanIN III), low-grade dysplasia (PanIN II) and their associated stroma were compared with normal controls by chi-square testing.

Results: Annexin V immunohistochemical staining of normal control ductal epithelium (mean 2.58) was significantly higher than low-grade dysplasia (2.43, $p=0.04$), high-grade dysplasia (2.0, $p<0.01$), and adenocarcinoma (2.23, $p=0.04$). Laminin staining of the normal control periductal stroma (mean 1.03) was significantly decreased relative to adenocarcinoma (1.92, $p<0.01$), high-grade dysplasia (1.96, $p<0.01$), and low-grade dysplasia (1.9, $p<0.01$).

Conclusions: ICAT-based proteomic strategies continue to yield biomarkers of interest for pancreatic ductal neoplasia, as confirmed by this immunohistochemical validation of annexin V and laminin.

1401 Increased Expression of Inhibitory B7 Family Members Associated with Chronic Hepatitic Necroinflammatory Disease

MW Cruise, R Kassel, TL Pruett, YS Hahn, JC Iezzoni. University of Virginia, Charlottesville; University of Virgina, Charlottesville.

Background: Several of the chronic hepatitic diseases are characterized by infiltrating lymphocytes, which are thought to be a key component in the pathophysiology of the disease. Recent data has demonstrated that PBL from patients with HCV and HBV express increased levels of PD-1 and regulation of this pathway may contribute to treatment failure and inability to resolve the infection. The immunomodulatory PD-1 along with its receptors, B7-H1 and B7-DC, induces tolerance and dampens the immune response. However the expression of these proteins within the liver is not well studied. We examined the expression profiles of PD-1 and its ligands to determine the utility of these molecules as markers of clinical disease.

Design: Liver biopsy from 74 patients were examined: HBV(n=11), HCV(n=17), AIH(n=14), NAFLD(n=13), and normal(n=19). Study exclusion criteria included: HIV+, acute HAV, antiviral therapy, cirrhosis, and EtOH abuse. Normal patients demonstrate elevated LFTs with normal histology. Blinded analyses was performed on the biopsies utilizing the Ishak modified HAI and fibrosis score or the NAS system, as appropriate. The biopsies were stained for CD3, PD-1, B7-H1, B7-DC and MHC I and graded by quartiles, reflecting frequency and intensity of expression.

Results: Liver biopsies from patients with HBV, HCV, and AIH demonstrated an increase in intrahepatic PD-1 positive lymphocytes, as compared to NAFLD and normal biopsies. While the PD-1 is expressed on primarily CD3 cells, the PD-1 ligands are expressed on Kupffer cells, LSECs, leukocytes, and hepatocytes. HBV, HCV, and AIH demonstrate increased B7-H1 and B7-DC expression by liver parenchymal cells and leukocytes. The increase is statistically significant and demonstrates a positive correlation with the Ishak scores.

Conclusions: The biopsies demonstrate an increase in the hepatic expression of B7-H1 and B7-DC along with increased numbers of infiltrating PD-1 positive lymphocytes

in chronic viral and autoimmune hepatitic diseases. These increases correlate with the level of inflammation and fibrosis across these etiologies, however they do not correlate with damage in NAFLD. These findings document the expression profile of this class of molecules and may suggest a possible target for therapy (humanized antibody recently released for phase I trial) as well as a marker for treatment outcomes.

1402 The Importance of NFKappa-B and COX-2 Expressions in Pancreatic Adenocarcinomas

S Erdamar, O Aydin, A Dirican, G Dogusoy, S Goksel. Cerrahpasa Medical College, Istanbul, Turkey.

Background: It's thought that NFKappa–B plays an important role regulation of apoptosis and also in angiogenesis, invasion. COX-2 is transcriptionally activated by NFkappa-B. We aimed to analyse the prognostic significance of NFkappa-B and COX-2 expression in pancreatic adenocarcinomas.

Design: We analyzed 65 patients with resectable ductal adenocarcinoma of the pancreas that had undergone a pancreaticoduodenectomy at Cerrahpasa Medical College, Istanbul, between 2003 and 2007. Tissue microarray (TMA) blocks were built using representative tumor blocks for each case. TMA blocks were cut in 4 microns and sections were immunostained with commercially obtained antibodies for COX-2 and NFKappa-B. The survival associated with both antibody expression was assessed by Kaplan-Meier survival analysis and multivariate Cox proportional hazards regression models that controlled for other known prognostic factors associated with pancreas cancer mortality.

Results: The mean age was 62,3 (32-85) in our study group. Mean survival was 22,5 months (1-105). Mean tumor size was 3,5 cm (0,6-11 cm). We found expression of COX-2 was upregulated in 43 of 65 cases (67%) and the expression of COX-2 was associated with the diameter (> 3 cm) of the tumors ($p < 0.05$), but not with the age, gender, tumor location, differentiation, lymph-node metastases and TNM stage. Expression of NFKappa-B was observed in 42 of 65 cases and its expression was more frequent in invasive components than in intraductal components. Expression of NFKappa-B was associated with metastasis to lymph nodes and other organs. A correlation was also found between NFKappa-B expression and the COX-2 in the tumour.

Conclusions: The increased expression of COX-2 may be responsible for rapid proliferation of pancreatic cancer. NFKappa-B play an important role in neoplastic spread through lymph node involvement.

1403 Detection of Hepatitis C Virus Core and NS3 Protein in Paraffin-Fixed Liver Tissue by Using a Modified Immunodetection System

M Ficarra, H LeBeau, S Florman, F Regenstein, S Dash, S Haque. Tulane University Health Sciences Center, New Orleans, LA.

Background: Hepatitis C virus (HCV) is a common blood borne hepatotrophic virus that causes chronic liver disease, cirrhosis and hepatocellular carcinoma. Diagnosis of chronic HCV infection and response to antiviral therapy in the clinical practice is currently established mostly by clinical and morphologic criteria and by detection of virus by a highly sensitive RT-PCR method. However, a reliable method to detect viral antigen in the liver tissue should be rapid, reliable, cost-effective, and a routine step in patient medical care. Aim: To develop an immunohistochemical method that can reliably detect the expression of HCV antigen in the formalin-fixed liver tissue of chronically infected humans. Design: In this study, HCV positive and HCV negative paraffin-fixed liver explants specimens were randomly selected from the files of Tulane University Health Sciences Center. Formalin fixed liver tissue sections were stained for HCV core and NS3 protein by using two different mouse monoclonal antibodies. Immunostaining was performed using a protocol that includes a Biotin-Free Universal HRP-Polymer detection method. Results: The polymer detection system is sensitive enough to detect the expression of HCV core and NS3 protein in the liver tissue. We were able to localize cytoplasmic expression of core and NS3 protein in all the HCV positive livers but not in the controls. In each case approximately 20- 40 % of hepatocytes showed positive staining to both antibodies. The immunoreactivity was also seen within some Kupffer cells and macrophages. Conclusions: We developed a method that can reliably detect HCV protein in paraffin-embedded, formalin-fixed liver tissue from chronically infected patients. This method can be utilized for routine histological evaluation of HCV in pathology laboratories.

1404 Abundant Infiltration of Immunoglobulin G4 – Positive Plasma Cells: Autoimmune Pancreatitis vs Pilonidal Sinus

Y Fukumura, M Takase, K Suda, H Abe, K Mitani, T Hayashi, T Yao. Juntendo University, Bunkyo-ku, Tokyo, Japan; Tokyo-West Tokushukai Hospital, Akishima, Tokyo, Japan.

Background: Abundant IgG4-positive plasma cells (G4-P) infiltrate in autoimmune pancreatitis (AIP) and its related diseases (AIP-Ds), hence immune mechanism via regulatory T cells (Treg) has been proposed in these disease entities. In our daily practice, many G4-Ps are observed not only in AIP-Ds but also in some non-AIP-Ds such as gastric ulcer, radicular cyst, and pilonidal sinus (PS). The aim of this study was to compare the amount of G4-P, ratio of G4-P / IgG1-positive plasma cells (G1-P), and CD25-positive lymphocytes between AIP and PS, in order to see the possible contribution of Treg in these disease entities.

Design: The study group consisted of pancreas from 4 AIP and skins from 10 PS. Formalin-fixed, paraffin embedded sections were prepared from these lesions. Sections were stained with H&E and with the antibodies IgG4, IgG1, and CD25. The amount of G4-Ps were scored (-), (1+), (2+), or (3+) according to Kamisawa's criteria.

Results: All the 4 cases of AIP showed up to (2+); diffuse and, in particular, periductal / interlobular infiltration of G4-Ps with storiform fibrosis were seen in all cases. The G4-P / G1-P ratio was 40.5 % to 120.5%. CD25 positive cells were less than 1 / HPF. PS cases showed G4-P score, (-) in 4 cases (40%), (1+) in 3 cases (30%), and (2+) in 3 cases (30%). In all PS cases, G4-Ps infiltrate mostly in granulation layer around the sinus of the PS. G4-P / G1-P ratio was 10.5 % to 150 %. CD25 positive cells were less than 1 / HPF.

Conclusions: (a) This study indicates that some cases of PS can show abundant G4-P infiltration and high G4-P / G1-P ratio, similar value as AIP, suggesting that histological G4-P score and G4-P / G1-P ratio are not enough for identifying AIP / AIPDs in our daily practice. To see the accompanying storiform fibrosis or granulation reaction may be helpful for the differential diagnosis. (b) In this study, only a few CD25-positive cells were seen both in AIP / PS, suggesting little contribution of Treg in AIP / AIPDs as well as in PS, at least with local level. Since this result may conflict with some recently published paper, which show higher serological level of Treg in AIP, additional study may be needed to investigate the other downstream members of 'T-reg to G4-P pathway' in these diseases.

1405 Black Cohosh Induced Acute Hepatotoxicity Featuring Centrilobular Necrosis and Autoimmune Hepatitis

G Guzman, C Wojweda, ER Kallwitz, SJ Cotler. University of Illinois, Chicago; Case Western Reserve University, Cleveland.

Background: There are a growing number of case reports of hepatotoxicity in patients taking black cohosh (*Cimicifuga racemosa*), an over-the counter herbal supplement used to alleviate menopausal symptoms and irregularities. Most reports described acute hepatic necrosis, although one paper detailed a case with clinical features of autoimmune hepatitis. Our aim is to report the second and third cases of acute hepatotoxicity attributable to black cohosh use with histological features of autoimmune hepatitis.

Design: Case reports.

Results: Case 1. A 42 year old woman presented with a two month history of progressive malaise, nausea, and vomiting. Mild icterus without stigmata of chronic liver disease was noted on physical exam. She had been taking black cohosh for menopausal symptoms for 6 months. Her total bilirubin level was 3.1 mg/dl, AST 696 U/L, ALT 1457 U/L, alkaline phosphatase 94 U/L, and INR 1.2. Case 2. A 53 year old woman presented for evaluation of elevated liver enzymes detected at health screening four months previously. She complained of right upper quadrant abdominal pain and fatigue. She had been taking an herbal supplement that contained soy protein and black cohosh within the past year. Laboratories showed an AST 478 U/L, ALT 443 U/L, alkaline phosphatase 188 U/L, total bilirubin 2.0 mg/dl and an INR of 2.0. Both patients had no history of any other liver diseases and denied alcohol and drug use. Both had negative work-ups for viral hepatitis A, B, and C serologies, hepatitis C virus RNA by PCR, acute CMV, EBV, hemochromatosis gene analysis, and ceruloplasmin levels, anti-nuclear, anti-smooth muscle, anti-liver kidney microsomal antibodies, and anti-mitochondrial antibody. The histologic features of both cases show acute hepatitis displaying prominent centrilobular hemorrhage and necrosis consistent with severe drug induced liver injury. While clinical features of autoimmune hepatitis were lacking, the histology showed characteristics of autoimmune-like liver injury with an interface hepatitis consisting of a dense lymphoplasmacytic infiltrates, hepatocyte rosetting and oncocytic changes. Both patients responded to corticosteroids, supporting an immune mediated component to the liver injury.

Conclusions: Hepatotoxicity attributable to black cohosh should be included in the list of differential diagnoses for acute liver necrosis mimicking autoimmune hepatitis.

1406 RUNX1T1 Is a Novel Metastasis-Associated Tumor Suppressor Gene in Pancreatic Endocrine Carcinomas

NA Hafez, L Turner, J Skaf, S McCarthy, NA Nasir, A Hakam, D Coppola, P Hodul, LK Kvols, A Nasir. Moffitt Cancer Center, Tampa, FL.

Background: RUNX1T1 is a gene present on chromosome 8. It had been shown to play different and significant role when it changes biological phenotype.The t(8;21)(q22;q22) was described thoroughly in acute myelogenous leukaemia that resulted in the transcription factor fusion protein, RUNX1-RUNX1T1 (also known as AML1-ETO). RUNX1T1 role was not described in Pancreatic Endocrine Tumors (PETS).

Design: Five clinically-localized primary (CLP)-PETS from 5 adult patients and 6 well-differentiated (WD) metastatic primary (MP)-PECAs from 6 other adult patients were profiled on Affymetrix U133 2.0 gene chip. The data were RMA normalized and t-test was used to identify genes differentially expressed in MP-PECAs vs. CLP-PETs. This gene set was further refined by excluding those with a significant frequency of Type I errors. Published literature was reviewed to select 'candidate progression genes' for further validation on the original frozen PETs/PECAs and also on independent test sets of archival MP-PECAs and CLP-PETs, using qRT-PCR. For real time PCR, TaqMan assays specific for those genes were spotted on TaqMan® Arrays (ABI). For real-time data normalization, IPO8 was tested and was found stable across samples and was hence used as the endogenous control gene.

Results: 217 transcripts were differentially expressed between MP-PECAs and CLP-PETs, using p-value <0.05 and fold-change values >1.5. Among those with a fold-change >2, several exhibited a high level of reliability, based on similar patterns of differential expression for multiple probe sets targeting the same mRNA. On microarray, RUNX1T1 was down regulated and directional in all studied tumors. It was 2 folds or more down regulated in MP-PECAs compared NMP-PETs on microarray. When RUNX1T1 expression in nucleic acid extracted from frozen samples was measured using TaqMan® Arrays, it was found to be under-expressed in MP-PECAs relative to NMP-PETs by a factor of 5.84 with a P value of 0.008. We also found a similar trend of down-regulation of RUNX1T1 on archival tumor sets, but with less obvious fold change.

Conclusions: RUNX1T1 is a novel 'putative tumor suppressor gene' in sporadic primary WD-pancreatic endocrine carcinomas that had synchronous liver metastases at the time of its resection. Further studies are required to investigate the clinical utility of this gene as a progression biomarker in pancreatic endocrine tumors and for developing new molecular therapy for these aggressive tumors.

1407 High Frequency of Overexpression of Transcriptional Intermediary Factor 1 Gamma (TIF1γ) in Pancreatic Ductal Adenocarcinoma and Its Precursor Lesions

CH Hajdu, E Blochin, L Zhang, F Francis, H Yee, L Chiriboga, P Lee, R Xu. New York University School of Medicine, New York, NY; Mount Sinai School of Medicine, New York, NY.

Background: Approximately 50 % of pancreatic adenocarcinomas show deletion or inactivation of SMAD-4/DEPC-4, a member of Transforming Growth Factor β (TGF-β) family. We hypothesize that TIF1γ, recently identified as a novel cofactor of SMAD2/3, competitive to SMAD4, may have a similar role in pancreatic cancer development.

Design: Eleven cases of mucinous cystic neoplasm (MCN) with and without pancreatic intraepithelial neoplasia (PanIN), 12 cases of IPMN, 13 cases of PanIN lesions, and 15 cases of pancreatic duct adenocarcinoma (PDA) were randomly selected from the archival Surgical Pathology files of the NYU Langone Medical Center and Mount Sinai Medical Center and confirmed by H&E slide review. Four micron-thick, formalin-fixed and paraffin-embedded tissue sections were immunostained with monoclonal mouse or rabbit anit-TIF-1 γ and TGF-β II receptor using Ventana automated stainer. The intensity of immunostains is defined as 1+ (baseline expression in normal ductal epithelium), 2+ (moderate) and 3+ (high). Abnormal expression in more than 30% cancer cells is considered to be positive.

Results: Compared to baseline expression in the nuclei of normal ductal epithelium, 11 of 11 (100%) cases of MCNs, 10 of 12 IPMNs (80%), and 15 of 15 PDAs (100%) show overexpression of TIF1γ. Interestingly TIF1γ overexpression is not observed in any of the 10 cases of low-grade PanIN (grade I, gastric type) associated with MCNs, but is seen in 10 of 13 (77%) independent PanINs (mostly grade II and III). Overexpression of TGF-β II receptor protein is present in 5 of 16 cases (31%) of MCN, 4 of 12 (30%) IPMN, and none of the low grade PanINs associated with MCNs. Downregulation of TGF-β II receptor protein is seen in 2 of MCNs and none of the other lesions.

Conclusions: The high frequency of overexpression of TIF1γ in pancreatic precancerous lesions and PDAs suggests that this protein may play a critical role in the early oncogenesis of pancreatic adenocarcinomas. Unlike SMAD4, TIF1γ is overexpressed in a high frequency in all three precursor lesions of pancreatic cancer, which may potentially serve as a screening marker for early diagnosis.

1408 Clinicopathological Correlation and Grading of Graft Versus Host Disease of the Liver

S Hukku, G Bentley. Wayne State University/Detroit Medical Center, Detroit, MI.

Background: Liver is the second most frequently involved target for graft versus host disease (GVHD), after skin, in patients with history of hematopoietic stem cell transplant. Prognosis is dependent on the overall grade of GVHD of which liver is an important parameter. There are no clear guidelines for grading GVHD of liver. The purpose of the study is to provide a clear, reproducible grading system for GVHD of the liver.

Design: Eighty-six liver biopsy specimens from hematopoietic stem cell transplant recipients obtained between 1999 to 2008, with a clinical suspicion of GVHD were reviewed to evaluate the histopathological changes of GVHD and iron deposition. Associations between these results and liver enzymes (AST, ALT, Alkaline phosphatase, total bilirubin) were sought. Cases with no morphological evidence of GVHD and hep B/C positivity were excluded. Seventy-three cases of GVHD were graded as mild, moderate and severe as follows: Mild: minimal lymphoplasmocytic infiltration of portal triads, nuclear anisocytosis and mild lymphocytic infiltration involving epithelium of **some** bile ducts. Moderate: moderate to severe portal inflammation and involvement of **most** bile ducts. Severe: moderate to severe portal inflammation and involvement of most bile ducts (moderate grade) **plus** lobular inflammation **or** bile duct loss **or** increased portal fibrosis. Iron (Prussian blue stain) deposition was scored minimal, mild, and moderate to severe: Minimal: scattered periportal hepatocytes with stainable iron. Mild: most periportal hepatocytes with stainable iron. Moderate/Severe: extension into lobules to virtually all hepatocytes with stainable iron.

Results: We found we could histologically divide GVHD into three categories: mild, moderate and severe, which have a statistically significant correlation with AST and Alkaline phosphatase levels. Severe Iron deposition may symptomatically mimic GVHD including elevations of transaminases. Our results show an inverse relationship of iron deposition with the severity of GVHD.

Results

GVHD	Mild (n=25)	Moderate(n=28)	Severe(n=20)	p value
AST	187±175	374±313	489±336	0.002
ALT	397±472	474±363	544±545	0.563
Alk.Phos	307±286	500±337	562±434	0.040
Total Bilirubin	7.6±12	4.2±4.4	5.2±5.0	0.311

Conclusions: GVHD of the liver can be reliably graded as mild, moderate and severe. There is a stastically significant correlation between severity of GVHD and elevation of AST and Alkaline phosphatase. Also, severe iron deposition should be included in the differential for GVHD.

1409 Von-Meyenburg Complexes Are Colonic Adenoma Equivalent in Liver

D Jain, L Qin. Yale University School of Medicine, New Haven, CT; Mount Sinai Medical Center, New York, NY.

Background: More than 80% of intrahepatic cholangiocarcinoma (CC) arise in non-cirrhotic livers, often without any underlying chronic liver disease. No precursor lesions for such sporadic CC are known. We have previously shown morphologic and molecular evidence that biliary-microhamartomas /Von-Meyenburg complexes (VMC) can occasionally transform into pre-neoplastic adenomatous lesions and CC. VMCs are known to increase with age and we suspect majority of sporadic CC arise from VMCs.

Design: All hepatic resections or explants containing CC from two institutions during 1985-2008 period were studied. Only intrahepatic (I-CC) and hilar (H-CC) tumors were included in the study. Numbers of VMCs present within and outside the tumors were recorded, and presence of any intermediate lesions/adenomatous transformation was specificially looked for. The tumors were histologically classified as per WHO classification. In addition, tumors that showed architectural resemblance to VMC characterized by angular profiles of the tumor glands, dilated lumen often containing inspissated secretions/bile and with intervening hyalinized/ desmoplastic stroma were called "VMC-like". Age and sex matched hepatic resection for metastatic colonic carcinoma were used as controls.

Results: A total of 79 cases of CC carcinoma {48 I-CC, 31 H-CC, age range 27-90Y, mean age 60Y, M:F=1.4:1) were identified. Of these 49(62%) had no known background liver disease and only 7(8%) had cirrhosis. Associated liver disorders included sclerosing cholangitis (primary/secondary) (14), hepatitis C (5), hepatitis B (5), NASH (7) and others disorders (3). VMC were identified in 15 (31.2%) of I-CC and 7 (22.5%) of H-CC. VMC were present within the tumor (6 cases), outside the tumor (9 cases), or at both locations (7 cases). Two or more VMCs were seen in 9 cases. Intermediate forms/adenomatous lesions were identified in 10 cases. 34 (43%) cases showed at least some areas of the tumor that were considered VMC-like. Only 7% of the controls showed presence of VMC compared to 27.8% CC cases and the results were statistically significant ($p<0.05$).

Conclusions: There is a significant association between the presence of VMCs in liver and development of intrahepatic or hilar CC, and VMCs likely represent the precursors of CC, especially in apparently normal appearing livers. Patients with increasing numbers of VMCs are likely at a higher risk of developing CC. Further studies establishing the molecular link between VMC and CC are needed to understand the natural history of these lesions.

1410 Early Hepatic Stellate Cell Activation in Fibrosing Cholestatic Hepatitis

CP Jenkins, LR Dixon. University of Florida, Gainesville, FL.

Background: Recurrent hepatitis C (RHCV) after liver transplantation (post-LT) is almost universal, and in some patients takes an aggressive course characterized histologically by pericellular/sinusoidal fibrosis and cholestasis, known as fibrosing cholestatic hepatitis (FCH). FCH progresses rapidly often resulting in graft failure within a few months. The hepatic stellate cell (HSC) is the predominant source of extracellular matrix and type I collagen in the liver. Smooth muscle actin (SMA) immunoreactivity is present in HSCs, and early activation of portal HSCs in post-LT recipients has been shown to predict subsequent fibrosis in RHCV. The degree of HSC activation in FCH has not been studied, and may prove useful in establishing a diagnosis of FCH as well as differentiating FCH from a severe, but more slowly progressive, RHCV.

Design: Subjects were selected from an established database of post-LT hepatitis C patients. Subject groups included patients who developed FCH (n=8) and those with severe RHCV (fibrosis score of >/=3 of 6 at 2 years post-LT, n=6). Control subjects were selected from this same patient pool, and consisted of stable post-LT patients (fibrosis score of </=2 of 6 at 2 years post-LT, n=5). Immunohistochemistry was performed on paraffin sections of formalin-fixed tissue using the ABC/peroxidase method with SMA on biopsies at 1 week and 4 months post-LT. Staining patterns and intensity were recorded and compared between study groups.

Results: SMA reactivity at 1 week post-LT was severely increased in the majority (63%, n=5) of FCH and in all severe RHCV patients. At 4 months post-LT the SMA reactivity was also severely increased in the majority (88%, n=7) of FCH and severe RHCV (67%, n=4) patients. Stable post-LT patients exhibited none (n=1) to mild (n=4) SMA reactivity at 1 week post-LT and none (n=1) to moderate (n=3) reactivity at 4 months post-LT. Four FCH patients expired within 10 months post-LT, all having severe SMA reactivity at 4 months post-LT.

Conclusions: The FCH and severe RHCV patients had greater SMA reactivity/HSC activity at both 1 week and 4 months post-LT than stable post-LT patients. The prevalence of severe HSC activation at 4 months post-LT was greater in the FCH patients than in RHCV patients allowing possible means to differentiate the two. Activation of portal HSCs at 1 week and 4 months in post-LT hepatitis C patients is a specific marker for progressive fibrosis to distinguish those who will have either an aggressive RHCV or FCH course and may help to select patients who would benefit from early aggressive therapy.

1411 Chromosomal Gains Demonstrated by Fluorescent In Situ Hybridization Are Helpful in the Diagnosis of Atypical Hepatocellular Neoplasms

S Kakar, JP Grenert, E Pease, O Adeyi, LD Ferrell. UCSF, San Francisco; Univ of Toronto, Toronto, Canada.

Background: It can be difficult to distinguish well-differentiated hepatocellular carcinoma (HCC) from hepatic adenoma (HA) based on morphology alone.Gains of chromosomes 1 and 8 are the earliest cytogenetic abnormalities in HCC, and have not been observed in HA.We explored the utility of fluorescent in situ hybridization (FISH) to identify cytogenetic aberrations for the diagnosis of atypical hepatocellular neoplasms occurring in noncirrhotic liver.

Design: FISH analysis using centromeric probes for chromosomes 1,8,X and locus specific probe for c-myc was performed in 35 hepatocellular neoplasms(HA=11, AHN=12, HCC=12). The signals were counted in 100 tumor nuclei per case as well as 200 normal hepatocyte nuclei. The designation of AHN was used in two situations: HA-like morphology in atypical setting (women ≥50 years and ≤15 years, and all men) and HA-like morphology with focal atypical areas (small cell change,abnormal trabeculae) that were insufficient for a definite diagnosis of HCC.

Results: None of the HAs showed gains at any of the four chromosomes (0/11). Gains involving at least one locus were seen in 7 (58%) well-differentiated HCCs and 7

(58%) AHNs (see table). Gains of chromosome 1 were seen in all AHNs (100%) and 6 (85%) HCCs. Gains of all loci tested (chromosomes 1,8,X and c-myc) were seen in 3 AHNs and 2 HCCs. One HCC case showed c-myc gains with no other abnormalities. Recurrence and/or metastasis were observed in 3 (25%) AHNs.

Conclusions: Cytogenetic aberrations characteristic of well-differentiated HCC are seen in majority of AHNs (males of any age, females outside the 15-50 year group or with focal atypical morphology). These tumors can recur and metastasize even though they morphologically resemble adenoma. Chromosome 1 gain by FISH was the most common abnormality and was observed in all the abnormal AHN cases. However the sensitivity of the FISH assay using centromeric probes is relatively low as only 58% of histologically diagnosed well-differentiated HCC were cytogenetically abnormal. Examination of additional loci and use of locus specific probes in addition to centromeric probes is likely to increase the sensitivity of diagnosis.

	No gains	1+ only	1+ X+	1+,8+,myc+,X+	myc+ only
AHN (n=12)	5	3	1	3	0
HCC (n=12)	5	4	0	2	1

Drs. Kakar and Grenert are equal contributors

1412 Increased Liver Cell Steatosis and Apoptosis Represent a Mechanism towards Increased Liver Injury in Experimental Liver Fibrosis

C Kalogeropoulou, I Tsota, P Zabakis, V Tzelepi, T Petsas, D Kardamakis, A Tsamandas. University of Patras School of Medicine, Patras, Greece.

Background: Liver cell steatosis seems to have a generally benign prognosis, either because most hepatocytes are not significantly damaged, or mechanisms that replace injured hepatocytes are induced. Apoptosis has been linked to liver cell depletion and ensuing liver fibrosis. This study assesses the effect of liver cell steatosis and apoptosis on the disease severity, in experimental liver fibrosis.

Design: The study comprised 54 male Wistar rats divided in 2 groups: A (n=6) controls and B (n=48): CCl4 injection (intraperitoneally 2ml/kg/BW-1:1 vol in corn oil twice weekly). In group B rats were sacrificed at 4, 8, 12 weeks. SGPT values were measured in blood samples. Steatosis (% of hepatocytes affected) was graded as follows: 0 (<5%), 1 (5%-30%), 2 (31%-70%), 3 (>70%). Liver tissues were evaluated for **I)** Bax, Bcl-2, TNFα, and active caspase-3 mRNA (RT-PCR) and protein (Western blot), **II)** liver stellate cell activation (immunostain for αSMA) and **III)** apoptosis (TUNEL method). Results were expressed following computerized analysis.

Results: Rats of groups B displayed higher SGPT values compared to controls ($p<0.001$). In group B, a direct correlation between liver cell apoptosis and degree of steatosis was recorded ($r=0.58$, $p<0.01$). Increased steatosis was associated with: **I)** decreased Bcl-2 mRNA levels ($r=-0.34$ $p<0.05$), **II)** increased Bax/Bcl-2 mRNA and protein ratio ($r=0.63$ and 0.74 $p<0.01$), **III)** active caspase-3 ($r=0.64$, $p<0.01$). In addition, a direct correlation was revealed between **I)** apoptosis and stellate cell activation ($r=0.46$, $p<0.05$) and **II)** TNFα levels and active caspase-3 ($r=0.68$, $p<0.01$).

Conclusions: In cases of experimental liver fibrosis, liver cell steatosis may contribute to hepatocytic injury. Further research is warranted in order to clarify the molecular pathways responsible for the proapoptotic effect of steatosis and whether this increase in apoptosis contributes directly to progression of liver injury in cases of liver cirrhosis.

1413 The Role of Oval Cell Activation and Oxidative Stress in Two Different Models of Experimental Cirrhosis

C Kalogeropoulou, I Tsota, P Zabakis, T Petsas, D Kardamakis, A Tsamandas. University of Patras School of Medicine, Patras, Greece.

Background: Oval cells (OC) are liver stem cells involved in the progress of liver disease and hepatocellular carcinoma development. In animals, the combination of oxidative liver damage and inhibition of mature hepatocyte proliferation increases the numbers of OC. This study investigates whether OC increase in experimental liver fibrosis and tries to clarify the mechanisms for this response.

Design: The study comprised 102 male Wistar rats divided in 3 groups: A (n=6) controls, B (n=48):CCl4 injection (intraperitoneally 2ml/kg/BW-1:1 vol in corn oil twice weekly), C (n=48): thioacetamide administration in drinking water (300 mg TAA/L) for 3 months. In group B rats were sacrificed at 4, 8, 12 weeks and in group C at 1, 2 and 3 months. Liver tissues were evaluated for: a) H_2O_2 production (inducer of cell cycle inhibitors), b) content of reduced glutathione (GSH-regulator of reactive oxygen species), c) expression of cytokeratin 7 (CK7) and AFP mRNA (OC phenotype), d) OC proliferation (%Ki67$^+$ OC). H_2O_2 production was expressed as integrated counts x10^6 and GSH content as μg/mg protein. Cells with morphologic features of oval cells that expressed CK 7 and AFPmRNA were scored.

Results: The table shows the results. Groups B and C showed higher hepatic mitochondrial production of H_2O_2 lower GSH content and higher OC accumulation, compared to group A (controls). In subgroups B3/C3, with the greatest H_2O_2 production, the highest number of OC was recorded, implying that there was the maximal degree of inhibition of mature hepatocyte proliferation.

Conclusions: This study demonstrates that in experimental liver fibrosis (irrespective of the model used for cirrhosis induction), OC accumulation evolves due to inhibition of mature hepatocyte proliferation. OC differentiate into intermediate hepatocyte-like cells after a regenerative challenge. However, cirrhosis is not required for OC accumulation. OC activation during experimental liver fibrosis may increase the risk for hepatocellular cancer, similar to that observed in the Solt-Farber model of hepatocarcinogenesis in rats.

Groups	H_2O_2	GSH	CK7	AFPmRNA	Ki67*
A	23	16	2.3±0.2	2.4±0.3	1.8±0.1
B1	39[a]	10[b]	14.2±4.1[c]	16.3± 6.2[d]	13.8±4.2[e]
B2	48[a]	8[b]	35.3±6.1[c]	37.4±8.5[d]	34.2±6.6[e]
B3	64[a]	7[b]	55.6±7.2[c]	57.3±8.6[d]	48.3±7.3[e]
C1	40[f]	9[g]	15.3±5.2[h]	18.1±7.4[i]	15.1±6.4[j]
C2	49[f]	7[g]	37.1±8.4[h]	39.2±9.3[i]	36.3±7.2[j]
C3	67[f]	6[g]	58.7±9.1[h]	59.6± 9.7[i]	51.4±8.7[j]

[a, c, d, e, f, h, i, j] : $p<0.001$ and [b, g] : $p<0.05$ when compared to controls. *: Ki67 + oval cells

1414 FOXP3 Positive Tumor-Infiltrating Lymphocytes in Hepatocellular Carcinoma: A Clinicopathologic Study

MJ Kapadia, J Alexander, LE Kernochan, MM Yeh. University of Washington, Seattle, WA.

Background: Tumor-infiltrating lymphocytes represent the host immune response to neoplasms. Recent studies have found that CD4+CD25+ forkhead box P3 (FOXP3) regulatory T-cells are increased in both peripheral blood and tissues from patients with hepatocellular carcinoma (HCC). Cumulative data suggest that these lymphocytes negatively regulate anti-tumor immunity by suppressing the activity and proliferation of effector T-cells, contributing to the failure of immune-mediated elimination of tumor cells. However, the prognostic value of regulatory T-cells in HCC remains unclear. We further investigated the association of regulatory and CD8+ T-cells in HCC with clinicopathologic characteristics.

Design: The number of CD3, CD8, and FOXP3 positive lymphocytes among the intra-tumor lymphocytes in 131 HCCs was assessed by immunohistochemistry using CD3, CD8, and FOXP3 antibodies. Numbers of lymphocytes were counted in the three highest density regions of FOXP3 expression within each HCC and tested for association with clinicopathologic features. HCC differentiation and Edmonson-Steiner (ES) grade was assessed at the consensus of two authors.

Results: Lower CD3:FOXP3 ratio was associated with poorer HCC differentiation ($p = 0.0117$). Lower CD8:FOXP3 was also associated with poorer differentiation and higher ES grade (Figures, $p = 0.0107$ and 0.0398, respectively). There were no significant associations involving vascular invasion, pathologic stage, or recurrence.

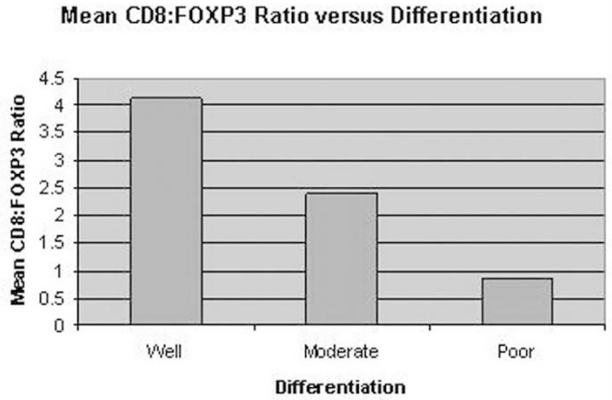

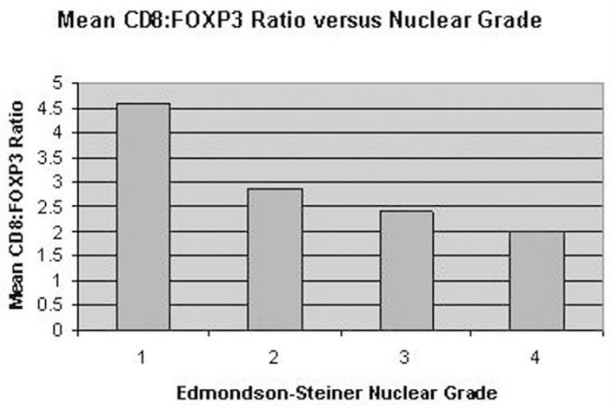

Conclusions: The phenotype of the intra-tumor T cell response in HCC has a significant association with tumor differentiation and ES grade. The data suggest that CD4+CD25+FOXP3+ regulatory T-cells may have a role in the modulation of the tumor immune response and that a higher percentage of them may be an unfavorable prognostic indicator. These findings could have implications for the design of immunotherapeutic approaches.

1415 Hepatocellular Carcinoma, Renal Cell Carcinoma Metastatic to Liver, and Adrenal Carcinoma Metastatic to Liver: Immunostaining for Bile Salt Export Pump as a Marker of Hepatocellular Differentiation

AS Knisely. King's College Hospital, London, United Kingdom.

Background: Bile salt export pump (BSEP) is an ATP-binding cassette transporter normally expressed only at the apical (canalicular) membrane of hepatocytes. If BSEP expression persists in hepatocellular neoplasms, to detect BSEP immunohistochemically might be useful in identifying hepatocellular differentiation.

Design: Formalin-fixed, paraffin-embedded archival samples of 25 tumours resected from liver and assessed on clinicopathologic grounds as hepatocellular carcinoma (HCC; 15), renal cell carcinoma metastatic to liver (RCC; 5), and adrenal cortical carcinoma metastatic to liver (ACC; 4) were immunostained for BSEP by standard techniques, using a polyclonal, affinity-purified antibody raised in rabbit. Degrees of HCC differentiation covered a spectrum from cells with minimal nuclear pleomorphism, resembling hepatocytes and rosetted around accumulations of material resembling bile ("well-differentiated"), to cells with extreme nuclear pleomorphism and scant and amphophilic or clear cytoplasm, lacking resemblance to hepatocytes and disposed without evident secondary structure ("poorly differentiated"). Using commercially available antibodies, parallel sections were immunostained for 5 additional canalicular antigens, including 2 transport proteins homologous to BSEP, multiple drug resistance associated protein 2 (MRP2; lacking in the Dubin-Johnson syndrome) and multidrug resistance protein 3 (MDR3; lacking in several cholestatic disorders); 2 ectoenzymes, neutral endopeptidase (CD10) and alanyl aminopeptidase (CD13); and carcinoembryonic antigen (using a polyclonal antibody; pCEA), as well as for the hepatocyte-associated cytoplasmic antigen carbamoyl phosphate synthetase (CPS; OCH1E5 / HepPar-1). Expression was scored as present or absent, with 3 descriptors (polarised membranous, diffuse membranous, and cytoplasmic).
Results: In HCC, polarised canalicular-antigen expression (BSEP, CD10, CD13, pCEA, MDR3, MRP2) was lost as differentiation worsened. CPS expression persisted in some moderately poorly differentiated HCC but was lost in worst-differentiated HCC. RCC expressed CD10, CD13, pCEA, MRP2, and MDR3, but not BSEP or CPS; ACC expressed only pCEA.
Conclusions: Unlike other canalicular antigens, BSEP expression in neoplasms appeared specific for hepatocellular differentation. It was, however, less robust than CPS expression. To immunostain for BSEP expression may have limited diagnostic value in relatively well-differentiated tumours.

1416 Intrapancreatic Cholangiocarcinomas. A Clinicopathological Study

I Konstantinidis, CR Ferrone, M Genevay, GY Lauwers, V Deshpande. Massachusetts General Hospital, Boston, MA.
Background: Intrapancreatic cholangiocarcinomas (ICC) are distal bile duct tumors that may be indistinguishable from pancreatic ductal adenocarcinomas (PDAC). The diagnosis of ICC is dependant on the pattern and extent of bile duct involvement, including the presence of dysplasia, although PDAC may also show common bile duct (CBD) involvement. However, there have been no prior attempts to pathologically explore ICC. The aim is to define the pathology of ICC, and examine the clinico-pathologic correlates thereof.
Design: We reviewed 100 pancreaticoduodenectomy specimens between 1989 and 2008 with tumors located adjacent to the CBD. The tumor microscopically involved the CBD in 64 cases, and these formed the study group. Two patterns of tumor growth were recognized: type I tumors demonstrated circumferential and symmetrical involvement of the bile duct, while type II tumors were asymmetrical with the epicenter of the tumor located away from the CBD. The presence of PanIN 2 and 3 (high-grade) and bile duct dysplasia was recorded. Demographic, nodal status and outcome data was documented. An additional 450 resected PDACs served as controls.
Results: We classified 37 patients as type I and 27 as type II. While there were no differences in the morphological appearance of the invasive carcinoma, group I lesions were associated with bile duct dysplasia, (46% vs 11%, p=0.03) whereas group II lesions were statistically more likely to be associated with high-grade PanIN (41%vs 8%, p=0.002). There were no significant differences in tumor size, nodal metastasis or overall survival between the both groups. In comparison to PDACs, the study group showed a significantly improved median survival (35 months vs. 19 months; log rank p=0.0006). When comparing the two groups with PDAC, overall survival was significantly better for type I tumors (46 months vs. 19 months, log rank p=0.001) but not type II tumors (32 months vs. 19 months, log rank p=0.12).
Conclusions: Peribiliary adenocarcinomas are a heterogeneous group. Tumors centered around the bile duct (group I) represent true ICC, while other forms of peribiliary intrapancreatic adenocarcinomas may be more closely related to PDACs. Genetic studies may aid in the refinement of this classification.

	Median age (years)	Females (%)	Size (cm)	Nodal status N1	Median survival (months)
Type I	65	25	2(0.4-5.5)	19(51%)	46
Type II	66	57	2(0.4-3.9)	17(63%)	32
p value	NS	p=0.009	NS	NS	NS

1417 BCL10 Is a New Sensitive and Specific Marker of Pancreatic Acinar Cell Carcinoma

S La Rosa, F Franzi, S Marchet, G Finzi, AM Chiaravalli, D Vigetti, F Sessa, C Capella. Ospedale di Circolo, Varese, Italy; University of Insubria, Varese, Italy.
Background: Acinar cell carcinoma (ACC) is a rare pancreatic cancer which may be difficult to distinguish from other pancreatic tumors, especially from islet cell tumors. The diagnosis depends on the demonstration of an acinar differentiation, easily obtained with antibodies recognizing various pancreatic enzymes that, although specific, show different levels of sensitivity. The rarity of this cancer, which also implies an occasional use of these antibodies in most laboratories, may lead to misdiagnosis. The C-terminal portion of the BCL10 protein shows homology with carboxyl ester hydrolase (CEH), an enzyme produced by pancreatic acinar cells. Routinely, anti-BCL10 antibodies are used for the diagnosis of MALT lymphomas.
Design: The aim of this study was to investigate the usefulness of a C-terminal-BCL10 monoclonal antibody (clone 331.1) in the diagnosis of pancreatic ACCs. Using immunohistochemistry, electron microscopy and western blotting, we examined normal pancreases and a series of 107 pancreatic tumors including ACCs, mixed acinar-endocrine carcinomas, ductal adenocarcinomas, intraductal papillary-mucinous, mucinous cystic, serous microcystic, endocrine, and solid pseudopapillary tumors. In addition, various normal tissues, cases of pancreatic metaplasia of the gastro-esophageal mucosa, cases of ectopic pancreas, gastrointestinal endocrine tumors, salivary and breast acinic cancers, gastric adenocarcinomas, four of which showing acinar differentiation, and hepatocellular carcinomas were included in the study.
Results: BCL10-immunoreactivity was restricted to acinar cells of normal and ectopic pancreas, of pancreatic metaplasia and of ACCs. It was ultrastructurally localized in zymogen granules. The BCL10 expression paralleled that of CEH as demonstrated by Western blotting and CEH immunohistochemistry. In addition, the anti-BCL10 antibody proved to be more sensitive in detecting ACCs and pancreatic metaplasia than antibodies directed against other pancreatic enzymes like trypsin, amylase, lipase, and CEH.
Conclusions: We suggest using BCL10 antibody for diagnosing pancreatic ACCs and whenever an acinar differentiation is suspected in gastrointestinal neoplastic and metaplastic lesions. In addition, the opportunity to use BCL10 as a marker of both ACCs and MALT lymphomas has the advantage that a single antibody can be employed for diagnosing two different neoplasms.

1418 HFE Gene Mutations in AAT Deficiency and HCV Cirrhosis

M Lam, M Torbenson, M Yeh, P Vivekanandan, L Ferrell. UCSF, San Francisco, CA; Johns Hopkins, Baltimore, MD; Univ of Washington, Seattle, CA.
Background: HFE gene mutations for C282Y and H63D are seen in 11.6% and 27.4% of US Caucasians, respectively. Studies have suggested an increased risk for advanced fibrosis in chronic hepatitis C (HCV) patients with these mutations. Cirrhotic patients without HFE defects may also have iron overload, causing cardiac failure on rare occasion post liver transplant. To further examine the association between HFE mutations and iron overload in cirrhosis, we examined endstage HCV and alpha-1 antitrypsin deficiency (AAT), the latter noted for its variable clinical phenotype, to determine if HFE mutations may be enriched or enhance iron overload.
Design: Charts were reviewed for 45 AAT and 33 HCV cirrhotic explants for evidence of iron overload; iron was graded by iron stain, scale 0-4; AAT was confirmed by PASD or immunostain. Analysis for C282Y, H63D, and other rare HFE mutations was performed by PCR and sequencing. Statistical analysis of iron grade between groups was performed.
Results: Analysis showed a similar frequency of mutations in HCV cirrhotics compared to expected for the general population, with total frequencies of C282Y=15% and H63D=27% (C282Y/wt=4; C282Y/H63D=1; H63D/H63D=2; H63D/wt=6). Total frequencies for AAT were C282Y=2% and H63D=42% (C282Y/wt=1; H63D/H63D=2; H63D/wt=17). The frequency of H63D mutations in AAT vs expected was higher (42% vs 27%) but not statistically significant, p=0.119. Iron stains on 44 AAT showed: 0+(N=8), 1+(N=18), 2+(N=5), 3+(N=11), 4+(N=2); on 33 HCV showed: 0+(N=0), 1+(N=9), 2+(N=16), 3+(N=8), 4+(N=0); no statistical difference noted. Other rare mutations identified include one S65C mutation in HCV and one novel A271S mutation in AAT; this patient had 4+ iron in the liver explant and later developed heart failure with cardiac iron. No other patients developed heart failure, regardless of degree of iron in the liver explant or HFE mutation status.
Conclusions: We were unable to confirm a greater than expected frequency of HFE mutations in HCV or AAT cirrhotics. Although H63D mutations are high (42%) in patients with AAT, this was not statistically significant, and its role in AAT cirrhosis is unclear. A novel A271S HFE mutation was found in one AAT case with heart failure and cardiac iron deposits; this suggests that HFE testing for the C282Y and H63D mutations in AAT and HCV patients without clinical signs of iron overload pretransplant is not predictive of significant iron overload and risk for cardiac failure following transplant.

1419 IgG and IgM Immunostaining of Inflammatory Cells, Histopathology and Serology in 63 Cases of Overlap Syndrome, Autoimmune Hepatitis and Primary Biliary Cirrhosis, with Special Attention to Overlap Syndrome

H Lee, CK Ma, AH Ormsby, VV Shah. Henry Ford Hospital, Detroit, MI.
Background: Autoimmune hepatitis (AIH) - Primary biliary cirrhosis (PBC) Overlap syndrome (OS) is a vaguely defined entity that demonstrates clinical, serological, and histological features of both AIH and PBC, of which the criteria for diagnosis are not standardized. As an extension of a recently published abstract (1), we investigated and compared the IgG and IgM staining pattern in established cases of OS, AIH and PBC focusing on the cases of OS. Serologic data were reviewed.
Design: AIH (26), PBC (26) and OS (11) cases including needle biopsies and hepatectomies were retrieved from the files at Henry Ford Hospital (1998-2008). Representative sections including recuts and tissue microarrays from formalin fixed, paraffin embedded tissue blocks were stained for IgG and IgM. The percentage of IgG or IgM positive inflammatory cells including plasma cells and plasmacytoid lymphocytes was approximated. The degree of inflammation and fibrosis was evaluated using Ishak's scoring system.
Results: IgG positive cells outnumbered IgM positive cells in 6 of 11 OS cases, 4 OS cases showed more IgM positivity, and 1 was equivocal. Anti-mitochondrial antibody (AMA) and anti-nuclear antibody (ANA) and/or anti-smooth muscle antibody (ASMA) were both positive in 2/11 OS, and both negative in 2/11.

	Result					
	IgG>IgM	IgM≥IgG	HAI	Fibrosis	AMA positivity	ANA±ASMA positivity
OS(n=11)	6/11	5/11	6(2-10)	3	3/11	7/11
AIH(n=26)	26/26	0/26	4(1-7)	3	2/26	21/26
PBC(n=26)	12/26	14/26	8(2-12)	3	20/26	8/26

Conclusions: AIH-PBC overlap syndrome does not demonstrate either IgG or IgM predominance ($p > 0.2$ by Fisher's exact test,) regardless of the degree of inflammation or fibrosis ($p > 0.5$ by unpaired t-test). HAI of OS is in between that of AIH and PBC. Our findings in the AIH and PBC group validate the findings of the reference study

with IgG versus IgM predominance being significantly different in these two groups ($p < 0.001$). OS appears to be a heterogeneous group with no predictable IgG or IgM predominance in the periportal inflammatory infiltrate. 1. JA Daniels, MS Torbenson, RA Anders, JK Boitnott. IgM and IgG immunostaining differentiates primary biliary cirrhosis from autoimmune hepatitis. Mod Pathol. 2008:21;303A

1420 Prognostic Implications of and Relationship between CpG Island Hypermethylation and Repetitive DNA Hypomethylation in Hepatocellular Carcinoma

HS Lee, BH Kim, NY Cho, SH Shin, JJ Jang, KS Suh, GH Kang. Seoul National University College of Medicine, Seoul, Republic of Korea; Cancer Research Institute, Seoul National University College of Medicine, Seoul, Republic of Korea.

Background: This study aims to determine the relationship between CpG island DNA hypermethylation and global genomic DNA hypomethylation and their prognostic implications in hepatocellular carcinoma (HCC). The association of DNA methylation changes with clinicopathologic factors and the chronological ordering of DNA methylation changes along multistep hepatocarcinogenesis were also assessed.

Design: HCC (n=20) and non-neoplastic liver samples (n=72) were analyzed for their methylation status at 41 CpG island loci and three repetitive DNA elements (*LINE-1*, *ALU*, and *SAT2*) using MethyLight or combined bisulfite restriction analysis. After selection of 19 CpG island loci showing cancer-specific DNA methylation, another set of 99 HCC samples were analyzed for these loci.

Results: The number of methylated genes in HCC was significantly higher in HCC patients with a cirrhotic liver than in HCC patients with a non-cirrhotic liver (8.8 vs. 6.1, P<0.001). HCC from female patients showed a higher number of methylated genes than HCC from male patients (9.9 vs. 7.2, P=0.004). The genes *CRABP1* and *SYK* showed significant association between CpG island hypermethylation and patients' poor survival. *SAT2* hypomethylation occurred earlier than *LINE-1* or *ALU* hypomethylation along the multistep hepatocarcinogenesis. Depending on the type of CpG island locus, a direct, inverse, or no relationship between CpG island hypermethylation and repetitive DNA hypomethylation was observed in HCCs.

Conclusions: The varying relationships between hypermethylation of individual CpG island loci and hypomethylation of repetitive elements suggests that they are not mechanically linked. *SYK* and *CRABP1* hypermethylation may serve as useful tumor markers for prognostication of HCC patients.

1421 Hepatocellular Carcinoma with Progenitor Cell Features: High Expression of Invasion and Epithelial Mesenchymal Transition-Associated Genes

J-E Lee, B-K Oh, J Choi, S-M Yoon, T-H Um, YN Park. Yonsei University College of Medicine, Seoul, Republic of Korea.

Background: Recently, it has been reported that hepatocellular carcinomas (HCCs) with progenitor cell features have more aggressive biological behavior in both *in vivo* and *in vitro* studies.

Design: We investigated expression levels of the following genes in 44 HCCs by real-time reverse transcriptase (RT)-polymerase chain reaction (PCR) or immunohistochemistry: Progenitor cell markers of cytokeratin (CK) CK19 and CD133; multidrug resistance (MDR) genes of MDR1 and MDR-associated protein (MRP) MRP1; invasion-associated genes of urokinase plasminogen activator receptor (uPAR), villin 2 (VIL2), and matrix metalloproteinase (MMP) MMP1 and MMP2; and epithelial-mesenchymal transition (EMT) regulators of Snail1 (Snail), Snail2 (Slug), Twist, and E- and N-cadherin. Correlations between expression levels of these genes and clinicopathological parameters were determined.

Results: HCCs with progenitor cell features, which showed high expression of CK19 or CD133 mRNA, revealed significantly more frequent vascular invasion compared to those without. HCCs with progenitor cell features had high mRNA levels of MRP1, uPAR, MMP1, MMP2, Snail, and Twist. Upregulation of Snail, Slug, and Twist were associated with increasing MRP1, uPAR, VIL2, and MMP2.

Conclusions: Our results suggest that HCCs with progenitor cell features have a potential for a more invasive phenotype with upregulation of invasion- and EMT- associated genes. Furthermore, elevated MRP1 expression might induce drug resistance in HCCs with progenitor cell features.

1422 Perinodular K19 Patterns Are Generic to Advanced Chronic Liver Disease, a Study of 176 Hepatocellular Nodules (HCN) in Explanted Livers

JKM Lennerz, N Vachharajani, WC Chapman, EM Brunt. Washington University St. Louis, St. Louis.

Background: In fibrotic chronic HCV and NASH, the epithelial-stromal compartment (ESC) hosts ductular reaction (DR), inflammation and fibrosis. Highlighted by type 2 keratin 7, DR is a reported diagnostic aid: indicative of perinodular stromal invasion by hepatocellular carcinoma (HCC) when absent. Proposed stem cell niches in the ESC include epithelial cells that express type 1 keratin 19 (K19). Study of the perinodular ESC of HCN is limited.

Design: Thirty-five coded slides from 32 patients with HCC in cirrhotic explants for HCV, Alcohol, HBV, cryptogenic, NASH, autoimmune, primary sclerosing cholangitis and Alagille's syndrome were used to mark 176 distinct HCN by H&E (EMB) as: cirrhotic nodule (CN), dysplastic nodule (DN), or HCC. Independent blinded review (JKL) noted 3 perinodular patterns of K19: (A) absent; (B) fragmented and thin cores of ovoid cells but not tubular formations; (C) circumferential, complex ductular structures, often multilayered. This study used virtual microscopy and statistical testing included intraclass-correlation-coefficient ICC and chi-square.

Results: By H&E, HCN were 54 HCC, 45 DN and 71 CN; the K19 IHC patterns were 62A, 41B and 67C (Fig. 1). The remaining 6 were 5 "nodule-in-nodule" (NIN) and 1 CN with mixed features of DN; K19 patterns were A(5 NIN) and C(1) respectively. As anticipated, K19 pattern of some DNs overlapped; with CN (24%), and HCC (26%). The ICC for H&E vs. K19 was 0.878 (p<0.02) overall; the distinction of non-HCC vs. HCC was also 'almost perfect' and the negative predicitve value of pattern A was 94%.

Conclusions: The study indicates very robust correlation of K19 patterns in the perinodular ESC with various HCN, regardless of liver disease: concentric tubular structures in ESC of CN, fragmented, attenuated cords <5 cells of DN, and absent in perinodular ESC of HCC. Thus the compelling relationship of intra- and extranodular pathology suggests the ESC as important in progression of CN and DN to HCC, and opens new approaches in the understanding of HCN pathogenesis.

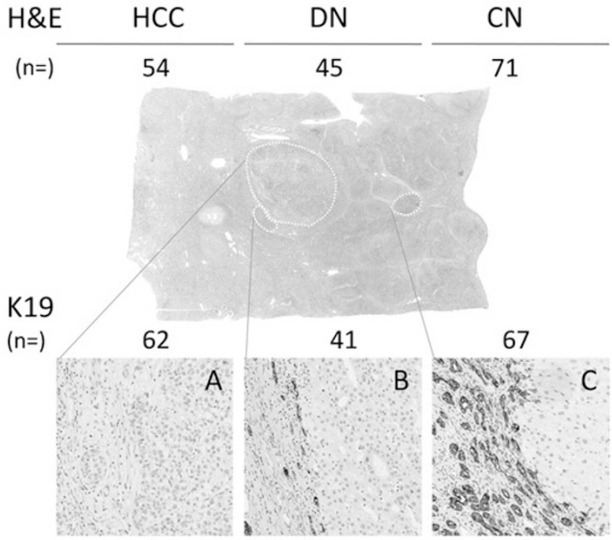

1423 Expression of Glypican-3 in Embryonal Sarcoma (ES) and Mesenchymal Hamartoma (MH) of the Liver: A Potential Diagnostic Pitfall

M Levy, D Dhall, J Zhang, L Miles, J Misdraji, LM Yerian, H Xu, CE Aguilar, HL Wang. Cedars-Sinai Medical Center, Los Angeles; Mayo Clinic, Rochester; Cincinnati Children's Hospital, Cincinnati; MGH/Harvard Medical School, Boston; Cleveland Clinic, Cleveland; University of Rochester Medical Center, Rochester.

Background: Glypican-3 (GPC3) is an oncofetal protein that has recently been demonstrated to be a useful diagnostic immunomarker for hepatocellular carcinoma and hepatoblastoma. Its expression in mesenchymal tumors of the liver, particularly ES and MH, has not been investigated.

Design: A total of 16 ESs and 12 MHs were retrieved from authors' institutions and stained for GPC3 using antibody 1G12. A case was considered negative if <1% of the cells of interest exhibited immunoreactivity. Positive staining was graded as weak, intermediate or strong, and as focal if 1-50% of the cells stained or diffuse if >50% of the cells stained.

Results: The ages of patients with ES ranged from 6-87 years (mean: 37.2 years; median: 23.5 years). Nine were male and 7 were female. The tumor sizes ranged from 2.4-20 cm (mean: 10.5 cm). The ages of patients with MH ranged from 0.2-72 years (mean: 12.8 years; median: 1.3 years). Six were male and 6 were female. The tumor sizes ranged from 2.4-34 cm (mean: 10.8 cm). Intermediate to strong cytoplasmic staining for GPC3 was observed in 8 (50%) ESs, of which 2 cases exhibited diffuse immunoreactivity and the remaining 6 showed focal positivity. The patients with GPC3-postive ESs tended to be younger (mean age: 29.9 years) than those with negative tumors (mean age: 44.5 years), although the difference was not statistically significant (P=0.17). Five MHs also exhibited GPC3 immunoreactivity (41.7%; 3 focal, 2 diffuse). However, positive staining was primarily seen in entrapped hepatocytes with a cytoplasmic/canalicular staining pattern; in only 2 cases was weak and focal immunoreactivity also observed in mesenchymal component. Interestingly, all the patients with positive staining were younger than 1.5 years old.

Conclusions: GPC3 is expressed in a subset of ESs and MHs of the liver. Caution should be exercised when evaluating a GPC3-expressing hepatic neoplasm, particularly in a needle biopsy, when the differential diagnosis includes poorly differentiated hepatocellular carcinoma and hepatoblastoma. The observed GPC3 staining patterns may be also helpful in the rare instance of ES arising in MH since the former appears to be more likely positive for GPC3.

1424 S100P, von Hippel-Lindau Gene Product (pVHL) and IMP3 Serve as a Useful Immunohistochemical Panel in Helping Diagnose Adenocarcinoma on Endoscopic Bile Duct Biopsy

M Levy, F Lin, H Xu, D Dhall, BO Spaulding, HL Wang. Cedars-Sinai Medical Center, Los Angeles, CA; Geisinger Medical Center, Danville, PA; University of Rochester Medical Center, Rochester, NY; Dako North America, Carpinteria, CA.

Background: Histologic distinction between benign and malignant bile duct epithelial lesions on endoscopic biopsies can be extremely challenging because of limited material, crush artifact, and compounding inflammatory and/or reactive changes. The aim of this study was to evaluate the diagnostic value of S100P, pVHL and IMP3 (KOC) on bile

duct biopsies because they all have been shown to be sensitive and specific markers for pancreatic ductal carcinoma.
Design: A total of 72 bile duct biopsies were immunostained for S100P, pVHL and IMP3. These included 40 adenocarcinomas and 32 benign biopsies, with histologic diagnoses confirmed by subsequent Whipple resections or follow-up biopsies in the majority of the cases. The stains were considered positive if ≥1% of the cells of interest exhibited immunoreactivity. Positive stains were graded as weak, intermediate or strong, and as focal if 1-50% of the cells stained or diffuse if >50% of the cells stained.
Results: Thirty-six (90%) adenocarcinomas exhibited strong nuclear and cytoplasmic staining for S100P, of which 30 (83.3%) showed diffuse immunoreactivity. Intermediate to strong cytoplasmic staining for IMP3 was observed in 30 (75%) tumors (15 diffuse, 15 focal). Completely negative staining for pVHL was observed in 35 (87.5%) tumors. In 5 tumors, focal or diffuse membranous and cytoplasmic pVHL immunoreactivity was observed. Twenty-seven (67.5%) tumors showed a S100+/IMP+/pVHL- staining pattern, 7 (17.5%) with a S100P+/IMP-/pVHL- pattern, and 1 (2.5%) with a S100P-/IMP3+/pVHL- pattern. All 32 nonneoplastic biopsies were completely negative for IMP3, and all were positive for pVHL with a diffuse staining pattern in 30 (93.8%) cases. Eight (25%) nonneoplastic biopsies showed focal S100P positivity.
Conclusions: An immunohistochemical panel consisting of S100P, pVHL and IMP3 can be very helpful in distinguishing reactive epithelial changes from adenocarcinoma on challenging bile duct biopsies. S100P has the highest sensitivity (90%) and IMP3 has the highest specificity (100%) in detecting adenocarcinoma. The findings of focal S100P expression with reciprocal loss of pVHL immunoreactivity in a few nonneoplastic biopsies suggest a utility of these markers in the detection of epithelial dysplasia that may be beyond histologic recognition.

1425 Mesothelin and B72.3: Can Their Expression Patterns Help Distinguish Neoplastic Cysts of the Pancreas?

S Li, D Jhala, N Jhala. University of Alabama at Birmingham, Birmingham, AL.
Background: Mesothelin is a GPI-anchored cell surface protein. Previously, it has been established that it is expressed in pancreatic adenocarcinoma but not in reactive ductal epithelial cells. B72.3 is an oncofetal antigen and a known tumor associated glycoprotein which is expressed in the majority of human adenocarcinomas including colorectal, pancreatic, gastric, ovarian, endometrial, mammary, and non-small cell lung cancer. Previous studies demonstrated that it is immunoreactive in pancreatic adenocarcinoma but negative in normal pancreatic ductal cells. Little is known about mesothelin and B72.3 expression in cystic pancreatic neoplasm. Present study was undertaken to determine if mesothelin and B72.3 are differentially expressed in various cystic neoplasms of the pancreas.
Design: The study group included 52 surgically resected cases incorporating pancreatic adenocarcinoma (ACA, n= 35), intraductal papillary mucinous neoplasm (IPMN, n = 9), mucinous cyst adenoma (MCA, n= 5), and serous cyst adenoma (SCA, n = 3). Adjacent non neoplastic ducts served as control groups. Pancreatic endocrine neoplasms, pseudo cysts and solid pseudo papillary neoplasms being non epithelial tumors were not included in the study population. Percent positivity and intensity of mesothelin and B72.3 expression were determined by immunohistochemistry method using formalin-fixed, paraffin-embedded full tissue sections. A Fisher's exact test was performed to determine the difference in expression patterns.
Results: Mesothelin expression was noted in 32 of 35 cases of ACA (91%), 6 of 9 cases of IPMN (67%), 1 of 5 cases of MCA (20%), and 0 of 3 cases of SCA (0%). Mesothelin expression was diffuse and more intense in ACA, weak in IPMN, and rare weak positive expression in MCA. All 2 cases of cystic ACA were strongly positive for mesothelin. The difference was statistically significant (p = 0.0023). Benign pancreatic tissue was present in 16 cases of ACA which were all negative for mesothelin. B72.3 expression was diffuse and intense in all cases of ACA (including 2 cases with cysts) and IPMN. In contrast, it was focal and weak in MCA and SCA. B72.3 expression was statistically significantly (P = 0.03) different between IPMN and other non malignant epithelial cysts (MCA and SCA).
Conclusions: Our results suggest that both mesothelin and B72.3 may serve as powerful markers to distinguish neoplastic epithelial cysts in equivocal cases. This result can have major impact in distinguishing various neoplastic epithelial cysts on cytology specimens.

1426 High Levels of Expression of Human Stromal Cell-Derived Factor-1 (SDF-1) Are Associated with Worse Prognosis in Patients with Pancreatic Ductal Adenocarcinoma

J Liang, S Zhu, R Bruggeman, D Evans, R Zaino, D Zander, H Wang. Penn State Hershey Medical Center, Hershey, PA; U.T. M.D Anderson Cancer Center, Houston, TX.
Background: Recently, stromal cell-derived factor-1 (SDF-1, CXCL12), together with its specific receptor, CXCR4, have been shown to mediate invasiveness and metastatic behavior in a number of cancers, including ovarian, prostate, bladder, breast and pancreatic cancers. The expression and significance of SDF-1 in human pancreatic ductal adenocarcinoma (PDA) have not been studied in detail.
Design: We prepared a tissue microarray consisting of 1.0-mm cores of tumor (two cores per tumor) and paired non-neoplastic pancreatic tissues from 72 pancreaticoduodenectomy specimens of PDA. Cytoplasmic expression of SDF-1 was evaluated by immunohistochemistry with mouse anti-human SDF-1/CXCL12 antibody (dilution 1:6000). The staining results were categorized as SDF-1-high (H) (strong cytoplasmic staining of 10% of tumor cells) or SDF-1-low (L) (no staining or weak staining of <10% of tumor cells). Statistical analyses were performed using SPSS software and survival was evaluated by Kaplan-Meier log-rank test.
Results: 25/72 (35%) PDAs demonstrated high levels of SDF-1 expression . The median overall and disease-free survival rates for patients with SDF-1-H PDAs were 26.1 and 11.1 months, respectively, compared to 44.3 and 22.3 months for patients with SDF-1-L tumors (log-rank test, p=0.047 and p=0.021). High SDF-1 expression was associated with poor overall and disease-free survival in univariate analysis (p=0.051 and p=0.024). In multivariate analysis, high SDF-1 expression was significantly correlated with poor overall and disease-free survival (p=0.019 and p=0.02) independent of age, gender, tumor size and differentiation.
Conclusions: High levels of SDF-1 expression are associated with poor overall and disease-free survivals in patients with PDA. SDF-1 may serve as a useful independent prognostic marker for PDA.

1427 Quantification of Mouse Genome in Xenografts of Human Pancreatic Cancers by Species-Specific Length Polymorphisms

MT Lin, LH Tseng, H Kamiyama, M Kamiyama, P Lim, JR Eshleman. Johns Hopkins University School of Medicine, Johns Hopkins Hospital, Baltimore, MD; National Taiwan University Hospital, Taipei, Taiwan.
Background: Establishing cancer cell lines from primary tissues is essential for many research areas of cancer biology. Isolation of human cancer cell lines, from pancreatic cancers and other solid tumors, is surprisingly difficult, primarily due to overgrowth of fibroblasts and other mesenchymal stromal cells during the early stages of *in vitro* culture. Cancers can be maintained by serial xenografting in athymic mice or severe combined immunodeficient (SCID) mice.
Design: We have developed a molecular detection assay to monitor the human/mouse genomic "chimerism" from DNA samples extracted directly from xenografts and from human pancreatic cell lines established *in vitro* after explanting the tumors. The assay was designed based on deletion/insertion variation between human and mouse genomes, a strategy similar to the use of amelogenin gene polymorphism to determine human female/male chimerism. The percentage of mouse DNA was calculated according to the relative peak height of PCR products analyzed by capillary electrophoresis.
Results: Three markers from chromosomes 9 and 10 showed accurate prediction of mouse genome ratio and were successfully combined into a multiplex PCR reaction. The assay was used to quantify 24 mouse xenografts of human pancreatic cancers. The results of chimerism analysis were also used to select flasks with highest percentage of human cells for subsequent passage of cultures and to confirm the purity of pancreatic cancer cell lines for subsequent biomedical studies.
Conclusions: In the current study, we have developed a PCR assay for rapid and robust quantification of mouse genome in xenografts of human pancreatic cancers. The results facilitate DNA sequencing of human pancreatic cancers and in vitro establishment of human pancreatic cancer cell lines.

1428 "Two Toned Hepatocytes": A Striking Histologic Change Likely Due to a Drug Effect

Q Liu, KE Tanaka, KM Whitney, J Hart. Montefiore Hospital, New York; University of Chicago, Chicago.
Background: Unusual and unexpected histological features can result in a time consuming & expensive work-up. We report 4 patients with a striking light microscopic change evident in liver biopsies that ultimately appeared to represent a drug effect. A review of major textbooks of hepatic pathology and a MEDLINE search revealed no prior mention of this peculiar histologic finding.
Design: Over 11 years we received 4 liver biopsies that exhibited a unique appearance in routine H&E stains. The cases were seen in consultation to exclude unspecified metabolic storage disease. The hepatocyte cytoplasm appeared condensed & finely granular toward the bile canalicular surface, while the other half of the cytoplasm was clear and finely vacuolated. This change, which imparted a striking "two-toned" appearance, was evident diffusely in each lobule. Mild hepatocellular & canalicular cholestasis was present in each case, but there was no steatosis, fibrosis, or necrosis. In PAS stains the condensed granular cytoplasm stained strongly, while the clear finely vacuolated cytoplasm was negative, further heightening the "two-toned" appearance. HBV immunostains were negative in all cases. Rebiopsy for EM in one case revealed hepatocytes with markedly dilated endoplasmic reticulum & moderate numbers of mitochondria.
Results: The biopsies were obtained to evaluate jaundice & increased LFTs. The 1st patient, a 51 y.o. M, was taking 20 Ibuprofen/day and significant alcohol for broken ribs. LFTs included: TB = 3.6, AST=140, ALT=120, Alk P=600. The 2nd patient, a 5 m.o. F with biliary atresia, s/p Kasai, was receiving antibiotics & acetaminophen for ascending cholangitis. LFTs included: TB=2.2, AST=159, ALT=114, Alk P=553. The 3rd patient, a 44 y.o. F with AIDS and necrotizing pancreatitis, received >30 medications in the 4 mos. before biopsy, including antibiotics & anti-convulsants. LFTs included: TB=0.5, AST= 136, ALT=125, Alk P=1796. The 4th patient, a 74 y.o. M, was on multiple anti-fungal agents & antibiotics. LFTs included: TB = 0.4, AST = 35, ALT = 53, Alk Phos = 2271. All patients had negative HAV, HBV and HCV serologies. In all patients LFTs normalized after discontinuation of medications, with no further liver dysfunction with up to 11 year follow-up.
Conclusions: Unusual histological changes can provoke expensive work-up (e.g., immunostains, EM, external consultation) & additional medical procedures. The histologic feature reported here most likely represents a hepatotoxic effect due to an interaction between multiple drugs.

1429 Foxp3 and IgG4 Expression in Subtypes of Autoimmune Pancreatitis

RV Mandal, K Notohara, V Deshpande, AB Farris, M Lisovsky, TC Smyrk, GY Lauwers, M Mino-Kenudson. Massachusetts General Hospital, Boston, MA; Kurashiki Central Hospital, Kurashiki, Japan; Mayo Clinic, Rochester, MN.
Background: "Autoimmune pancreatitis" (AIP) is probably a heterogenous category, including lymphoplasmacytic sclerosing pancreatitis (LPSP) and idiopathic ductocentric chronic pancreatitis (IDCP). LPSP appears to represent the pancreatic manifestation of systemic IgG4-related fibrosclerosing disease; however, the nature of IDCP has not been well studied. Forkhead box P3 (Foxp3) is a specific transcription factor expressed

by CD4+CD25+ regulatory T cells (Tregs). Large numbers of Foxp3+ Tregs have been found in organs involved by systemic IgG4-related fibrosclerosing disease and it is hypothesized that Tregs might be involved in IgG4 class switching and fibroplasia. The aim of this study was to evaluate and compare Foxp3 and IgG4 expression between LPSP and IDCP.

Design: Surgically resected LPSP (n=22) and IDCP (n=13) cases were evaluated for several pathologic features characteristic of AIP including: the extent of inflammation, inflammatory pseudotumor-like changes, and obliterative phlebitis. Foxp3, IgG4, and IgG1 immunostains were performed and an average number of Foxp3+ Tregs/HPF and an IgG4+ plasma cell/IgG1+ plasma cell ratio (IgG4/IgG1) were compared between the LPSP and IDCP cases and were correlated with the histologic parameters.

Results: Large numbers of Foxp3+ Tregs were found in both LPSP and IDCP cases (mean: 49.6/HPF vs. 37.3/HPF, respectively, p=0.12). The mean IgG4/IgG1 was higher in the LPSP group than in the IDCP group (1.23 vs. 0.31, respectively, $p < 0.001$). The numbers of Tregs correlated with IgG4/IgG1 in the LPSP group (p=0.025), but no such correlation was observed in the IDCP or entire cohort. There was no significant difference in any of histologic parameters between cases with $\geq$ 40 Tregs/HPF and those with < 40 Tregs/HPF in the LPSP, IDCP or entire cohort. Conversely, a higher IgG4/IgG1 ($\geq$ 0.50) was associated with dense lymphoplasmacytic infiltration in lobules (p=0.023), extensive obliterative phlebitis (p=0.004), and a larger caliber of obliterated veins ($p < 0.001$) in the entire cohort.

Conclusions: The increase in Tregs is associated with a high IgG4/IgG1 ratio in LPSP, but not in IDCP. The results support the hypothesis that Tregs might be involved in IgG4 class switching in LPSP that is, in turn, associated with characteristic histologic features. The large number of Tregs seen in IDCP may simply represent immune reactions to various stimuli such as infection.

1430 Temporal Evolution of Amoxicillin-Clavulanate Induced Liver Injury

H Mani, R Saxena, JH Hoofnagle, DE Kleiner. NCI, NIH, Bethesda; Indiana University, Indianapolis; NIDDK, NIH, Bethesda; For the Drug Induced Liver Injury Network (DILIN).

Background: Although the widely used combination of amoxicillin-clavulanate is a well known cause of idiosyncratic hepatotoxicity, the temporal course of its associated liver disease is not adequately documented.

Design: Cases of amoxicillin-clavulanate-induced liver injury with liver biopsies available for review were identified in the data set of DILIN, a prospective study and database on drug-induced liver disease. Liver biopsies were independently reviewed in a blinded manner and injury patterns classified as one of 4 patterns: acute hepatitis, acute cholestasis, chronic cholestasis, or mixed hepatocellular-cholestatic. R ratio (ALT to alkaline phosphatase) was used to classify biochemical profiles, using standard criteria. Pathology injury patterns were compared to temporal biochemical profiles, based on the date the implicated drug was begun.

Results: Among 122 DILIN cases with available causality review and biopsies, 9 were attributed to amoxicillin-clavulanate, making it the second most common drug associated with DILI. Patients were 42-87 (mean 61) years old; 7 were males. Patients presented with cholestatic (2 cases), mixed (5 cases) or hepatocellular (2 cases) biochemical profiles, 10 to 36 (mean 25) days after starting therapy. 7 cases were considered definite DILI, 1 very likely and 1 probable DILI; 1 biopsy was inadequate. Of the 8 cases with biopsies, 6 had similar temporal biochemical profiles, with R rising to a mixed or hepatocellular profile before declining to the cholestatic range. In these patients, the 2 earliest biopsies showed acute cholestasis with little inflammation, and the 4 biopsies at later time points showed mixed hepatocellular-cholestatic pattern, irrespective of R at biopsy. One patient biopsied during a sharp rise in R value showed acute hepatitis without cholestasis and the last with a persistent cholestatic biochemical profile showed chronic cholestasis with bile duct paucity.

Conclusions: Amoxicillin-clavulanate-induced liver injury progresses temporally from a hepatocellular or mixed to a cholestatic biochemical profile in most cases. Biopsy reveals acute cholestasis in the early phase progressing later to a mixed hepatocellular-cholestatic injury pattern. Pathologic patterns in the two variant cases corresponded with their biochemical profiles. These findings suggest that, in amoxicillin-clavulanate induced liver injury, biopsy pathology reflects temporal biochemical injury profiles as a whole.

1431 Histopathology of *De Novo* Autoimmune Hepatitis in Children

A Manuyakorn, RS Venick, SV McDiarmid, CR Lassman. Siriraj Hospital, Bangkok, Thailand; UCLA, Los Angeles.

Background: *De novo* autoimmune hepatitis (d-AIH) is a well-recognized complication of pediatric liver transplantation (LTx). The diagnosis is often based on elevated liver function tests (LFTs) and the presence of autoantibodies (a-Abs). The histology of d-AIH was first described in 1998. We present detailed histologic data from the largest series to date of biopsies in pediatric liver transplant patients with d-AIH.

Design: Between 1984 and 2008, 685 patients <18 y/o underwent 883 liver transplants (LTx). 70 recipients (10.2%) were identified as having developed d-AIH based on clinical parameters and biopsy. Liver biopsies obtained at or near the time of diagnosis were retrieved. Pathologic evaluation included scoring of interface, lobular and perivenular necroinflammatory activity, plasma cells density in each location, rejection activity index, apoptotic bodies, and fibrosis.

Results: Biopsies were available for re-review in 53 of 70 patients. Indication for LTx was biliary atresia (51%), fulminant hepatic failure (24%) and metabolic liver disease (15%). The mean time from LTx to development of d-AIH was 6.7 years. The majority of patients had strongly positive a-Ab titers and 43% had multiple positive a-Abs (ANA, dsDNA, SMA). 85% of patients had resolution of LFT abnormalities following treatment. In 38 biopsies (72%) the predominant pattern of injury was hepatitis. Pure lobular hepatitis was present in 7 (18%), pure interface hepatitis in 2 (5%), and pure perivenular hepatitis in only 1 (3%). Mixed interface/lobular hepatis was present in 8 (21%), mixed lobular/perivenular in 4 (11%), mixed interface/perivenular in 2 (5%) and mixed interface/lobular/perivenular in 14 (36%). Severe necroinflammatory activity was present in 7 (18%). In 7 biopsies (13%) convincing features of acute rejection in addition to hepatitis were present. In 2 (4%) there was ductopenia and in 5 (9%) there was minimal non-specific infiltrate. While perivenulitis was seen in 21 (40%), central vein endotheliitis was seen in only 3 (6%). Dense plasma cell infiltrates were seen in 30% of biopsies. 54% of patients had stage 2/4 or 3/4 fibrosis at presentation.

Conclusions: The dominant histologic pattern in biopsies of patients with a diagnosis of d-AIH is lobular hepatitis with or without interface and perivenular hepatitis. Plasma cell infiltrates were observed in all zones. Rejection histology was seen in only 13 % of cases. More than half of the patients had at least stage 2 fibrosis at presentation.

1432 The Role of Hepatic Steatosis in Acetaminophen Hepatotoxicity

A Manuyakorn, N Logan, D Gjertson, JC Hong, S French. Siriraj Hospital, Bangkok, Thailand; UCLA, Los Angeles.

Background: Acetaminophen, is the leading cause of drug induced acute liver failure in the United States. There are some potential factors such as heavy alcohol use, antitubercular agents, antiepileptic medications, and malnutrition that may render the liver more susceptible to injury from acetaminophen. Nonalcoholic fatty liver disease (NAFLD) has been associated with elevated liver tests, fibrosis and cirrhosis. The histologic similarity between fatty liver due to metabolic syndrome and heavy alcohol use raises the possibility that patients with NAFLD may be more susceptible to acetaminophen toxicity. We sought to determine if there was an association between steatosis and extent of liver injury at the time of transplantation.

Design: Patients who underwent liver transplantation for liver failure secondary to acetaminophen toxicity between 1992 and 2008 were identified from the UCLA pathology database. Pathologic evaluation included extent of hepatocellular necrosis and extent of steatosis. The clinical records of the patients were reviewed for: body mass index, liver function tests (LFTs), acetaminophen levels, hepatotrophic viral serologies, history of diabetes, hypertension and heavy alcohol use. The hepatocellular necrosis and steatosis were compared by Fisher's exact test.

Results: 37 patients (27 female) with mean age of 34 years (range 17-57) were identified and grouped by extent of necrosis. The majority (81%) had submassive hepatic necrosis (necrosis beyond zone 3) whereas seven patients had necrosis limited to zone 3. There was no correlation between extent of steatosis and extent of necrosis (p value=0.65). 86% of the group with submassive necrosis and 70% with zone 3 necrosis had moderate to severe steatosis (>33%). There was no obvious difference in LFTs, acetaminophen level and the other clinical parameters listed in the designs.

Conclusions: Here we demonstrate that the majority of patients suffering from acetaminophen induced acute liver failure show moderate to severe steatosis at the time of transplantation. There is no correlation between extent of steatosis and extent of hepatic necrosis. Clinical parameters that would indicate metabolic syndrome also appear to be unrelated to the extent of necrosis. This study suggests that patient's with metabolic syndrome may not have increased sensitivity to acetaminophen toxicity as is seen with heavy alcohol use. Further studies with a larger number of patients may provide statistical significance to this observation.

1433 Neoadjuvant Chemotherapy Followed by Two-Step Hepatectomy for Bilateral Hepatic Colorectal Liver Metastases. Clinical and Histological Outcomes with a Focus on the "Dangerous Halo"

G Mentha, S Terraz, P Morel, A Andres, E Giostra, A Roth, L Rubbia-Brandt, P Majno. University Hospitals of Geneva, Geneva, Switzerland.

Background: Bilobar hepatic colorectal metastases (HCRM) require a multidisciplinary approach. Our study describes the clinical and histological outcomes of patients undergoing neo-adjuvant chemotherapy and two-step hepatectomy for bilateral HCRM.

Design: A series of 23 patients was reviewed. HCRM were studied using the standardised Tumour Response Grade (TRG) classification**.** In addition, we defined a *dangerous halo* the clustering of cancer cells infiltrating the liver tissue for several millimetres at the periphery of a metastasis, regardless of any signs of response in HCRM and quantified as *absent*, *focal* (less than 50% of circumference the metastasis) and *diffuse* (more than 50% of the circumference of the metastasis). Sinusoidal obstruction syndrome (SOS) and NRH in the non-tumoral liver, frequently associated with oxaliplatin, were graded.

Results: There was no mortality or grade III morbidity. Median survival was 45 months, and 1-5 years Kaplan Meier estimates were 95%, 90%, 73%, 48% and 27%. On histology at the first operation there was a *dangerous halo* in 46% of the patients, of variable importance, regardless of the response to chemotherapy of HCRM. The dangerous halo increased in prevalence (59%) and importance between the first and the second operation. SOS or NRH appeared at least as severe at the second procedure, and not affected by the longer interval from the last cycle of chemotherapy.

Conclusions: Neoadjuvant chemotherapy followed by two-step hepatectomy is feasible and may be advantageous to the patient. The appearance of a dangerous halo around the liver metastases requires adapting of the surgical technique to decrease the risk of local recurrence.

1434 Biomarkers as Predictors of Rapidity of Fibrosis in the Liver Allograft of Hepatitis C Patients

Z Meriden, T Pasha, R Wells, R Reddy, G Makar, EE Furth. University of Pennsylvania, Philadelphia, PA.

Background: Recurrent hepatitis C with subsequent highly variable rates of fibrosis post liver transplantation is the leading cause of allograft loss. We hypothesized that early increased collagen synthesis, bile duct proliferation, epithelial to mesynchemal transition, and other features may predict the rapidity of subsequent liver fibrosis.

Design: For 476 hepatitis C liver transplant (1999-2007) patients**,** the stage of fibrosis (METAVIR 0-4) from each post-transplant liver biopsy was recorded with respect to time post-transplantation. Rapid (52 patients) and slow (61 patients) fibrosis were defined as having at stage 3 (bridging) by 24 months, and stage 0 or 1 at 24 months or later, respectively. The stage 0 biopsy was 1. scored for hepatitis activity and number of apoptotic hepatocytes 2. immunostained and scored (0-3) for Hsp47 (a collagen chaperone protein), CK19 (expressed in bile ducts), and vimentin (a marker of epithelial to mesynchemal transition). The area under the Receiver Operator Characteristic curve (AUC), a measure of test diagnostic utility (1= perfect test, 0.5=no utility), was calculated for all immunostains with the exception of vimentin which was scored on a binary scale and analyzed by Chi Square. The number of rejection episodes was determined.
Results: By year 8, 61% of our entire transplant population had cirrhosis; 78% of rapid fibrosers (RF) had cirrhosis by year 2, while only 4% of slow fibrosers (SF) had fibrosis by year 8. Hsp47 was not different in RF vs. SF (AUC= 0.61; *P=0.13*). However, CK19 was predictive of rapid fibrosis (AUC = 0.71; *P=0.003*), as was vimentin staining (81% RF vs. 52% SF, *P=0.022*). Stage 0 biopsies of RF had more hepatocyte apoptosis than SF (mean apoptotic cells/hpf ± SD = 0.30 ± 0.37 vs. 0.08 ± 0.15; *P = 0.001*) with no difference in hepatic activity. RF had more numbers of acute rejection episodes than SF (number of patients with 1 or more acute rejection episodes = 65% vs. 18%, *P <0.0001*). The rate of fibrosis over time was constant for each group.
Conclusions: CK19 and vimentin are good markers predictive of rapidity of liver allograft fibrosis in patients transplanted for hepatitis C, implicating the bile ductular reaction and epithelial to mesynchemal transition as critical early processes. While the inflammatory hepatic activity is not predictive of the rate of fibrosis, the level of hepatocellular apoptosis is. Importantly, the rate of fibrosis is established early in the post-transplant period, as this initial rate dictates long-term outcome.

1435 Pathology of Pancreas in Inflammatory Bowel Disease: An Etiology of Idiopathic Ductocentric Chronic Pancreatitis?

M Mino-Kenudson, TC Smyrk, K Notohara. Massachusetts General Hospital, Boston, MA; Mayo Clinic, Rochester, MN; Kurashiki Central Hospital, Kurashiki, Japan.
Background: "Autoimmune pancreatitis" (AIP) is probably a heterogenous category, including (at least) lymphoplasmacytic sclerosing pancreatitis (LPSP) and idiopathic ductocentric chronic pancreatitis (IDCP). LPSP appears to represent the pancreatic manifestation of systemic IgG4-related fibrosclerosing disease; however, the nature of IDCP has not been well studied. IDCP has been reported in patients with inflammatory bowel disease (IBD). Thus, we reviewed resected pancreata of IBD patients to characterize the morphology, and to assess the possible link between IBD and IDCP.
Design: The study group consisted of 9 patients with IBD (7 ulcerative colitis [UC] and 2 Crohn's disease [CD]). Their resected pancreata were classified into IDCP, LPSP, and others. Study cases classified as IDCP were compared with IDCPs of non-IBD patients (n=21) for the following characteristic features of AIP: the extent of inflammation in interlobular and intralobular ducts, lobules and fibrosis, reactive epithelium of ducts, inflammatory pseudotumor-like changes, obliterative phlebitis, lymphoid aggregates, and an IgG4/IgG1 ratio. The demographic data were also compared between the 2 groups.
Results: In 6 of 7 UC cases, the pancreatic pathology was classified as IDCP. LPSP was seen in the remaining UC patient who had undergone ileocolectomy 7 years prior to Whipple resection. One CD patient showed patchy neutrophilic ductal inflammation with diffuse lobular atrophy and perivenular granulomatous inflammation, recapitulating her colonic morphology, and the other, periductal lymphocytic inflammation with mild, diffuse lobular atrophy and no granulomas. When compared with IDCPs of non-IBD patients (M:F = 11:10, age: 15 - 73 years [mean: 45 years]), IDCPs of the 6 UC patients (M:F = 3:3, age: 43 - 80 years [mean: 57 years]) exhibited more prominent eosinophilic infiltrate (p = 0.023) and a markedly smaller IgG4/IgG1 ratio (mean 0.09 opposed to 0.31 of the non-IBD group, p = 0.001). There was no difference in other clinicopathological features between the 2 groups.
Conclusions: In this study, although limited by a small sample size, pancreatic manifestations in UC are often classified as IDCP. When compared to non-IBD cases, UC-related IDCPs are associated with more prominent eosinophilic infiltrate and a markedly smaller IgG4/IgG1 ratio. The results may support the hypothesis that IDCP represents the morphology of a heterogeneous group that includes UC.

1436 Histopathology of Idiopathic Portal Hypertension in Patients with HIV Infection Treated with HAART

R Miquel, P Chang, JL Blanco, M Laguno, J Gonzalez-Abraldes, J Bosch, JC Garcia-Pagan, M Bruguera. Hospital Clinic, IDIBAPS, UB, Barcelona, Spain.
Background: Idiopathic portal hypertension (IPH) describes the clinical entity of pre-sinusoidal portal hypertension in the absence of cirrhosis and other known etiologies of liver dysfunction. Patients with IPH often have preserved liver function but present with symptoms of portal hypertension, mainly variceal bleeding, splenomegaly and thrombocytopenia. The histological features associated with IPH involve a wide spectrum of non-specific changes, being the key feature the absence of cirrhosis. Recently, several cases of IPH in patients with Human Immunodeficiency Virus (HIV) infection have been reported.
Design: The aim of this study is to examine the histological profile of liver biopsies in HIV patients who presented with IPH.
Results: A total of eight HIV patients on HAART were identified over the last three years. Five presented with variceal bleeding, one with ascites and two with radiologycal and endoscopic features of IPH. Portal and systemic hemodynamics showed normal or mildly elevated hepatic venous pressure gradient in 6 patients and intrahepatic vascular shunts in 5. Viral hepatitis, autoimmunity, alcohol abuse, genetic and metabolic disorders and underlying thrombophilic abnormalities were excluded. Fourteen liver biopsies from these patients were reviewed (5 percutaneous, 9 transjugular). Cirrhosis was not present, and 12 out of 14 biopsies showed Metavir F0/F1. Absence of a patent portal vein radical (PVR) was a constant finding in all biopsies, with a variable degree of portal tract involvement. In 6 patients PVR was absent in more than 50% of portal tracts, and all biopsies had a percentage of portal tracts without PVR above 30%. Occasionally, other PVR changes such as phlebosclerosis or herniation were identified. Abnormal periportal vascular channels, focal sinusoidal dilatation and perisinusoidal fibrosis were identified in 8 biopsies each. Foci of regenerative hepatocytes were present in all biopsies, being in places vaguely nodular. No significant inflammation or steatosis was observed.
Conclusions: HIV-related IPH is characterized histologically by a heterogeneous spectrum of lesions. The most consistent finding is the presence of abnormal portal vein radicals, which may be interpreted as a progressive vascular obliterative disorder. The etiology remains elusive, and potential agents such as endothelial injury, related to drug toxicity or cytokine-induced damage, deserve further studies.

1437 Diagnostic Utility of Immunoglobulin Subclasses in Autoimmune Liver Diseases

RK Moreira, MK Washington. Vanderbilt University, Nashville, TN.
Background: Plasma cells are seen in autoimmune hepatitis (AIH), primary biliary cirrhosis (PBC), and primary sclerosing cholangitis (PSC). Previous studies have shown that assessment of immunoglobulin subclasses in plasma cells by immunohistochemistry (IHC) may be useful in distinguishing PBC from AIH. Limited data exists regarding the immunophenotype of plasma cells in PSC . The prevalence and significance of IgG4-positive cells in autoimmune liver diseases has not been well studied. We investigate the role of IgM and IgG IHC in the differential diagnosis of autoimmune liver diseases on liver biopsies, and the prevalence and significance of IgG4-positive cells.
Design: Fifty biopsies from untreated patients diagnosed with autoimmune liver disease at our institution from 1993 to 2006 were selected. IHC for IgM, IgG (Cell Marque, 1:20.000), and IgG4 (Zymed, 1:800) were performed and the concentration of positive plasma cells (per mm^2) was assessed.
Results: 21 patients with AIH (8 males (M), 13 females (F), mean age 32, range 4-63), 15 patients with PBC (1 M, 14 F, mean age 53, range 43-71), and 14 patients with PSC (9 M, 6 F, mean age 31, range 7-67) were included. A predominance of IgG-positive plasma cells is seen in AIH (90% of cases) and PSC (75% of cases), while IgM-positive plasma cells predominate in PBC (92.8% of cases). The IgM /IgG ratio (<1 or >=1) accurately distinguishes PBC from AIH in 91.4% of cases, and PBC from either AIH or PSC in 87.5% of cases (PPV=76.4%; NPV=95.6%). However, considerable overlap exists between PSC and either PBC and AIH by this method. The total number of plasma cells in AIH (mean=9.75 cells/mm^2) tends to be higher than in PBC or PSC (mean=6.19 and 5.16 cells/mm^2, respectively, $p<0.05$). Significant numbers of IgG4-positive plasma cells were seen in 28% of AIH cases, but only rare positive cells in PBC and PSC cases. IgG4-positive AIH cases were more likely to present with advanced fibrosis compared to IgG4-negative cases (66.6% vs 30%). No association was found with other IgG4-related conditions, presence of autoimmune diseases, response to steroids, or severity of inflammation on liver biopsy.
Conclusions: PBC and AIH can reliably be distinguished on initial biopsy by their IgM/IgG immunophenotype, while significant overlap exists between the latter two conditions and PSC. Our data indicates that IgM and IgG IHC may be a useful tool in evaluating autoimmune liver disease. A subset of AIH cases shows positive IgG4 cells, which may be a marker of more aggressive disease.

1438 Pregnancy Associated Fulminant Hepatic Failure; a Clinicopathologic Study

BV Naini, CR Lassman. David Geffen School of Medicine at UCLA, Los Angeles, CA.
Background: Pregnancy associated fulminant hepatic failure is a rare but fatal condition for which emergent liver transplantation (LT) is the only viable option. The etiology is broad and includes distinct entities of acute fatty liver of pregnancy (AFLP), preeclampsia/eclampsia and HELLP (hemolysis, elevated liver enzymes and low platelet) syndrome; the histologic features of these entities have been described in the literature based on studies performed more than a decade ago.
Design: We performed a retrospective study of all cases of pregnancy associated liver failure necessitating transplantation at our institution from 1984-2008. Eight cases were identified, the largest single-center report of LT for pregnancy related liver diseases. Clinical data including the gestational age at the onset of liver dysfunction, date of delivery and LT, and laboratory studies including viral and autoimmune serologies were collected by medical record review. We performed a comprehensive histologic exam of the explants.
Results: Patients ranged in age from 23-37. None had prior clinical history of liver disease, and all presented with fulminant hepatic failure. Six delivered live healthy babies (4 C/S, 2 vaginal), and 2 had fetal loss (1 stillbirth). The onset of liver failure relative to LT ranged from a few days to 1.5 months. LT in 1 case happened at 18 weeks of gestation; for the remainder, the date of LT ranged from 2 days to 1.5 months post partum. Histologic evaluation of all cases showed hepatocellular necrosis ranging from patchy zone 3 to massive panlobular necrosis. Four cases had moderate to severe portal lymphocytic infiltrate; viral and autoimmune serologies were negative in 3 of 4 cases; 1 case had positive surface and core hepatitis B antibodies but no surface antigen. Steatosis ranged from none (5 cases), mild pericentral (2 cases) to moderate macrovesicular steatosis (1 case). Sinusoidal fibrin thrombi were not identified in any of the cases. One case demonstrated a background of bridging fibrosis with an elevated copper and a presumptive diagnosis of Wilson's disease was made.
Conclusions: In our experience of 8 patients with pregnancy associated liver failure and a clinical diagnosis of HELLP syndrome, all showed extensive necrosis but none showed the characteristic histologic features described for AFLP, eclampsia or HELLP syndrome. Three cases had infiltrates suggestive of hepatitis but had negative serologies, and one case had Wilson's disease.

1439 Expression of Matrix Metalloproteinase Type 9 in Hepatocellular Carcinoma and Correlation with Histopathologic Parameters

D Nart, N Incili, M Zeytunlu, M Kilic, Z Karasu, F Yilmaz. Ege University Faculty of Medicine, Izmir, Turkey.

Background: Matrix metalloproteinases (MMP-9) are known to play an important role in the cell migration during cancer invasion by degrading extracellular matrix proteins. This study aimed to determine the role of MMP-9 in hepatocellular carcinoma (HCC) carcinogenesis.

Design: Eighty-nine cases who underwent transplantation for HCC in cirrhotic liver were selected for this study. The tumor charecteristics such as nodule number, maximal diameter, portal vein invasion were reviewed. Parafin sections were immunostained with antimouse monoclonal antibodies for MMP-9 (GE-213, 1:10, Neomarkers). The intensity of immunostaining and the percentage of immunoreactive cells were evaluated. The Pearson Chi Square analysis was used.

Results: In 31 patients (34,8%) HCC presented as a solitary nodule, 15 (16,9%) as two nodules; 9 (10,1%) as three nodules; and 34 patients (38,2%) as more than three nodules. There were 61 patients (68,5%) with maximal diameter of the largest tumor between 1-3 cm, 17 patients (19,1%) with maximal diameter of the largest tumor between 3-5 cm and 11 patients with maximal diameter of the largest tumor exceeding 5 cm. The histopathological grade of differentiation of the tumors was assessed as "well" in 20 patients (22,5%), moderate in 52 (58,4%), and poor in 17 (19,1%). While 47 patients had no sign of vascular involvement, 36 tumors showed segmental vasculer invasion (40,4%) and six large vessel involvement (6,7%). Among 89 HCC, the incidence of a positive (+) and (++) expression of MMP-9 in carcinoma cells was 30,3% (23/89) and 43,8% (39/89), respectively. There was no immunostaining in 23 tumors (25,8%). There was a significant correlation between increased MMP-9 expression and poor differentiation (p=0,001). A significant correlation between MMP-9 expression and large tumor (>5 cm) was also observed. There was a positive correlation between large vascular invasion and MMP-9 immunoreactivity (p=0,002).

Conclusions: In this study, our results indicate a positive association between MMP-9 expression and histopathologic parameters indicating poor prognosis. We conclude that MMP-9 expression in HCC may aid to predict poor outcome.

1440 Histologic Description of Pancreatectomy Specimens after Current Neoadjuvant Therapies

NJ Nolan, JB Stokes, TW Bauer, RB Adams, EB Stelow. University of Virginia, Charlottesville, VA.

Background: Most patients who develop pancreatic ductal adenocarcinoma (PDA) are considered to be unresectable at the time of their diagnosis. For those who are considered to be resectable, surgery allows for their only possible cure. Occasionally patients will be considered "borderline resectable" usually based on anatomic criteria. They receive neoadjuvant chemoradiation therapy and can then be considered for resection if they show no evidence of progressive disease throughout their treatment. Most information regarding this method of treatment has been published in the surgical literature and we are not aware of a detailed description of the associated histologic changes. Here, we describe our experience with these specimens.

Design: Sixteen patients with borderline resectable PDA underwent resection (pancreaticoduodenectomy=14) following neoadjuvant chemoradiation therapy (capecitabine and 50 Gy of radiation). Histology was reviewed. The tumor response was determined based on the percentage of viable tumor. Grade 1 was defined as >90% viable tumor, Grade 2a had 50-89% viable tumor, Grade 2b had 10-49% viable tumor, Grade 3 had < 10% viable tumor and Grade 4 showed complete response. Specific histologic findings and staging information were noted. Follow-up data were pursued.

Results: Three cases (18.75%) demonstrated grade 1 response, 5 cases (31.25%) grade 2a response, 2 cases (12.5%) grade 2b response, and 6 cases (36.5%) grade 3 response. Eight of sixteen (50%) cases were pathologically down-staged. Histologic response was variable and non-specific. Most cases (15) showed prominent dense fibrosis throughout sections of tumor. Coagulative necrosis (8 cases), prominent hemorrhage, cholesterol material and mucin pools (sometimes perineural) were less commonly seen. Viable perineural invasion was seen in 8 cases. Viable tumor was present at margin in 4 cases. At a mean follow-up of 10 months, degree of response did not correlate with recurrence or death.

Conclusions: The histologic response to neoadjuvant chemoradiation is nonspecific. Fibrosis is the most frequent histologic finding while a minority of cases had other features including coagulative necrosis and mucous pools. Neoadjuvant therapy results in pathologic downstaging of tumor in half of borderline resectable patients. More than one-third of cases show more than 90% tumor death using today's chemoradiation regimens. Further follow-up is needed to evaluate the relationship between response and survival.

1441 The Role of Biopsies in the Diagnosis of Autoimmune Pancreatitis (Lymphoplasmacytic Sclerosing Pancreatitis)

K Notohara, TC Smyrk, N Mizuno, M Mino-Kenudson. Kurashiki Central Hospital, Kurashiki, Japan; Mayo Clinic, Rochester, MN; Aichi Cancer Center Hospital, Nagoya, Japan; Massachusetts General Hospital, Boston, MA.

Background: Lymphoplasmacytic sclerosing pancreatitis (LPSP) represents the pancreatic manifestation of IgG4-related systemic fibrosclerosing diseases and appears to be the most prevalent subtype of "autoimmune pancreastitis (AIP)". Because of the difficulty in differentiating AIP from pancreatic cancer clinically, pancreatic biopsy is now being considered as an attractive diagnostic tool. The aim of our study was to evaluate the accuracy and interobserver concordance of the biopsy diagnosis of LPSP.

Design: 69 pancreatic biopsies (35 fine needle aspiration biopsies [FNABs], 32 trucut biopsies [TCBs] and 2 excisional biopsies) diagnosed as non-neoplastic diseases were collected. Without clinical information, 3 pathologists categorized each biopsy as diagnostic of LPSP (group 1, G1), suspicious but not diagnostic of LPSP (group 2, G2), or not suggestive of LPSP (group 3, G3). Insufficient biopsies were also noted as such. Both diagnoses made before and after reviewing IgG4-immunostain (IG4-IS), when it was available (n=22), were recorded. The pathologic diagnoses were correlated with clinical records.

Results: 21 FNABs were considered as insufficient materials by 2 or more pathologists, and were excluded from further analysis. Each pathologist categorized 14, 16 and 10 of the remaining 48 biopsies as G1, and 7, 16 and 13 as G2. Without IG4-IS, the complete agreements of G1 and G3 were achieved in 4 and 14 biopsies, respectively. K value for G1 was only fair (0.34), although all observers agreed that periductal inflammation, obliterative phlebitis and storiform fibrosis were the diagnostic hallmarks for G1 diagnosis of LPSP. With IG4-IS, κ value for G1 improved to 0.43 (moderate). When G1 and G2 were grouped together (G1/2), the complete agreement of G1/2 was achieved in 17 biopsies (κ value 0.50 [moderate]). G1/2 diagnosis was made on 26 of 32 TCBs by 2 or more pathologists, and 25 of these cases carried a clinical diagnosis of AIP. Clinical AIP was also seen in 4 of the remaining 6 patients with TCBs. G1/2 diagnosis by 2 or more pathologists was not achieved in any of 14 FNABs, although 9 of these patients had clinical AIP.

Conclusions: Diagnosis of LPSP on biopsies is challenging, most likely because small tissue samples fail to contain diagnostic hallmarks for LPSP. However, TCB (with IG4-IS) appears to be a useful tool to support the clinical diagnosis of AIP.

1442 Risk Factors and Histologic Pathways of Fibrosis Progression and Architectural Distortion in Chronic Hepatitis C Virus Infection after Liver Transplantation

EO Ochoa, G Alarcon, Z Gao, DT Tran, AJ Demetris. University of Pittsburgh Medical Center, Pittsburgh, PA; Hospital Universitario de la UANL, Monterrey, Nuevo Leon, Mexico; University of Calgary, Calgary, AB, Canada.

Background: Chronic hepatitis C virus (HCV)-induced cirrhosis is the leading indication for liver transplantation (OLT) and recurrent disease is universal. The rate of fibrosis progression is variable, but significantly accelerated compared to native livers, which enables pathologists to closely monitor histologic pathways responsible for liver injury and architectural distortion.

Design: 67 highly selected HCV+ OLT recipients were divided into two groups based on the presence or absence of bridging fibrosis ≤ year 3. Those with co-existent conditions that might accelerate fibrosis progression were excluded. Donor and recipient demographic, clinical and laboratory parameters were evaluated for an association with fibrosis progression. A subset of 23 patients had early (1-12 months) and late (2-5 yrs) biopsies available for comparison.

Results: Demographic and clinical factor analysis (n=67) showed that older donor age (> 40 yrs; p=0.048) and older recipient age (p=0.0269) were associated with rapid fibrosis progression, which more often led to graft failure (p=0.0005), re-transplantation (p=0.007) and death (p=0.014). Histologic findings in early biopsies (n=23) of rapid progressors showed more severe interface hepatitis (> 2 Ishak scale; p=0.025); portal inflammation (>2; p=0.025); total mHAI score > 5 (p=0.010); lymphoid aggregates (p=0.004) and hepatocyte ballooning (p=0.025). Late biopsies of rapid progressors showed more severe interface hepatitis (>2; p=0.0195); lobular necro-inflammatory activity (p=0.0545); portal inflammation (p=0.0245); total mHAI score (>6; p=0.0195); and prominent ductular reactions (p=0.0195), which caused stellate portal tract expansion (p=0.0001) and was responsible for the architectural distortion.

Conclusions: The combination of more severe necro-inflammatory activity/injury in older donor livers in early biopsies predicts the development in later biopsies of a more prominent ductular reaction, stellate portal expansion, and recurrent cirrhosis followed by allograft failure. These observations are consistent with default activation of the ductular reaction as an important mechanistic contributor to architectural distortion in allografts and identifies at risk patients early after transplantation for therapeutic intervention.

1443 Peripancreatic Soft Tissue Involvement by Pancreatic Ductal Adenocarcinomas: Incidence, Patterns and Significance

I Oliva, S Bandyopadhyay, I Coban, O Basturk, N Culhaci, D Kooby, J Sarmiento, C Staley, N Adsay. Emory Univ., Atlanta; WSU, Detroit; NYU, NY.

Background: Involvement of peripancreatic soft tissues (PST) is one of the main parameters in the current TNM staging of resected pancreatic ductal adenocarcinoma (PDA); however, defining PST by histologic parameters can be highly problematic due to abundant baseline pancreatic adipose tissue, absence of pancreatic capsule, and difficulty delineating pancreatic lobules, which becomes further blurred in the setting of compression-related secondary changes such as atrophy and fibrosis.

Design: In order to evaluate the true PST involvement by PDA, an orange-peeling method of dissection for pancreatic head resections was devised in which all the PST was shaved-off from the pancreatic surfaces before sectioning the specimen further. The PST was then separated into 7 defined anatomic regions and from each, at least one section was obtained for the purposes of both PST evaluation and also identification of microscopic LNs.

Results: PST involvement in patients with PDA was detected in 103 of 109 (94.5%) when evaluated by this method. In many cases, this appeared to be away from the main tumor, unappreciated by the gross examiners, and in some, PST involvement was represented as small microscopic foci, or scattered isolated solitary ducts (ISD). Many of these ISDs were so well differentiated that they could be easily mistaken for PanINs. Some were surrounded by muscular vessel wall, indicating that they are in fact intravascular tumor cells carcino-endothelializing the inner surfaces of the vessels, and as such representing a peculiar, insidious form of spread into PST. Separately, among these 109 cases, 19 would have qualified as pT1 by stage criteria (≤2 cm). However, 16 of these 19 had PST involvement, placing them into the pT3 category instead (by the TNM 6th edition).

Conclusions: PST involvement by PDA is very common (94.5%) when examined by the orange-peeling method. The incidence and subtle patterns of infiltration into PST, such as isolated solitary ducts and carcino-endothelialization, indicates the importance of careful evaluation of these regions, illustrates the highly insidious nature of PDA, and more importantly, provides more insight to the reasons of its incurability. Since PST involvement indicates pT3 in the current TNM staging, it appears that most resected PDAs cannot qualify as pT1 or pT2 if carefully examined.

1444 Incidence and Significance of Common Bile Duct Involvement in Resected Pancreatic Ductal Adenocarcinomas: Should It Be Represented in the TNM Staging?

IV Oliva, S Bandyopadhyay, I Coban, O Basturk, D Kooby, J Sarmiento, C Staley, N Adsay. Emory University, Atlanta, GA; WSU, Detroit, MI; NYU, New York, NY.

Background: It is not clear whether involvement of the common bile duct (CBD) is a parameter to be included in staging of pancreatic ductal adenocarcinoma (PDA). Current TNM defines pT3 as "tumor extends beyond the pancreas." CAP and others interpret this as invasion of "common bile duct &/or duodenum (including ampulla)," whereas, the recent AFIP fascicle states that "involvement of the bile duct should be designated as T3 only when the carcinoma extends beyond the pancreas to involve the extrapancreatic biliary tree."

Design: The incidence of extension to CBD by PDA was analyzed in 72 consecutive pancreatodudodenectomy specimens dissected carefully by a unified approach. These 72 cases were composed of only conventional PDA. Cases with neo-adjuvant therapy were excluded. CBD involvement was defined as 1) grossly identified and microscopically confirmed stricture of CBD, and 2) invasive carcinoma cells extending into the wall of the CBD. Where available, the location of the CBD involvement was also noted.

Results: CBD involvement was seen in 70 of 72 cases (97%). 34 were identified grossly with possible CBD involvement (characterized as: stricture, obstruction, dilation, encased in or abutting), and subsequently confirmed microscopically. In 37 cases with adequate documentation available, 22 involved the retroampullary CBD, and 15 involved the middle region of resected CBD. The 2 cases with no CBD involvement were women, aged 69 and 64, with tumor size 1.8 cm and 2.5 cm, respectively (slightly smaller than the average, 3.6 cm). Interestingly, one of these CBD negative patients presented with jaundice (total bilirubin 8.2 mg/dL).

Conclusions: Our study confirms that involvement of CBD is seen in virtually all cases (97%) of resectable PDA, and therefore it supports the stance taken in the recent AFIP fascicle that invasion into the CBD in a pancreatoduodenectomy specimen does not necessitate up-staging of the tumor to T3. This study also highlights the difficulty of determining the origin of some pancreatobiliary-type adenocarcinomas occupying the head of the pancreas, and whether they are arising from peribiliary ductules, CBD mucosa, or the pancreas itself.

1445 Differential Expression of Selected MicroRNA Species in Pancreatic Ductal Adenocarcinoma and Intraductal Papillary Mucinous Neoplasm

NC Panarelli, XK Zhou, JA Campbell, Y-T Chen, RK Yantiss. Weill Cornell Medical College, New York, NY.

Background: MicroRNAs (miRNAs) are small noncoding RNAs involved in the post-transcriptional regulation of gene expression. Aberrant expression of miRNAs has been implicated in the oncogenesis of many solid tumors, including pancreatic neoplasms. We investigated the expression of 5 miRNAs (*miR-21, miR-221, miR-100, miR-155*, and *miR-181b*) previously shown to be over-expressed in pancreatic ductal adenocarcinoma (PDA) to evaluate their potential to distinguish between PDAs, intraductal papillary mucinous neoplasms (IPMN) and non-neoplastic pancreatic tissues.

Design: Manually dissected tissue sections obtained from 16 PDAs, 12 IPMNs, and 15 non-neoplastic pancreatic tissues were evaluated for miRNA expression using quantitative RT-PCR. Control experiments that amplified endogenous small RNA U6 were also performed to normalize the expression data of the 5 miRNAs. The mean miRNA expression levels were statistically compared between PDA, IPMN and normal pancreas using ANOVA and Tukey's test, and the fold differences were calculated.

Results: We found consistently increased expression of *miR-21, miR-221, miR-100, miR-155*, and *miR-181b* in PDA compared to IPMN ($p \leq 0.01$ for all comparisons), with fold changes ranging from 1.91 (*miR-181b*) to 9.06 (*miR-21*). Similarly, all 5 miRNAs showed increased expression in PDAs compared to adjacent non-neoplastic pancreatic tissues (1.62 to 4.17 fold changes, $p<0.05$ for all comparisons). In contrast, IPMNs showed decreased expression of *miR-21* and *miR-221* compared to non-neoplastic pancreatic tissues ($p=0.03$ and $p=0.01$, respectively) but no significant differences were noted with respect to the expression of *miR-100, miR-155,* and *miR-181b*. One IPMN displayed a miRNA expression profile similar to that of PDA, but this lesion was associated with an invasive carcinoma, suggesting a difference in miRNA expression between the non-invasive and invasive components.

Conclusions: Pancreatic ductal adenocarcinomas show significantly increased expression of *miR-21, miR-221, miR-100, miR-155*, and *miR-181b* compared to non-neoplastic pancreatic tissues and non-invasive IPMNs, whereas IPMNs display decreased expression of *miR-21* and *miR-221*. These results suggest that miRNA analysis may represent a useful adjunct to the pathologic evaluation of pancreatic lesions, and its diagnostic potential in cytopathology specimens should be further explored.

1446 Steatohepatitis in Childhood and Adolescence: Histopathologic, Clinical and Serologic Correlates, a Review of 30 Cases

V Prasad, A Hughes, M Uddin, C Boesel. Nationwide Children's Hospital, Ohio State University, Columbus, OH.

Background: Steatohepatitis (SH) is an important pattern of hepatic injury in adults and children, and can lead eventually to cirrhosis. Although incompletely understood, alterations in cytokines and inflammatory mediators paired with hepatic insulin resistance are proposed pathways of damage. SH is being encountered more frequently in children. Obesity is an emerging problem in childhood SH. We reviewed 30 cases of SH diagnosed in the last 8 years, examined the liver biopsies and correlated with serologic findings and electron microscopic (EM) features when available.

Design: We reviewed liver biopsies, clinical information including drug intake and autoimmune gastrointestinal profiles (AGIP), and electron microscopy (when available) in 30 patients followed at a tertiary care teaching hospital, from 2000 to 2008.The patients ranged in age from 8 to 18 years with a median of 14.5 years, 23 were male and 7 female. 9/30 cases had available EM studies. The liver biopsies, electron photomicrographs, laboratory data and clinical charts were reviewed.

Results: All 30 cases had Steatohepatitis with varying degrees of fibrosis (8/30). 15/30 had abnormal AGIP, with positive Anti-Nuclear or positive Anti Smooth muscle antibodies. 9/30 patients were obese (6 male, 3 female), 6/30 had biliary dyskinesia, 2/30 had a prior diagnosis of autoimmune hepatitis, 3/30 had a history of seizures and were on Valproate, while 3/30 had Diabetes mellitus (all female). 2/30 had autistic spectrum disorders (1 with Asperger's syndrome). 2/30 showed histological features of auto immune hepatitis. Of 9 cases examined by EM, 8 showed accumulation of neutral fat and dilated endoplasmic reticulum. 2/9 showed mitochondrial para-crystalline inclusions (PCI). One case had decreased activity of antimycin A sensitive decylubiquinol-cytochrome C reductase (Electron transport chain complex III) indicating a defect in complex III.

Conclusions: Steatohepatitis is being recognized more often in childhood, and obesity is an emerging problem. 50% of our cases showed abnormal AGIP with 2 cases showing autoimmune hepatitis, which may be challenging in the diagnosis and management. Valproate and medications used in the management of autistic spectrum disorders can cause SH. Girls with diabetes have an increased risk for SH. Cirrhosis is a legitimate concern, and accurate diagnosis and grading of fibrosis is vital for optimal management and therapeutic modification in children with SH. PCI on EM may be encountered, but interpreted with caution.

1447 Focal Nodular Hyperplasia after Orthotopic Liver Transplantation

SH Ra, CR Lassman. David Geffen School of Medicine at UCLA, Los Angeles, CA.

Background: Liver nodules are not uncommonly encountered in the post-transplant liver. The vast majority of these lesions represent hepatocellular carcinoma and infrequently nodular regenerative hyperplasia. Focal nodular hyperplasia (FNH) is a localized hyperplastic overgrowth of hepatocytes typically associated with vascular anomalies. There is scant information in the literature regarding the presence of focal nodular hyperplasia in post- transplant livers. Focal nodular hyperplasia has been well characterized in native livers, but only one case has been described in a transplanted liver.

Design: We review the clinical and pathologic features of 4 patients with the diagnosis of focal nodular hyperplasia after orthotopic liver transplantation.

Results: There were 3 male and 1 female patients, ranging in age from 2-63 years. Two of the patients were originally transplanted for cirrhosis secondary to biliary atresia, one for hepatitis C, and one for hepatitis B&C and alcohol use. The time from transplant to a diagnosis of FNH ranged from 15-118 months. Three patients presented with an incidental solitary liver nodule; one presented with with two liver nodules. All four patients had increases in alkaline phosphatase and one patient had increased ALT and AST. The main considerations before diagnosis were hepatocellular carcinoma and lymphoma. The diagnosis of FNH was made on core needle biopsy in 2 cases, wedge biopsy in 1 case, and at autopsy in 1 case. The nodules ranged in size from 1.7 to 6.9 cm. Three patients had conditions associated with altered vascular perfusion; 2 had portal vein thrombosis and 1 had a partial allograft from a living donor. One patient underwent resection of the FNH; the other 2 patients are being followed clinically.

Conclusions: FNH can present as a hepatic nodule after orthotopic liver transplantation. Due to altered vascular perfusion in the post-transplant livers, we believe that FNH is more common than reported in the literature and should not be confused with hepatocellular carcinoma. FNH should be considered in the differential diagnosis of hepatic nodules within the post-transplant liver, especially in patients with co-existing vascular perfusion abnormalities.

1448 Advantages and Pitfalls of Glypican-3 Immunohistochemistry in the Distinction of Hepatocellular Carcinoma and Metastatic Carcinomas

R Ramachandran, LW Browne, S Kakar. UCSF, San Francisco, CA.

Background: Immunohistochemistry for glypican-3 (GPC), a membrane-anchored proteoglycan, has been advocated for the diagnosis of hepatocellular carcinoma (HCC). However, the experience with this antibody is still limited and its expression in adenocarcinomas of various sites and other metastatic tumors that can mimic HCC has not been widely studied.

Design: GPC immunohistochemistry (IHC) was performed on tissue microarrays generated from hepatocellular carcinoma (n=162), adenocarcinomas (n=139) including cholangiocarcinoma and metastatic adenocarcinomas from colon, pancreas, breast and lung. Polygonal cell tumors that can often be mistaken for HCC were also studied including renal cell carcinoma (RCC,n=139), neuroendocrine tumors (NE,n=14), melanoma (n=52) adrenocortical carcinoma (ACC,n=25) and angiomyolipoma (AML,n=57). IHC for polyclonal carcinoembryonic antigen (pCEA), hepatocyte paraffin 1(HepPar) and monoclonal epithelial glycoprotein (MOC-31) was also done.

Results:

Marker expression in tissue microarrays

	GPC-3 (%)	HepPar (%)	MOC-31 (%)	pCEA (%)
HCC	104/162 (64)	100/147 (68)	13/146 (9)	72/163 (44)
RCC	0/97	0/97	76/96 (79)	-
Adenocarcinoma	3/139 (2)	1/140 (~0)	128/143 (90)	122/139 (88*)
NE	0/15	0/15	8/14 (57)	0/15
Melanoma	2/51 (4)	0/58	3/52 (6)	8/58 (14)
ACC	0/25	0/24	0/25	0/23
AML	0/57	0/56	2/57 (4)	0/65

*expression in a non-canalicular pattern

GPC, HepPar and canalicular pCEA were expressed in 64%, 68% and 44% of HCC respectively. All 3 markers were expressed in 26% of HCC. GPC alone was seen in 12%, HepPar alone in 15% and pCEA alone in 1 case (<1%). Rare melanomas (4%) and adenocarcinomas (2%) showed GPC expression. All other adenocarcinomas and polygonal cell tumors were negative. MOC31 was expressed in majority of adenocarcinomas, NE and RCC, but also in 13 (9%) HCC. GPC expression was seen in 9/13 MOC31+ HCC; of these GPC was the only positive heptocellular marker in 6 cases.

Conclusions: GPC has high specificity for HCC with negative or rare expression in metastatic adenocarcinomas, RCC, NE, ACC and AML. The reported GPC expression in melanomas has ranged from 0-80%, and was observed in 4% in this series. MOC31, an excellent adenocarcinoma marker can be strongly expressed in 9% of HCC. GPC is the only hepatocellular marker expressed in 12% of HCC and when combined with HepPar, it increases the sensitivity of HCC diagnosis to >90% and identifies all HCC cases with MOC31+ expression.

1449 The Role of Post-Reperfusion Biopsy (PRB) in the Era of Extended Criteria Donor (ECD): Clinicopathologic Correlation and Follow-Up Analysis of 50 Liver Transplant Patients, a Prospective Study

M Raoufi, C Ma, A Ormsby, H Vakil, K Brown, MA Huang, D Moonka, M Abouljoud. Henry Ford Hospital, Detroit, MI; Wayne State University, Detroit, MI.

Background: Organ shortage drives transplant surgeons to consider organs with extended criteria for transplant. A PRB at the time of transplant would serve the purpose of detecting existing pathology as well as obtaining baseline morphology for comparison with follow-up biopsies (FUBs). In this prospective study, we evaluate how and to what extent morphological changes in PRBs correlate with histologic findings in FUBs and clinical outcomes.

Design: Between January-July 2007, total of 50 liver transplants were performed in our center. Histologic sections of PRBs and FUBs (including H & E, trichrome and iron stains) were examined on a routine basis. All patients were followed till September 2008 and relevant clinical and laboratory data were recorded.

Results: Mean follow-up time was 518.4 days (range: 431-608). Mean time between PRB and FUBs was 94.9 days (SD $\pm$ 120.62) for the first FUB (40 cases), 111.2 days (SD $\pm$ 21.67) for the second FUB (16 cases), and 235 days (SD $\pm$ 123.85) for the third FUB (8 cases). Major histologic findings in PRBs included: preservation injury (21 cases), macrovesicular steatosis (mild to moderate: 12 cases; severe: 4 cases), portal triad chronic inflammation and fibrosis (15 cases), and pericellular fibrosis (3 cases). Major histologic findings in FUBs included: acute cellular rejection (6 definite and 4 indeterminate cases), recurrent hepatitis C (6 cases), centrilobular necrosis (4 cases), and cholestasis (5 cases). After comparing pathological findings in PRBs and FUBs and correlating the findings with clinical and lab data, the following observations were made: 1) None of the major pathologic findings in PRBs persisted in FUBs, regardless of cause of end stage liver disease; 2) In patients with and without any type of pathology in PRBs, no significant differences were found in liver function tests, length of hospital stay, and survival rates.

Conclusions: Our experience indicates: 1) Transplanting organs with pre-existing pathologic changes does not adversely affect the outcomes, and 2) PRBs can reliably serve as a baseline measure of existing pathology in donor organs. Given the low morbidity of such biopsies and continued expansion of donor criteria, having PRB is appropriate to better understand the long-term impact of baseline pathologic findings.

1450 Muscularis Mucosae vs. Muscularis Propria in Gallbladder, Cystic Duct and Common Bile Duct: Smoothelin and Desmin Immunohistochemical Study

K Raparia, QJ Zhai, MR Schwartz, L Peters, SS Shen, AG Ayala, JY Ro. The Methodist Hospital, Houston, TX.

Background: The muscle layer in the gallbladder, cystic duct and common bile duct is not well defined and it is still unresolved whether it is muscularis mucosae or muscularis propria. Smoothelin is a novel smooth muscle-specific contractile protein expressed only by fully differentiated smooth muscle cells in the muscularis propria, and not by proliferative or noncontractile smooth muscle cells in muscularis mucosae. In this study, we attempt to characterize the property of muscle layers in gallbladder, cystic and common bile ducts by immunohistochemistry using desmin and smoothelin.

Design: Formalin-fixed paraffin-embedded sections of the gallbladder (15 cases), cystic duct (11 cases) and common bile duct (10 cases) were stained for smoothelin (1:100; Abcam Inc, Cambridge, MA) and desmin (1: 200; Dako, Carpinteria, CA). Staining intensity was evaluated as weak and strong. The staining pattern score was evaluated as follows: 0 or negative ≤ 5%; +1 or focal=5% to 10% positivity; +2 or moderate=11% to 50% positivity; and +3 or diffuse >50% muscle cells positivity.

Results: With desmin, strong and diffuse (+3) staining was observed in all gallbladders (15/15, 100%) highlighting one continuous layer of muscle. In contrast, the muscle layer was discontinuous and interrupted in all cystic ducts and in most of the common bile ducts highlighted by the desmin stain. Smoothelin intensely stained (more than 2+) muscle fibers in the gallbladder wall similar to that observed with desmin staining (10/15, 67%). In contrast, the common bile duct predominantly had absent or weak and focal immunostaining (0 or 1+ staining) with smoothelin (7/10, 70%) with only a few cases (3/10, 30%) having 2+ staining. Cystic ducts also showed absent or weak and focal immunostaining with smoothelin with 5 of 11 cases (44%) showing 2+ immunostaining with smoothelin.

Conclusions: 1) In the gallbladder, the continuos muscle layer appears to be muscularis propria and no muscularis mucosa is present. 2) In cystic and common bile ducts only attenuated and incomplete muscle layer is present, suggesting no or limited contractile function. 2) Differentiating these anatomic muscle structures may be important for the pathologic staging of carcinoma in these organs.

1451 Fibrolamellar Carcinomas Arise in Livers with Depleted Mitochondrial DNA

HM Ross, P Vivekanandan, M Torbenson. Johns Hopkins Hospital, Baltimore, MD.

Background: Fibrolamellar carcinoma (FLC) is a unique subtype of hepatocellular carcinoma (HCC) with characteristic demographic and histological features. Previous studies of FLC using electron microscopy have demonstrated a proliferation of mitochondria, which correlates with the distinctive oncocytic appearance of this tumor. Mitochondrial changes can be associated with cancer development but their role in FLC has not been well studied. In this study, we investigated the levels of mitochondrial DNA within FLC, control HCC with typical morphology, and the paired non-neoplastic liver tissues for both of these groups.

Design: Mitochondrial DNA levels were quantitated by real time PCR in 4 FLC, 10 control HCC, and in the paired non neoplastic tissues. To further examine the background non-neoplastic liver tissues, paraffin-embedded specimens from 11 individuals with FLC (average 30 years) and ten controls with HCC that arose in non-cirrhotic livers (average 40 years) were studied and scored for mega-mitochondria, lipofuscin, fatty change, and arterialization of portal tracts.

Results: Surprisingly, mitochondrial DNA levels within FLC were on average 33% lower than in control HCC ($16x10^7$ versus $24x10^7$ copies mitochondrial DNA/ug total DNA) , p=0.04. This observation held true when mitochondrial DNA levels were normalized to both the micrograms of total tissue DNA as well as nuclear DNA as measured by real time PCR. Interestingly, mitochondrial DNA levels were also lower in the background livers of individuals with FLC as compared to the HCC controls ($9x10^7$ vs $29x10^7$ copies mitochondrial/copies genomic DNA). Careful histological examination of the background livers showed no differences in fatty change, lipofuscin deposition, or mega-mitochondria but did show enhanced arterialization within the small portal tracts of cases with FLC (5/11) versus those with typical HCC (0/10). The enhanced arterialization manifested as increased numbers and prominence of small arterial profiles. These findings suggest that baseline defects in mitochondria in the livers of individuals with FLC may lead to sufficient hypoxia to induce increased arterialization of the liver.

Conclusions: FLC have decreased mitochondrial DNA levels despite their oncocytic appeareance. In addition, the background livers demonstrate decreased mitochondrial DNA levels as well as an enhanced arterialization in some cases. These findings suggest FLC are associated with a fundamental mitochondrial biogenesis defect or diffuse mitochondrial injury.

1452 Sinusoidal Obstruction Syndrome and Nodular Regenerative Hyperplasia Are Major Hepatic Lesions Associated with Oxaliplatin Based Chemotherapy for Colorectal Liver Metastases and Partially Prevented by Bevacizumab

L Rubbia-Brandt, GY Lauwers, H Wang, PE Majno, K Tanabe, A Zhu, C Brezault, O Soubrane, EK Abdalla, J-N Vauthey, G Mentha, B Terris. University Hospital, Geneva, Switzerland; Massachusetts General Hospital, Boston, MA; M.D. Anderson Cancer Center, University of Texas, Houston, TX; University Hospital, Geneva, Switzerland; Hopital Cochin, Paris, France; Hopital Cochin, Paris, France.

Background: Surgical resection of hepatic colorectal cancer metastases (HCRM) is the only curative treatment available. Preoperative chemotherapy is used to downsize HCRM and achieve respectability. Oxaliplatin (OX) is commonly used because of its tumor efficacy. We performed a detailed assessment of non-tumoral hepatic lesions associated to OX, assessed histological effects of bevacizumab (anti-VEGF antibody) recently introduced to OX, and proposes a histological scoring system.

Design: A multiinstitutional series of surgically resected HCRM (n = 385) was reviewed. Type and grade of hepatic lesions were analyzed.

Results: Amongst 274 resection treated by OX, 54% had moderate to severe sinusoidal obstruction syndrome (SOS), related to rupture of the sinusoidal barrier. Peliosis, centrilobular perisinusoidal/venular fibrosis and NRH developed in 10.6%, 47%, 24.5% respectively, directly related to severity of SOS. In contrast, the 111 livers treated by surgery alone remained normal. Hepatic lesions were lower in the group treated with OX with bevacizumab compared to the one treated by OX alone, including lower incidence of SOS (31.4% vs. 62.2% respectively; $p<0.05$), of peliosis (4.3% vs. 14.6% respectively), of NRH (11.4% vs. 28.9% respectively), of centrilobular/venular fibrosis (31.4% vs. 52% respectively) ($p<0.001$).

Conclusions: Pathologists should have a high index of suspicion that non tumorous liver of patients treated with OX may display distinctive lesions involving SOS, NRH and fibrosis that may potentially impact on clinical outcomes. Bevacizumab may partially prevent these lesions.

1453 Chemotherapy-Induced Vascular Liver Injury in Metastatic Colorectal Cancer: Analysis of 275 Resected Liver Specimens Shows Nodular Regenerative Hyperplasia and Parenchymal Extinction Lesions but Not Sinusoidal Dilatation Are Associated with Oxaliplatin

P Ryan, A Pollett, S Nanji, CA Moulton, S Gallinger, M Guindi. University of Toronto, Toronto, Canada; Mount Sinai Hospital, Toronto, Canada; University Health Network, Toronto, Canada.

Background: The use of newer chemotherapeutic agents prior to resection of colorectal cancer liver metastases has been with linked with parenchymal liver injury. In particular chemotherapy-associated steatohepatitis (CASH) and diffuse sinusoidal injury have been linked to use of irinotecan and oxaliplatin, respectively. We assessed liver injury in 275 cases from 2002-2007 and correlated findings with chemotherapy use.

Design: Cases were reviewed retrospectively while blinded to preoperative treatment. Features scored semi-quantitatively [using established criteria where available] included: steatosis and steatohepatitis [NASH activity score]; sinusoidal dilatation [Rubbia-Brandt]; hepatic and portal vein loss; nodular regenerative hyperplasia (NRH); congestive changes; and parenchymal extinction lesion (PEL). 20 Cases with confounding factors, such as portal vein embolization or tumour obstructing vessels serving resected liver, were excluded from assessment of vascular injury.

Results: In the year prior to hepatic resection 40 patients received 5-fluorouracil (5FU) alone, 41 irinotecan with 5FU, 24 oxaliplatin with 5FU, 8 all three agents, and 162 did not receive chemotherapy. Steatohepatitis was identified in 6/275 cases (2.2%) - 1 received irinotecan and 5 did not receive chemotherapy. Multivariate analysis showed steatosis > 33% was associated with increasing BMI ($p < 0.001$) but not chemotherapy. Vascular lesions of any severity were identified in 126/255 cases; 56 of these received chemotherapy. Nodular regenerative hyperplasia ($p = 0.011$) and PELs ($p = 0.01$) were significantly associated with oxaliplatin. No significant associations were found with other vascular lesions including sinusoidal dilatation.

Conclusions: Unlike previous series, our findings suggest that sinusoidal dilatation is not significantly associated with Oxaliplatin. The assessment of chemotherapy-induced vascular liver disease if limited to sinusoidal dilatation misses more advanced parenchymal injuries (NRH, PELs) which may have clinical impact. No significant association was demonstrated in this series between the use of newer chemotherapeutic agents and CASH.

1454 Expression of Hepatocyte and Cholangiocyte Transcription Factors in Hepatocellular Carcinoma, Cholangiocarcinoma, and Combined Hepatocellular and Cholangiocarcinoma: Implication for the Process of Transdifferentiation

E Sasatomi, E Ochoa, K Isse, MA Nalesnik, T Wu, AJ Demetris. University of Pittsburgh Medical Center, Pittsburgh, PA.

Background: Hepatocyte nuclear factors (HNFs) are a subfamily of transcription factors that are known to play important roles in the division of hepatocyte and biliary lineages in early liver development. The purpose of the study is to examine the expression status of different HNFs in hepatocellular carcinoma (HCC), peripheral intrahepatic cholangiocarcinoma (ICC), and in the different histologic components of combined hepatocellular and cholangiocarcinoma (HCC-CC).

Design: Five cases of ICC, 6 cases of HCC and 7 cases of HCC-CC were gathered from the pathology archives of the University of Pittsburgh Medical Center (UPMC). By definition, unequivocal component of hepatocellular carcinoma with trabecular or solid nests separated by sinusoidal spaces (hcc) and cholangiocarcinoma component with tubular glandular structures accompanied by fibrous stroma (cc) were observed within the same nodule in cases of HCC-CC. Areas of sarcomatoid differentiation (src) were seen in two cases (29%) of HCC-CC. Immunohistochemical stains for HNF1α, HNF1β, HNF4, and HNF6 were performed in all cases.

Results: HCC was characterized by negative expression for HNF1α and HNF1β (Table 1).

Table 1. Expression status of HNFs in ICC, HCC and HCC-CC

	ICC	HCC	HCC-CC
HNF1α	20% (1/5)	0% (0/6)	43% (3/7)
HNF1β	100% (5/5)	0% (0/6)	57% (4/7)
HNF4	60% (3/5)	67% (4/6)	100% (7/7)
HNF6	40% (2/5)	17% (1/6)	71% (5/7)

HNF1β was expressed exclusively in ICC or cc component of HCC-CC (Tables 1 and 2).

Table 2. Expression status of HNFs in different components of HCC-CC

	cc	hcc	src
HNF1α	43% (3/7)	14% (1/7)	0% (0/2)
HNF1β	57% (4/7)	0% (0/7)	0% (0/2)
HNF4	71% (5/7)	86% (6/7)	50% (1/2)
HNF6	43% (3/7)	43% (3/7)	0% (0/2)

HNF4 and HNF6 were observed both in HCC and CC and in hcc and cc components of HCC-CC. Sarcomatoid component of HCC-CC was positive only for HNF4.

Conclusions: Because HNF1β was observed exclusively in the areas of cholangiocellular differentiation, HNF1β may play a role in the pathogenesis of cholangiocarcinoma. Immunostain for HNF1β may serve as a marker for biliary epithelial differentiation in the diagnosis of liver neoplasm.

1455 Insulin-Like Growth Factor-2 mRNA Binding Protein 3 (IGF2BP3) Expression May Be a Marker for a Unfavorable Prognosis in Pancreatic Ductal Adenocarcinoma

DF Schaeffer, D Owen, HJ Lim, E Mehl, AK Buczkowski, SW Chung, CH Scudamore, DA Owen, SSW Ng, DG Huntsman. The University of British Columbia, Vancouver, BC, Canada; BC Cancer Agency, Vancouver, BC, Canada.

Background: Pancreatic adenocarcinoma is a lethal disease with a 5-year survival rate of 4% and typically presents in advanced stages. In this setting therapeutic markers identifying aggressive tumors, could aid in management decisions. Insulin-like growth factor 2 mRNA binding protein 3 (IGF2BP3, also known as IMP3 or KOC) is an oncofetal RNA-binding protein regulating targets such as insulin-like growth factor 2 (IGF2) and ACTB (beta-actin) and has previuosly been demonstrated to be expressed in pancreatic adenocarcinoma.

Design: The expression of IGF2BP3 was evaluated by immunohistochemistry on a tissuemicroarray of 128 pancreatic adenocarcinoma with tumor grade 1, 2 and 3, according to WHO criteria. Non-neoplastic pancreatic parenchyma served as control tissue. Slides were reviewed by two pathologists, blinded to clinical outcome, and scored. Cut-off point for positive cases was any convincing cytoplasmic expression in more than 5% of tumor cells. Univariate disease specific survival analysis was performed by the generation of Kaplan- Meier curves and differences assessed with the log-rank statistic. Multivariable disease specific survival analysis was assessed with the Cox proportional hazards regression model.

Results: IGF2BP3 was found to be selectively overexpressed in pancreatic ductal adenocarcinoma tissues but not in benign pancreatic tissues, as previously reported. 9 (40%) patient samples of tumor grade 1 (n=24) and 27 (44%) of tumor grade 2 did express IGF2BP3. The highest rate of expression was seen in poorly differentiated specimen (Grade 3, n=42) with 26 (63%) positive samples. Overall survival was found to be significantly shorter in patients with IGF2BP3 expressing tumors ($p=0.001$; RR 2.3, 95% 1.2-4.8).

Conclusions: Although IGF2BP3 is expressed in a variety of malignant neoplasm (i.e. pulmonary SCC, ovarian CCC and RCC) prognostic value has only be demonstrated in RCC. Our data suggest, that IGF2BP3 denotes a subset of pancreatic adenocarcinomas with an extremly poor outcome and provides a rationale for developing therapies to target the IGF pathway in this cancer.

1456 Sclerosing Mesenteritis Involving the Pancreas: A Mimicker of Pancreatic Cancer

JR Scudiere, K Horton, J Herman, E Fishman, R Schulick, C Wolfgang, E Montgomery, R Hruban. The Johns Hopkins Medical Institutions, Baltimore, MD.

Background: Sclerosing mesenteritis, also known as mesenteric lipodystrophy, rarely involves the pancreatic parenchyma. When it does involve the pancreas, sclerosing mesenteritis can mimic pancreatic carcinoma both clinically and radiographically, creating substantial diagnostic and treatment challenges.

Design: We report 12 cases of sclerosing mesenteritis involving the pancreatic parenchyma, and review their clinical presentation, radiographic findings, pathology, and outcome.

Results: The clinical and radiologic impression for 7 of these 12 patients was a primary pancreatic neoplasm. The mean age at presentation was 56.7 years (range 16-78 years). Five patients were men and 7 were women. Of the 11 patients with recorded clinical presentation information available, 9 reported abdominal or epigastric pain, 5 reported weight loss, and 2 reported one or more of the following: back pain/pain radiating to the back, fever, abdominal bloating or distention, nausea with or without vomiting, and anorexia. In each case, the lesion formed a tumefactive mass with an infiltrative pattern that involved the pancreas. All cases had the 3 key histologic features of sclerosing mesenteritis- fibrosis, chronic inflammation, and fat necrosis- in the absence of known etiology. As in other locations, the cases of sclerosing mesenteritis involving the pancreas contained a mixture of lymphocytes, plasma cells, and scattered eosinophils. Of the 10 patients with treatment and follow-up information available, 5 responded to treatment (either resection, steroids, tamoxifen, azathioprine, or a combination) and 5 showed no response in follow-up ranging from several days to ten years after diagnosis. A dramatic response to immunosuppressive therapy is illustrated by the case of a 46-year-old woman who presented for treatment evaluation following the presumptive diagnosis of an inoperable pancreatic cancer.

Conclusions: Distinguishing patients with sclerosing mesenteritis involving the pancreas from those who have pancreatic cancer is crucial to appropriate management, as patients with sclerosing mesenteritis may benefit greatly from immunosuppression.

1457 Immunohistochemical and Molecular Characterization of Incipient Intraductal Papillary Mucinous Neoplasms

C Shi, S-M Hong, P Lim, JR Eshleman, M Goggins, RH Hruban. The Johns Hopkins Medical Institutions, Baltimore, MD.

Background: Intraductal papillary mucinous neoplasms **(**IPMN) are grossly visible mucin-producing epithelial neoplasms often with prominent papillary architecture that arise predominantly in the main pancreatic duct or its branches. "Incipient" IPMNs are histologically similar to IPMNs, but they are <1cm and fall short of size criteria for an IPMN. Some investigators have suggested that incipient IPMN may represent an early stage of the development of IPMN. The goal of this study is to characterize incipient IPMNs using immunohistochemical labeling and *KRAS2* gene mutation analysis.

Design: Formalin-fixed, paraffin-embedded sections were immunolabeled with antibodies to MUC-1, MUC-2, CDX-2, DPC4, E-cadherin, P53, P16 and cyclin D1. *KRAS2* gene status was analyzed by PCR DNA sequencing using DNA isolated from microdissected samples.

Results: Twenty two incipient IPMNs were identified: 16 with low-grade dysplasia and 6 with moderate dysplasia. The size of the incipient IPMNs ranged from 0.2 cm to 0.8 cm. MUC-1 was expressed in 5 of 22 lesions (22.7%), whereas MUC-2 expression was only detected in one lesion (4.5%). No lesions were immunoreactive for CDX2. DPC4 and E-cadherin expression were both intact in all of the lesions. P53 immunoreactivity was seen in 2 of 22 lesions (9.1%). Overexpression of cyclin D1 was present in 10 of 22 lesions (45.5%). Four of 20 (20%) lesions demonstrated loss of p16 expression. *KRAS2* gene sequencing revealed that 5 out of 6 lesions (83.3%) harbored a codon 12 mutation.

Conclusions: Incipient IPMNs demonstrated a high frequency of *KRAS2* gene mutations and low frequency of MUC-2 expression as seen in PanIN. On the other hand, similar to IPMN, they also showed a low rate of P16 loss. This data suggests that incipient IPMN may represent a transitional lesion between PanIN and IPMN lesions.

1458 Patients with Familial Pancreatic Cancer Have More and Higher Grade Precursor Lesions Than Do Patients with Sporadic Pancreatic Cancer

C Shi, AP Klein, M Goggins, M Canto, R Schulick, E Palmisano, RH Hruban. The Johns Hopkins Medical Institutions, Baltimore, MD.

Background: 10% of patients with pancreatic cancer (PC) have a family history of the disease. Individuals with a family history of PC have an increased risk of developing PC themselves. Significant effort has been placed in screening these at-risk individuals for early disease, but little is known of the precursor lesions associated with familial PC. The purpose of this study was to define the histologic features of the precursor lesions in patients with familial PC.

Design: The histologic findings in 51 pancreata surgically resected from patients with a strong family history of PC (familial PC, at least two first-degree relatives with PC in the kindred) were compared to the findings in 40 surgically resected sporadic PCs.

Results: Classic ductal adenocarcinoma was the most common type of infiltrating PC in both the familial (36/51, 71%) and sporadic groups (34/40, 85%). Other phenotypes identified in the familial group included 6 adenosquamous carcinomas (11 %), 7 intraductal papillary mucinous neoplasms with invasive carcinoma (IPMN+CA, 14%), 1 undifferentiated carcinoma and 1 signet ring cell carcinoma. The other histologic types identified in the sporadic group included 1 adenosquamous carcinoma (3%), 4 IPMN+CA (10%) and 1 undifferentiated carcinoma (3%). Non-neoplastic pancreatic parenchyma was available from 49 of the 51 familial PC cases. Precursor lesions, including pancreatic intraepithelial neoplasia (PanIN), IPMN and incipient IPMN, were quantified in these tissues. Multiple precursor lesions were present in all but 2 cases, and precursor lesions were significantly more common in the 49 familial cases than in the sporadic cases (1.9 ± 0.3 per slide versus 1.1 ± 0.2 per slide, $p<0.001$ after controlling for age). There were significantly more high-grade lesions (PanIN-3 and IPMNs with high-grade dysplasia) in the familial cases than in the sporadic cases ($p=0.032$). This association was stronger for PanIN3 ($p=0.003$) than for IPMNs with high-grade dysplasia ($p=0.06$).

Conclusions: Precursor lesions are more common than in patients with sporadic disease and tend to be of a higher grade in patients with a strong family history of PC. These findings have significant implications for the design of screening tests for the early detection of PC.

1459 Cirrhosis in Young Chronic Hepatitis B Patients with Low Viral Load and HBeAg-Negative Status: Result of Extended Screening for Co-Morbidities

K Sivarajah, OA Adeyi. University of Toronto/UHN, Toronto, ON, Canada.

Background: The natural history of hepatitis B contracted perinatally typically follows a period of immune-tolerant phase, followed usually in late teen by immune clearance phase, which if progressive leads to cirrhosis. Risk factors for progression to cirrhosis include high viral load, age, severity and frequency of inflammation in the immune clearance phase, positive e-antigen status, HCV co-infection, and fatty liver among others, and these are usually screened for at most centers. In this study we aimed at identifying other factors responsible for progression in patients with none of these usually screened risk factors.

Design: The records of UHN patients younger than 40 years biopsied for chronic viral hepatitis B over a period of 7 years (2001 -2007) were reviewed. Biopsies were reviewed and patients with stages 3 and 4 fibrosis on the modified Metavir scale were included. Their e-antigen status and viral loads were documented. Patients with known hepatitis C co-infection, previous antiviral therapy, and /or steatosis/steatohepatitis on biopsy were excluded. Additional clinical, serologic and biochemical data were sought with a view to determining other contributors to cirrhosis other than chronic hepatitis B.

Results: Twenty-six untreated HBV patients <40 years old with advanced fibrosis were identified over the study period. 10 patients aged 20 to 34 years were e-antigen-negative, of whom 4 (40%) tested positive for hepatitis D (HDV); 3 (30%) by urine and quantitative tissue copper measurement indicate possible co-exiting Wilson's disease (WD), and the remaining 3 (30%) patients have no other apparent explanation for their cirrhosis. 16 patients were e-Ag+ of whom 2 (12.5%) have possible WD. The e-Ag+ group have significantly higher viral load that the negative group (mean 5.5 logs versus less than 1 log).

Conclusions: Young chronic HBV patients with cirrhosis, especially those with low viral load and negative e-Ag, should be considered for extended screening for Wilson's disease and HDV; in this study 7 of 10 patients in this category tested positive for either HDV co-infection or WD.

1460 The Severity of Histological Lesions Is Predictive of Outcome in 138 Patients with Alcoholic Steatohepatitis

L Spahr, E Giostra, A Hadengue, L Rubbia-Brandt. University Hospitals of Geneva, Geneva, Switzerland.

Background: Diagnosis of alcoholic steatohepatitis (ASH) is based on histology (ballooning/Mallory bodies; steatosis; neutrophils). Additional features include bile pigment, iron deposits, and ductular reaction. Whether the intensity of histological damage is of clinical significance is ill-defined. We studied the prognostic value of individual features on liver biopsy, as well as other parameters (age, MELD and Maddrey) to predict the 90-day mortality in patients with ASH.

Design: 138 patients and biopsy-proven ASH admitted over a 3-year period were studied. Clinical scores were calculated at time of biopsy. A semi-quantitative evaluation was performed, while blinded to patients' outcome: macrovesicular steatosis (>50%: +1); microvesicular steatosis (present: +1); hepatocellular damage (numerous Mallory: +1; frequent ballooning: +1); neutrophilic infiltration (severe: +1); iron deposits (moderate/severe: +1); ductular reaction (marked: +1); and bile pigments (moderate/severe: +1). All patients had cirrhosis. The 3-month survival status was recorded.

Results: Survival was 74%. Thirty seven patients died (median time 26 days). At univariate analysis, age > 50 yrs, Maddrey ≥ 32, MELD > 19, bile pigments (all $p<0.001$), marked iron deposits ($p<0.015$), were associated with death. Bilirubin showed a weak but significant correlation with bile pigments (Kendall tau = 0.49, $p<0.0001$). On multivariate analysis (OR [95% CI]), an age > 50 yrs (**3.8** [1.35-10.9]; a Maddrey > 32 (**5.7** [1.7-19.7]; and bile pigments on biopsy (**2.5** [1.2-5.2] were independent predictors of death.

Conclusions: Apart from description of features for the diagnosis of ASH, histology identifies bile pigments with a prognostic significance, together with an age > 50 yrs and a Maddrey's score > 32.

1461 A Clinicopathologic Study of Mixed Acinar Ductal Carcinomas of the Pancreas

EB Stelow, F Bao, NJ Nolan, R Shaco-Levy, J Garcia, DS Klimstra. University of Virginia, Charlottesville, VA; Memorial Sloan-Kettering Cancer Center, New York, NY; Ben-Gurian University, Beer-Shiva, Israel.

Background: Pancreatic acinar cell carcinomas (ACCs) are clinically and pathologically distinct from pancreatic ductal adenocarcinomas (PDAs). Whereas endocrine differentiation has been well demonstrated in ACCs, significant ductal components are rare. This paper reviews the clinicopathologic features of a series of ACCs with prominent ductal differentiation.

Design: Cases of pancreatic ACCs with significant (>25% of the tumor) ductal differentiation were identied in the surgical pathology databases of two academic centers. Patient clinical information, gross and histologic features, and histochemical and immunohistochemical (IHC) results were recorded. Cases were tested for *KRAS2* mutations.

Results: Ten cases were identified (8 men and 2 women; age range 52-77 yrs). Only 1 patient presented with jaundice. All but 1 patient were treated with primary surgery and most received adjuvant therapy. All but 1 patient with follow-up had died (dead of disease=8; 9-52 mo; ave= 26 mo). Tumors measured between 2 and 5.5 cm and were ill-defined, nodular and multilobulated. Nine were located in the head of the pancreas. All but 2 exhibited extrapancreatic invasion. In most cases (8), the acinar phenotype predominated (>50%), and the tumors were composed of nodules of neoplastic acinar cells growing in acini, trabeculae and nests. Between 10 and 75% of the neoplastic nodules contained variable amounts of extracellular mucus, focally appearing colloidal. Between 10 and 25% of the tumors cells had a mixed phenotype with granular cytoplasm displaced either by multiple, foamy vacuoles or, by a single large mucous droplet that compressed the nucleus and rendered a signet-ring cell appearance. Two cases had areas recapitulating typical PDAs while the other portions of the tumors appeared akin to the mucinous acinar cell pattern described above. All cases had intracellular and extracellular mucus by mucicarmine stain. IHC results were as follows: trypsin+ (100%), chymotrypsin+ (88%), CK19+ (100%), B72.3+ (50%), CA19.9+ (88%), synaptophysin+ (focal) (33%), and chromogranin+ (focal) (22%). Two cases had *KRAS2* mutations.

Conclusions: Despite the early embryologic divergence of acinar and ductal cell lineages, rare pancreatic tumors have both acinar and ductal differentiation, usually predominantly the former. They produce mucin and express markers of both cell lineages. The clinical course is highly aggressive.

1462 Clinicopathologic Features in Earlier Interim Liver Allograft Biopsies May Predict Recurrent Hepatitis C-Associated Fibrosis Progression

MR Stitzel, AM Larson, MM Yeh. University of Washington Medical Center, Seattle, WA.

Background: The progression rate of recurrent hepatitis C virus (HCV)-associated fibrosis in liver allografts post orthotopic liver transplant (OLT) varies, in which the roles of both viral and host factors have been suggested. We studied the histologic features in interim (IT) allograft biopsies that subsequently developed early fibrosis progression due to recurrent HCV.

Design: Cases of OLT performed for HCV cirrhosis at a major liver transplant center during 2001-2008 were retrospectively reviewed. All recurrent HCV biopsies (bx) developing at least Batts/Ludwig (BL) stage 2 fibrosis within 4 years as progressors (PR) and those developing no or only stage 1 fibrosis in a similar time period (endpoint: EP) as non-progressors (NP) were included. Earlier IT bx within 15 months post OLT in PR and those in a similar period in NP when available were reviewed. After cases not meeting inclusion criteria and cases with rejection/complications were excluded, 32 PR and 22 NP remained. Histologic features including BL grade/stage, Ishak scores, acidophil body index (ABI: total acidophil body count/mm^2), steatosis, and cholestasis were assessed at the consensus of two authors blinded to fibrosis progression status and lab data.

Results:

Median or mean(*) histologic parameters in interim biopsies

	ABI*	BL Grade	BL Stage	Ishak Portal Inflammation	Ishak Periportal Injury*	Ishak Parenchymal Injury	Ishak Fibrosis
PR	0.594	2.5	1.5	2	1.75	2	2
NP	0.083	1	0	1	1	1	0
p-value	0.009	0.0341	0.0005	0.0027	0.0357	0.0060	0.0002

There was no significant difference in age, gender, and race between PR and NP. Mean duration from OLT to EP bx in PR and NP was 24 and 40 months, respectively ($p=0.02$) and from OLT to IT bx was 10 and 20 months, respectively ($p=0.07$). ABI, BL grade/stage, and Ishak scores of various inflammation/fibrosis parameters of IT bx were significantly higher in PR vs NP (Table); there was no significant difference in steatosis

and cholestasis. Liver function tests (LFT), including ALP, ALT, AST, and GGT were also higher in PR vs NP at time of IT bx (p: all<0.05).
Conclusions: Our findings suggest that acidophil body index, BL grade/stage, and Ishak scores in interim bx (10-20 months), along with LFT may predict subsequent progression of recurrent HCV-associated fibrosis. Large cohort and/or prospective studies are warranted to validate these observations.

1463 Molecular Divergence within Synchronous and Metachronous Intraductal Papillary Mucinous Neoplasms

L Stoll, JK Ryu, E Chen, S Egawa, M Ishida, M Akada, F Motoi, M Unno, RD Schulick, T Furukawa, RH Hruban, A Maitra. Johns Hopkins University, Baltimore; Tohoku University Graduate School of Medicine, Sendai, Japan; Tokyo Women's Medical University, Tokyo, Japan.
Background: Intraductal papillary mucinous neoplasms (IPMNs) are cystic precursor lesions of pancreatic adenocarcinoma, and demonstrate a propensity for multifocality. This can present as either synchronous or metachronous IPMNs. The molecular basis for multifocality is poorly defined.
Design: We evaluated a series of six synchronous and five metachronous cases of IPMNs collated from the United States and Japan. In addition to assessment of clinico-pathological features, expression of p53 and Dpc4 was analyzed by immunohistochemistry, and *KRAS2* gene sequencing was performed on laser microdissected tissue obtained from one multifocal synchronous and two metachronous IPMNs.
Results: The average age of patients with synchronous IPMNs at presentation was 70 years (61-83 years), with a female predominance (66%). In contrast, the average age at presentation of first metachronous lesion was 66 years (50-75 years), and all patients were male in this series. The pathology of synchronous IPMNs included moderate dysplasia (66%), high-grade dysplasia (carcinoma-*in-situ*) (17%), and IPMN with invasive carcinoma (17%). The pathology of metachronous IPMNs at first presentation were moderate dysplasia (40%) and high-grade dysplasia (60%); at recurrence, the lesions demonstarted moderate dysplasia (20%), high-grade dysplasia (20%), and IPMN with invasive carcinoma (60%). Neither aberrant loss of Dpc4 expression nor nuclear accumulation of p53 was observed in any of the non-invasive synchronous or metachronous IPMNs. In one metachronous IPMN pair, identical *KRAS2* mutations were seen in the primary and its recurrence, while in another metachronous pair, a *de novo* mutation was observed only in the recurrent lesion. In a multifocal synchronous IPMN, DNA from independently microdissected cysts demonstrated distinct codon 12 mutations (GGT-GAT or GGT-GTT), consistent with independent genetic hits in the same carcinogenic field.
Conclusions: Multifocal IPMN lesions likely represent independent clones of cystic neoplasia in the pancreas, further underscoring the need for continued follow up even in patients with resected non-invasive lesions.

1464 Useful Pathologic Features To Distinguish Telangiectatic/ Inflammatory Hepatocellular Adenoma from Other Benign Hepatocellular Tumors

AA Suriawinata, KH Lim, MI Fiel, L Qin, S Ward, DJ van Leeuwen, SN Thung. Dartmouth-Hitchcock Medical Center, Lebanon, NH; Singapore General Hospital, Singapore, Singapore; Mount Sinai Medical Center, New York, NY.
Background: Telangiectatic/inflammatory hepatocellular adenoma (TIHA) of the liver, previously described as "telangiectatic focal nodular hyperplasia", is a neoplasm that had been considered as a variant of focal nodular hyperplasia (FNH). Recent studies indicated that TIHA are monoclonal; therefore, TIHA was reclassified as a variant of hepatocellular adenoma (HA). Distinguishing one from another remains problematic when the specimen is small and clinical studies are inconclusive. To clarify TIHA diagnostic features, we studied gross morphology, histologic and immunohistochemical features of these benign tumors.
Design: We identified 13 archived cases (11 resections, 2 biopsies) of TIHA between 2000-6. For comparison, 13 resections of FNH and 16 of conventional HA were selected. Gross morphology and histologic features were evaluated for the presence of unpaired arteries, dilated sinusoids at least 30% of the lesion, trabecular thickness, cellular atypia, portal tract like structures (PTLS) containing dystrophic arteries, PTLS with bile ductules, steatosis in lesion and adjacent tissue, chronic inflammation; and detailed study of the vasculature including presence of thin and thick walled vessels, vessels draining directly into the sinusoids and clustered ectactic vessels. Selected representative sections were immunohistochemically stained for CK7, MIB-1, p53 and serum amyloid A (SAA).
Results: In addition to the characteristic soft and hemorrhagic gross morphology and the absence of central scar, we identified four histologic features useful to diagnose TIHA(p<0.001): ≥30% of dilated sinusoids, PTLS with bile duct, vessels draining directly into sinusoids and ectatic thin-walled vessels. Other features of TIHA, not statistically significant, but aid to the distinction of TIHA vs. HA are chronic inflammation and presence of thick walled arteries; and TIHA vs. FNH are cellular atypia and presence of unpaired arteries. CK7 reacted to ductular epithelium in TIHA and FNH, but absent in HA. SAA were positive in majority of TIHA and HA, but negative in FNH. The intensity of SAA staining correlated with the degree of inflammation in TIHA. MIB-1 and p53 were not helpful in differentiating these tumors.
Conclusions: We have identified a subset of pathologic features that are useful to the diagnosis and distinction between TIHA from other benign hepatocellular tumors.

1465 Prognostic Differences between Ampullary Carcinomas and Pancreatic Ductal Adenocarcinomas: The Importance of Size of Invasive Component

T Tajiri, O Basturk, A Krasinskas, I Coban, S Bandyopadhyay, E Levi, CK Chu, D Kooby, JM Sarmiento, C Staley, NV Adsay. Emory U., Atlanta; NYU, NY; U. of Pittsburgh, Pittsburgh; WSU, Detroit.
Background: Ampullary adenocarcinomas (AAC) are thought to be more indolent than pancreatic ductal adenocarcinomas (PDA); however, this impression is based mostly on clinical databases with vague inclusion criteria for AAC and lack of pathologic confirmation.
Design: 89 cases of resected invasive AAC were analyzed and compared with 113 cases of PDA. A tumor was classified as AAC only if **1)** the epicenter was located in the *ampulla/major papilla* and/or **2)** there was convincing preinvasive lesion (adenoma/CIS) in the *ampullary/papilla of Vater mucosa*. CBD, pancreatic, duodenal, periampullary-duodenal and retroampullary CBD carcinomas were excluded on critical review.
Results: Median overall survival (OS) of AAC was significantly better than that of PDA (38 mos *vs* 11 mos, p<0.001). 1-, 2-, and 3-year survival were 0.85, 0.68 and 0.51 for AAC *vs* 0.47, 0.21 and 0.11 for PDA. AAC overall tumor size was smaller than PDA size (2.73cm±1.57 *vs* 3.59cm±1.80; p<0.001). Further, size of the invasive component in AAC was significantly smaller than that of PDAs (1.66cm±0.91 *vs* 3.59cm±1.80; p< 0.001). In more than a third of AAC, the preinvasive component (adenoma and/or in-situ/intramucosal carcinoma) constituted more than half of the bulk of the tumor. The invasive component was ≤1cm in diameter in 26% of AAC compared with only 3% of PDA at presentation (p<0.001). AAC was also less likely to be associated with nodal disease (47% AAC *vs* 73% PDA , p<0.001); however, the lower incidence of lymph node metastasis in AAC also appeared to be releated to smaller size of invasion: the incidence of lymph node metastasis in ≤1.0cm, >1.0-≤2.0cm, >2.0cm groups in AAC were 23%, 42% and 70% respectively (spearman rank correlation, p=0.0005).
Conclusions: AAC carries better survival than PDA, although the comparison may be unfair due to differences in tumor size and invasive component size. AAC at presentation is substantially smaller than that of PDA. In a third of AAC, more than 50% of the tumor is preinvasive, presumably leading to detection before the tumor reaches a more detrimental stage. Incidence of lymph node metastasis is also significantly less common in AAC; however this is also possibly related to smaller size of invasion.

1466 FoxP3-Expressing T Regulatory Cells (T-regs) Increase with the Severity of Active Disease in Chronic Hepatitis C

AD Toll, JL Farber. Thomas Jefferson University Hospital, Philadelphia, PA.
Background: The hepatitis C virus (HCV) leads to chronic disease in 80% of those infected and is associated with a chronic inflammatory response that is mediated by both cytokine producing ($CD4^+$) and cytotoxic T cells ($CD8^+$). FoxP3-expressing, $CD4^+$, $CD25^+$ T cells (T-regs) are a subset of T lymphocytes that inhibit immune responsiveness and, thereby, control immunological reactions. Whether $FoxP3^+$ T regulatory cell-mediated suppression is a factor in HCV persistence and/or the course of chronic liver injury has not been defined. In order to assess the association between these T regulatory cells and the severity of chronic hepatitis C, we evaluated liver biopsies for the density of FoxP3-expressing cells in relation to the degree of inflammation.
Design: Forty liver biopsies from patients with chronic hepatitis C were obtained from the archives of the Department of Surgical Pathology of Thomas Jefferson University Hospital. The biopsies were selected to be equally divided between those with mild and moderate-severe necroinflammatory activity based on a modified histological activity index (HAI) after Ishak et al.(*J Hepatol* 22:696, 1995). The biopsies were stained for FoxP3 (eBioscience Cat #14-4777-82). A representative area of portal inflammation was photographed at 400X, and the percentage of $FoxP3^+$ cells relative to the total number of lymphocytes was calculated.
Results: The 20 cases of mild chronic hepatitis C had a mean necroinflammatory (HAI) score of 2.7 $\pm$ sd 1.1, whereas the moderate to severe cases had a mean HAI score of 7.6 $\pm$ sd 0.7 (p< 0.001, student t-test). The number of lymphocytes in a 400X field was greater in the moderate-severe cases than in the mild cases (412 $\pm$ sd 92 versus 182 $\pm$ sd 102; p<0.001, student t-test). The mean percentage of $FoxP3^+$ T cells among the mild cases was 7.4 $\pm$ sd 3.3. By contrast, the mean percentage of $FoxP3^+$ T cells among the moderate-severe cases was 14.2 $\pm$ 4.2 (p< 0.001, student t-test).
Conclusions: In chronic hepatitis C, $FoxP3^+$ T regulatory cells increased with greater inflammation that reflected, in turn, more severe liver disease. Thus, the density of T-regs reflected the activity of the chronic hepatitis. Such a conclusion does not support the hypothesis that greater activity in chronic hepatitis C is related to a reduced level of regulatory control by $FoxP3^+$ T cells (T-regs).

1467 Hepatitis C Infection: Can It Cause Hepatocellular Carcinoma in Non-Cirrhotic Livers?

M Torbenson, HD Daniel, MM Yeh. Johns Hopkins Univ, Baltimore, MD; Univ of Washington, Seattle, WA.
Background: Chronic hepatitis C viral (HCV) infection can lead to cirrhosis and hepatocellular carcinoma (HCC). It is generally believed that HCV is not oncogeneic per se, but that the presence of cirrhosis determines the increased risk for HCC. To date there is little data on HCC arising in HCV infected, but non-cirrhotic livers.
Design: To further study HCCs arising in this setting, we searched our files from 1982-2008 for HCCs resected for curative intent. Cases with clinical or serologic evidence of HBV coinfection were excluded. All remaining cases were tested for occult HBV by PCR in formalin-fixed, paraffin embedded tissues. The tumors were further tested for CTNNB1 (beta catenin) exon 3 mutations. TP53 was also tested for codon 249 mutations, a characteristic mutation strongly linked to aflatoxin exposure.
Results: 18 non-cirrhotic HCC cases arising in HCV were identified. All were negative for occult HBV infection. Average age at resection was 58 years (M:F=14:4), including 9 Whites, 5 Blacks, 2 Asians, and 2 Egyptians. Only 1 had additional risk factors for

fibrosis (iron overload and significant alcohol use). The cases were not enriched for unusual HCV genotypes:1A,1B,2B,3A,4, unavailable (n=3,3,2,1,2,7, respectively). HCV viral loads averaged 6.48 log IU/ml (available in 7 cases). Only 3 had serum AFP greater than 30 ng/ml: 5188, 2329, 2303 (available in 15 cases). 4 showed bridging fibrosis while 7 showed portal fibrosis; none were cirrhotic. The average tumor size was 5.9 cm and tumors were unifocal in 9 cases and multifocal in 9 cases. AJCC staging was: T1 (n=6), T2 (n=8), T3 (n=4). Histology of tumors (not available in 1 case due to necrosis) showed typical HCCs, with Edmonson-Steiner grades 1 (n=2), 2 (n=5), 3 (n=7), and 4 (n=3) and showed pseudoglandular (n=6), solid (n=9), or mixed (n=2) patterns. No mutations were seen in exon 3 of CTNNB1 or in TP53.

Conclusions: Our results clearly demonstrate that HCC can arise in livers chronically infected with HCV but without cirrhosis. The HCCs had typical histology with no enrichment for unusual growth patterns. In this cohort, occult HBV was not detected and there was no molecular evidence for aflatoxin exposure. These findings raise the possibility that in some cases HCV can be directly oncogeneic. It is also possible that established cirrhosis may have regressed in some cases. Regardless of the mechanism, these findings highlight an important and previously under-recognized risk for HCC in HCV infected individuals who do not have cirrhosis.

1468 The Role of Hepatic Progenitor Cell Activation and Periportal Ductular Reaction Presence in Chronic Hepatitis C and B. A Clinicopathologic Study

A Tsamandas, K Thomopoulos, I Syrokosta, D Dimitropoulou, C Karatza, C Gogos. Univ. of Patras, Patras, Greece.

Background: Hepatic progenitor cells (HPC) are liver stem cells that involved in the progress of liver disease. This study investigates the potential correlation of HPC activation and the resultant periportal ductular reaction (PDR) with disease severity and response to treatment, and impaired liver cell replication, in patients with HCV and HBV.

Design: The study included 284 liver biopsies obtained from 142 patients with HCV(n=77) and HBV(n=65). All patients received therapy and assigned as: [**HCV:**responders(A=29), non-responders(B=29), relapsers(C=19)], [**HBV**:"responders"(negative HBVDNA and LFTs normalization) (D=40) and "non-responders" (E=25). 77 HCV/65 HBV biopsies were obtained before treatment (A1/ B1/C1/D1/E1) and the remaining after (A2/B2/ C2/D2/E2). Paraffin sections were stained with antibodies to CK7, LCA, CD34, and p21. Cells with features of HPC (Roskams T, Hepatology 39:1739, 2004) that were CK7+/LCA(-)/CD34(-) were scored. The same reference was used to define PDR. The presence of HPC was also determined by gene analysis for AFPmRNA, performed on microdissected liver tissue samples. PDR was quantified as % of biopsy area.

Results: The table lists the results. Statistical analysis revealed significant correlation between **a)** HPC with fibrosis (HCV: p=0.0028, HBV: p=0.0041) and inflammation (HCV: p=0.0035, HBV: p=0.0052), **b)** PDR and fibrosis (HCV: p=0.0017, HBV: p=0.0024). Impaired hepatocyte replication (%p21+ cells) was independently associated with **a)** %HPC (HCV: p=0.0031, HBV: p=0.0048) and **b)** PDR (HCV: p =0.0042, HBV: p =0.0061). Multivariate analysis showed that PDR is independent factor for the prediction of fibrosis.

Conclusions: This study shows that in HCV and HBV cases, HPC activation and PDR degree, are significantly decreased in patients with response to treatment, implying that they are strongly correlated with disease severity. The fact that these factors are associated with impaired hepatocyte replication implies the presence of an alternative pathogenetic pathway during liver regeneration that leads to PDR and progressive liver fibrosis, with consequent liver failure.

Groups		HPC-CK7+	AFPgene	PDR
A	A_1	30.7±1.9*	32.5±2.1$^{£}$	28.8±4.5^{+}
	A_2	8.3±1.4*	9.2±1.8$^{£}$	4.6±1.4^{+}
B	B_1	53.4±6.3	54.2±8.1	48.3±7.1
	B_2	51.2±5.4	52.7±6.2	47.5±6.3
C	C_1	49.7±1.8	50.6±3.4	46.6±7.1
	C_2	47.3±4.3	46.9±7.2	43.5±5.2
D	D_1	29.3±3.4$^{\$}$	31.6±4.2$^{¥}$	26.3±5.1§
	D_2	7.2±1.1$^{\$}$	8.3±1.3$^{¥}$	3.9±1.2§
E	E_1	52.1±7.2	53.4±9.2	46.4±8.3
	E_2	50.9 6.3	51.8 7.4	46.3 7.1

*, £, +, $, ¥, § :p<0.001

1469 The Role of RCC-Ma in Evaluating Primary and Metastatic Clear Cell Carcinomas in the Liver

DL Tunnell, MP Bronner. Cleveland Clinic, Cleveland, OH.

Background: The differentiation between primary hepatocellular carcinoma (HCC) and metastatic renal or adrenocortical cell carcinoma (RCC, ACC) can be difficult. The neoplastic cytology and growth patterns can be indistinguishable. Immunohistochemistry for hepatocyte specific markers can be helpful but may not be definitive. The goal of this study was to evaluate RCC-Ma in primary HCC and hepatic metastases of RCC and ACC.

Design: From 1993-2007, thirty-two cases of hepatic metastases of RCC and seven of ACC were studied. Of the metastatic RCCs, 68% (22/32) were of the clear cell type, while none of the ACC metastases were clear cell tumors. Nine of the RCC cases also had available matched primary renal tumor, of which 77% (7/9) were clear cell type. Twenty-two cases of primary HCC were used as controls, 27% (6/22) of which were of clear cell morphology. Immunohistochemistry (IHC) for HepPar-1, CD10, polyclonal CEA and RCC-Ma were performed.

Results: The immunohistochemical results are indicated in the table.

IHC Marker	HCC Primary	ACC hepatic mets	RCC hepatic mets	RCC primary
RCC-Ma	0% (0 of 22)	0% (0 of 7)	28% (9 of 32)*	66% (6 of 9)*
CD10 (non-canalicular)	0% (0 of 22)**	42% (3 of 7)***	90% (29 of 32)*	100% (9 of 9)*
Polyclonal CEA	27% (6 of 22)	0% (0 of 7)	0% (0 of 32)	0% (0 of 32)
HepPar1	72% (16 f 22)	0% (0 of 7)	3% (1 of 32)	0% (0 of 9)

*Both primary and metastatic RCC demonstrated membranous and/or cytoplasmic staining with RCC-Ma and CD10. The CD10 cytoplasmic and membranous pattern in RCC was distinct from the **fine canalicular staining pattern present uniformly in liver. ***The staining pattern of CD10 in ACC was faintly cytoplasmic and also distinct from that in HCC and RCC.

Conclusions: RCC-Ma revealed a 66% sensitivity for primary RCC, which decreased to 28% in RCC hepatic metastases, whereas non-canalicular CD10 showed 90% sensitivity in hepatic metastases of RCC. The specificity for distinguishing metastatic RCC from primary HCC was 100% for RCC-Ma and 100% for CD10 (non-canalicular), as none of the 22 primary HCCs stained with RCC-Ma or had the cytoplasmic/membranous pattern of CD10. None of the markers was useful for distinguishing ACC from HCC. As a panel approach, these markers are diagnostically useful for distinguishing metastatic RCC from primary HCC.

1470 Periportal Apoptotic Bodies Are Helpful in Distinguishing Recurrent Hepatitis C from Rejection in Liver Allograft Biopsies

WS Twaddell, JH Lefkowitch. University of Maryland Medical Center, Baltimore, MD; Columbia University Medical Center, New York, NY.

Background: Hepatitis C virus (HCV) is the most common indication for liver transplantation worldwide. Histologic differentiation between acute rejection and recurrent chronic hepatitis C following transplantation is a common diagnostic dilemma. This study was undertaken to test the hypothesis that the presence of periportal apoptotic bodies (ABs) in allograft biopsies is a marker of acute rejection and is useful in establishing this diagnosis even in difficult cases where HCV recurrence is also present.

Design: The CUMC Surgical Pathology database was reviewed to select liver biopsies from 3 patient groups: Grp. 1 (non-transplant patients with chronic hepatitis C); Grp. 2 (allograft biopsies showing acute rejection after transplantation for causes other than HCV); and Grp. 3 (allograft biopsies from patients transplanted for chronic hepatitis C). The histologic criteria for acute rejection were those of the Banff consensus document, and recurrent hepatitis C was diagnosed using standard histologic criteria. For each case, H&E slides were evaluated for numbers of lobular and periportal ABs and the percent in each region was compared to the total number per case.

Results: The total number of ABs varied considerably among groups (Table 1).

Table 1

	HCV- No Transplant	Transplant- No HCV	HCV & Transplant
Density: Average ABs/Lobule	0.98 +/- 0.71	1.19 +/- 1.30	1.89 +/- 1.97
% ABs in Periportal Zone	12.08 +/- 10.16	23.11 +/- 14.96	19.87 +/- 15.02

Biopsies from Grp. 1 showed < 20% of all ABs in the periportal regions, whereas Grp. 2 biopsies showed >20% of total ABs in periportal regions. For Grp. 3, two distinct subgroups were identified: biopsies in which rejection was the predominant element showed 18-50% of total ABs to be present in periportal regions, while biopsies showing predominant features of recurrent HCV showed 0-19% of total ABs in periportal regions.

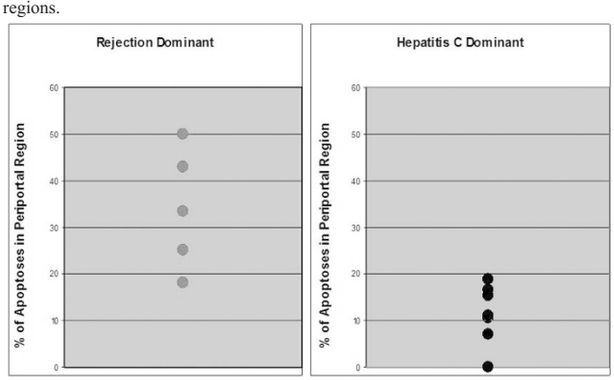

Conclusions: Routine chronic hepatitis C biopsies (non-transplanted) show a range in periportal apoptotic bodies, but very large numbers, particularly if more than 20% of the total number of ABs, favors a diagnosis of acute rejection.

1471 IMP3 Expression Can Distinguish Cholangiocarcinomas and Metastatic Pancreactic Ductal Carcinomas from Benign Bile Duct Lesions

DG Wagner, Q Yang, LA McMahon, BO Spaulding, HL Wang, H Xu. University of Rochester Medical Center, Rochester; Dako North America, Carpinteria; Cedars-Sinai Medical Center, Los Angeles.

Background: Insulin growth factor (IGF) messenger RNA binding protein 3 (IMP3), also known KOC and L523S, is expressed during embryogenesis and in malignancies. It functions to promote tumor cell proliferation by enhancing IGF-II protein expression. IMP3 expression in cholangiocarcinoma and pancreatic ductal carcinoma has been reported, but its diagnostic value in segregating these two types of malignancy from benign ductal lesions has not been investigated.

Design: Surgically resected or biopsied cholangiocarcinomas (intrahepatic, n=41; extrahepatic, n=4), metastatic pancreatic ductal carcinomas in the liver (n =4), pancreatic ductal carcinomas (n=20), bile duct adenomas (intrahepatic, n=5; extrahepatic, n=2) and bile duct hamartomas (n=11) were immunohistochemically studied using a monoclonal antibody against IMP3 (Dako). Cytoplasmic staining was considered positive. The percentage of positively stained tumor cells was recorded and the staining intensity was graded as weak, moderate or strong. A p value of <0.05, as determined by two-tailed Fisher exact test, was considered statistically significant.
Results: Thirty-nine of 45 (87%) cholangiocarcinomas were positive for IMP3, among which 35 cases showed moderate or strong cytoplasmic staining in >90% of tumor cells and 4 cases exhibited weak to moderate staining in 40-50% of tumor cells. Three of 4 (75%) metastatic pancreatic ductal carcinomas showed strong cytoplasmic staining in >90% of tumor cells. Of 20 pancreatic ductal carcinomas, 15 (75%) were moderately to strongly positive for IMP3 in >90% of tumor cells, and the remaining 5 cases showed a variable degree of cytoplasmic staining in 10-50% of tumor cells. IMP3 expression was not significantly different among these groups. In contrast, no IMP3 expression was detected in any of 7 bile duct adenomas or 11 bile duct hamartomas. The non-neoplastic bile ducts or ductules in tumor sections were also completely negative for IMP3 expression.
Conclusions: A large proportion of cholangiocarcinomas and metastatic or primary pancreatic ductal carcinomas highly expressed IMP3 but benign biliary lesions did not. These findings indicate that immunohistochemical detection of IMP3 expression can be utilized to distinguish benign bile ductal lesions from malignant pancreaticobiliary carcinomas, in particular when limited material from a needle core biopsy is evaluated.

1472 IMP3 Expression Can Distinguish Hepatocellular Carcinoma from Hepatocellular Adenoma

DG Wagner, Q Yang, LA McMahon, BO Spaulding, HL Wang, H Xu. University of Rochester Medical Center, Rochester; Dako North America, Carpinteria, Carpinteria; Cedars-Sinai Medical Center, Los Angeles.
Background: Insulin growth factor (IGF) messenger RNA binding protein 3 (IMP3), also known as K homology domain containing protein overexpressed in cancer and L523S, is predominantly expressed in embryogenesis. In recent years, IMP3 expression has been identified in multiple malignant neoplasms including hepatocellular carcinoma (HCC) (Jeng YM, et al. Hepatology, in press). The study by Jeng YM et al also indicated that IMP3 plays an important role in tumor invasion and metastasis and is a strong prognostic factor for patients with HCC. It is often difficult to segregate hepatocellular adenoma (HCA) from HCC when HCC is well-differentiated and/or limited tissue from a needle biopsy is examined. The aim of this study was to determine if immunohistochemical detection of IMP3 serves as a useful diagnostic tool in the distinction between these two hepatocellular neoplasms.
Design: Fifty-two surgical resected or biopsied specimens of well- to moderately-differentiated HCC (resection, n=16; needle, n=3) and HCA (resection, n=31; needle, n=2) were obtained from University of Rochester and Cedars-Sinai Medical Centers. Immunohistochemistry was performed using a monoclonal antibody against IMP3 (Dako). Cytoplasmic staining was considered positive. The percentage of positively stained tumor cells was recorded and the staining intensity was graded as weak, moderate, or strong.
Results: Immunohistochemical studies showed that 12 of 19 well- to moderately-differentiated HCCs (63%) were moderately to strongly positive for IMP3. Among them, 9, 1 and 2 cases showed 5-10%, 20% and >90% of tumor cells positively stained for IMP3, respectively. Interestingly, IMP3 protein was predominantly expressed in tumor cells at the periphery of the tumors. In contrast, no IMP3 expression was detected in any of 33 HCAs or non-neoplastic hepatic tissues.
Conclusions: A large proportion of HCCs expressed IMP3 with a predominant staining at the periphery of the tumors, but HCAs and non-neoplastic hepatic tissues did not. These findings indicate immunohistochemical detection of IMP3 expression can serve as an additional diagnostic tool in segregating well differentiated HCC from HCA or non-neoplastic hepatic tissues, in particular when limited material from a needle biopsy is evaluated.

1473 Naked Islets of Langerhans Are Frequently Found in Patients with Pancreatic Endocrine Neoplasms

R Wilcox, A Noffsinger. University of Chicago, Chicago.
Background: 90% of pancreatic endocrine cells reside within islets of Langerhans. The remainder lie scattered among the acini and along the larger pancreatic ducts. Rarely, isolated, naked islets have been reported outside the pancreas proper, in the peripancreatic fat. In our experience, this phenomenon usually occurs in the distal pancreas, and is more common in patients with pancreatic endocrine neoplasms. Based on this observation, we examined distal pancreatectomy specimens from patients with endocrine neoplasms and other pancreatic pathologies to determine the frequency with which naked islets occur.
Design: 29 distal pancreatectomy specimens were reviewed, 14 of which were performed for endocrine tumors, and 15 for other reasons (ductal adenocarcinoma, pancreatic pseudocyst, solid pseudopapillary tumor, mucinious cystadenoma). Naked islets, defined as islets sitting alone in the peripancreatic fat without accompanying ductal or acinar structures, were recorded as present or absent, and their distance from the closest adjacent pancreatic tissue was determined. These foci were clearly delineated from changes of chronic pancreatitis in that they lacked fibrosis or evidence of residual pancreatic structures. The clinical histories from all patients were reviewed. Stains for neuroendocrine markers and specific pancreatic endocrine products were performed in a subset of cases from patients with pancreatic endocrine tumors.
Results: 6 of the 14 distal pancreatectomies performed for endocrine tumors showed naked islets (43%). In 2 cases, the islets were present within 1 mm of the pancreatic parenchyma. In the remaining four cases, naked islets extended from 2 mm to over 1 cm beyond the pancreas proper. Immunohistochemical staining showed the same distribution of pancreatic endocrine products with naked islets as in the normal intrapancreatic islets. None of the patients with naked islets had any clinical features suggesting multiple endocrine neoplasia syndrome, nor were any of the tumors clinically functional. However, the 2 patients with the most extensive distribution of naked islets were the only 2 patients who were symptomatic (nausea, vomiting, night sweats). Among the 15 pancreata resected for non-endocrine lesions, 2 showed small foci of naked islets within 1 mm of the pancreas proper.
Conclusions: Naked islets are seen in a small proportion of distal pancreatectomy specimens, and are usually located within 1 mm of the pancreas proper. This finding is most commonly seen in patients with endocrine neoplasms (43%), and may be quite extensive in some individuals.

1474 The Significance of On-Site Evaluation of Image-Guided Core Needle Biopsy of Liver Masses

S Williams, S Sahoo, H Alatassi. University of Louisville, Louisville, KY.
Background: Image-guided core needle biopsy (CNB) is a safe, rapid and cost-effective procedure for sampling of liver masses. It is extremely important for the radiologist who obtains a core biopsy under ultrasound or CT guidance to accurately place the needle and sample the lesional tissue. Immediate evaluation of touch imprint cytology (TIC) of the core biopsy by a pathologist during the procedure not only ensures the lesion has been sampled, but also minimizes the number of needle punctures.
Design: A retrospective review of all image-guided CNB performed for the evaluation of liver masses over last 5 years was performed. In all cases, a pathologist was available for on-site evaluation of the TIC of the cores to assess sample adequacy. The aim of the study was to evaluate the impact of providing rapid interpretation in reducing the number of passes required before obtaining diagnostic material.
Results: Of the 70 CNB of liver masses, 54 were malignant (50 metastases and 5 hepatocellular carcinoma) and 13 were benign lesions (1 focal nodular hyperplasia, 5 cirrhotic nodules and 7 cases with non-specific findings). Three cases that were interpreted as inadequate on TIC remained inadequate on the final interpretation. Specimen adequacy was correctly interpreted 69 of 70 cases (99%): on the first pass in 51 cases (72%), on the second in 13 cases (19 %) and on the third in 6 cases (9%). Only in one case, the pathologist was unable to accurately diagnose the malignancy on TIC. In 3 cases, the immediate evaluation was that of a lymphoid malignancy which led to allocating part of the sample for flow cytometry.
Conclusions: Touch imprint cytology is very sensitive for evaluating specimen adequacy of CNB. Immediate evaluation of CNB prevented unnecessary passes in vast majority of cases and facilitated triaging the specimen for further testing.

1475 Adenosquamous Carcinoma of the Pancreas Harbors KRAS2, DPC4 and TP53 Molecular Alterations Similar to Pancreatic Ductal Adenocarcinoma

AK Witkiewicz, JB Brody, CL Costantino, CJ Yeo, PM McCue, RH Hruban. Thomas Jefferson University, Philadelphia, Philadelphia, PA; The Johns Hopkins University, Baltimore, MD.
Background: Adenosquamous carcinoma of the pancreas is one of the most malignant forms of pancreatic cancer.There is a lack of comprehensive molecular information about this rare tumor. We analyzed the pathologic and molecular features of eight cases of pancreatic adenosquamous carcinomas.
Design: For *KRAS2* and *p16/CDKN2a* mutational analysis, squamous and adenocarcinoma components of adenosquamous carcinomas were isolated by Laser Capture Microdissection . DNA sequencing was done by capillary gel electrophoresis. Immunohistochemistry was performed using the Envision Plus system (DAKO) with antibodies to DPC4 (Santa Cruz, 1:500), p53 (DAKO,1:100), E-cadherin (DAKO, 1:100), EGFR (Santa Cruz, 1: 100) and p16 (Novocastra, 1:100).
Results: We detected *KRAS2* gene mutations in all cases, all at codon 12, in both the squamous and adenocarcinomatous portions. All cases also showed loss of p16 protein; in three of these it was due to p16/CDKN2a gene exon 2 homozygous deletion. The majority of cases had loss of Dpc4 protein and nuclear p53 staining similar to the molecular signature found in pancreatic ductal adenocarcinoma. E-cadherin was either lost or reduced in almost all cases and all cases were EGFR positive. The squamous component stained with p63 antibody and this antibody was helpful in identifying squamous differentiation in adenosquamous carcinomas with an acantholytic growth pattern.

Immunohistochemical profile of adenosquamous carcinoma

	Dpc 4	P53	P16	E-Cadherin	P63	EGFR
Case 1	Lost	Negative	Negative	Lost**	Positive	Positive
Case 2	Lost	Positive*	Negative	Reduced***	Positive	Positive
Case 3	Lost	Negative	Negative	Lost	Positive	Positive
Case 4	Intact	Positive	Negative	Lost	Positive	Positive
Case 5	Lost	Negative	Negative	Reduced	Positive	Positive
Case 6	Intact	Positive	Negative	Normal	Positive	Positive
Case 7	Lost	Positive	Negative	Lost	Positive	Positive
Case 8	Intact	Positive	Negative	Reduced	Positive	Positive

* defined as nuclear staining in >75% of tumor cells. ** <10% of the neoplastic cells labeled, *** labeling in 10-50%

Conclusions: In summary, although pancreatic adenosquamous and ductal adenocarcinoma have overlapping molecular characteristics, frequent loss of E-cadherin and higher percentage of EGFR expression could account for the more aggressive nature of this tumor and thus could be potential therapeutic targets.

1476 Acidophil Body Index May Help Diagnosing Non-Alcoholic Steatohepatitis

MM Yeh, P Belt, EM Brunt, KV Kowdley, A Unalp, L Wilson, L Ferrell. University of Washington, Seattle, WA; Johns Hopkins University, Baltimore, MD; Washington University, St. Louis, MO; Virginia Mason Medical Center, Seattle, WA; University of California, San Francisco, San Francisco, CA.

Background: The histologic features of non-alcoholic steatohepatitis (NASH) consist of steatosis, lobular inflammation, and ballooned hepatocytes. It is not certain if other features, such as the quantity of acidophil bodies (AB), are associated with NASH. We quantified AB in liver biopsies and examined the correlation with the diagnosis of NASH and other histologic features reviewed by the NASH CRN Pathology Committee.

Design: We reviewed 159 liver biopsies (<2 cm in length were excluded) obtained from participants enrolled in the NASH CRN Database during 1/06 through 12/06 (>18 years old, n=129) including 95 definite NASH, 41 borderline for NASH, and 23 definitely not NASH. The total length and average width of the core biopsies were measured and the biopsy areas were calculated (mm^2). Total AB were counted and mean AB count per mm^2 was calculated (AB/mm^2) as acidophil body index (ABI).

Results: ABI was 0.04(±0.1) in definite NASH and 0.02(±0.0) in borderline/definitely not NASH groups combined (p=0.03) in all 159 biopsies; same correlation was also present in the 129 adult only biopsies (0.04±0.1 and 0.02±0.1, respectively, p=0.01). In all 159 biopsies, increased ABI correlated with greater lobular inflammation (p=0.01). Additionally, ABI tended to be higher when ballooned hepatocytes were "many" (p=0.05) and when NAFLD activity score (NAS) was greater than 3 (p=0.05). These correlations reached statistical significance in the adult population: ABI was 0.04±0.1 and 0.03±0.1 when ballooned hepatocytes were many vs absent/few, respectively (p=0.03) and 0.04±0.1 and 0.02±0.1 when NAS was 4-8 vs 0-3, respectively (p=0.03). Finally, ABI did not correlate with the degree of steatosis or stage of fibrosis in either the entire group or in adult only group.

Conclusions: There were significant correlations between the density of AB in liver biopsies and lobular inflammation, ballooned hepatocytes, NAS score, and the diagnosis of NASH in adult and pediatric biopsies. These results suggest the involvement of the apoptosis in NASH-associated liver cell injury. Acidophil body index may also be used as an additional histologic feature when a diagnosis of NASH is uncertain.

1477 Fibro-Inflammatory, Ductulo-Obliterative (FIDO) Lesions in Hepatitis C Cirrhosis

WM Yu, JS Lambe, A Gupta, JH Lefkowitch. Columbia Presbyterian Medical Center, New York, NY.

Background: Our center previously described cases of chronic hepatitis C with cirrhosis in which the nodules were entirely or partially obliterated by a combination of proliferating bile ductules, fibrosis, and inflammation (fibro-inflammatory, ductulo-obliterative or FIDO lesions). The current study was undertaken to determine the incidence of FIDO lesions in various types of cirrhosis. Immunohistochemical staining was used to develop a preliminary profile of these nodules.

Design: 61 explanted livers with varying etiologies including hepatitis C, hepatitis B, primary biliary cirrhosis, primary sclerosing cholangitis, and autoimmune hepatitis were identified in the pathology database from 2007 to 2008. The H&E slides for all the cases were retrieved and reviewed by the pathologists. The dimensions and calculated area of the reviewed sections on the slides were recorded. After the slides were examined, the number of FIDO lesions and the area encompassed by these lesions were tabulated. The formalin-fixed, paraffin-embedded tissues with the identified FIDO lesions were immunohistochemically stained with p21, CK7, SMA, and KI-67 antibodies.

Results:

	Hepatitis C	Hepatitis B	PBC	PSC	Giant cell hepatitis	Autoimmune hepatitis	Other etiologies
Number of cases	24	6	7	14	1	3	6
Number of cases with FIDO	6	0	0	1	0	0	2
Area encompassed by FIDO(cm^2)	14.8	0	0	3.53	0	0	7.17
Area examined (cm^2)	564.59	152.33	173.36	325.11	15.24	62.37	133.78
% encompassed by FIDO	2.62	0	0	1.09	0	0	5.36
% of cases with FIDO	25	0	0	7.14	0	0	33.33

24 cases of hepatitis C cirrhosis (HCV) and 37 cases of cirrhosis with other etiologies were reviewed. 6 of 24 HCV cirrhosis (25%) and 3 of 37 (8.1%) cases of non-HCV cirrhosis demonstrated FIDO lesions. For 3 cases, immunohistochemical stains were performed and showed ductules staining strongly with CK7, associated with SMA positive surrounding fibrosis. The ductular structures were negative for Ki-67 and p21 stains. The adjacent cirrhotic nodules, however, showed approximately 30-40% of the hepatocytes to have positive nuclear staining with p21 antibody.

Conclusions: In cirrhosis, progenitor cell activation with fibrosis and inflammation may obliterate all or part of cirrhotic nodules. These obliterative lesions appear to be specific to hepatitis C cirrhosis and result in loss of functional liver parenchyma. These lesions also resemble bile duct adenoma. The unique association of FIDO lesions with HCV-cirrhosis requires further investigation.

1478 Sensitivity and Specifity of IgG4 Staining in Ampullary Mucosa for Autoimmune Pancreatitis

WM Yu, A Gupta, HE Remotti. Columbia Presbyterian Medical Center, New York, NY.

Background: Autoimmune pancreatitis (AIP) is a type of chronic pancreatitis that may present as a mass lesion and mimic pancreatic carcinoma. Distinguishing AIP from neoplastic disease in the pancreas is critical to clinical management, since it is steroid responsive and usually does not require surgical intervention. AIP may be associated with increased numbers of IgG4-positive plasma cells in multiple organs. Studies have suggested immunostaining duodenal ampullary biopsies for IgG4 antibody as a useful method for diagnosing AIP. The presence of >10 IgG4-positive plasma cells per high power field (HPF) in a duodenal ampullary biopsy has been proposed by a group as a finding that supports the diagnosis of AIP. We examined duodenal ampullary mucosa in AIP and non-AIP specimens and investigated the feasibility of using the >10 IgG4-positive plasma cell/HPF cutoff in diagnosing AIP.

Design: Formalin-fixed, paraffin-embedded tissue sampling the ampullary region of Whipple resection specimens with autoimmune pancreatitis (3 cases) and control cases with adenocarcinoma (9 cases) were retrieved and were immunohistochemically stained with IgG4 antibody (Calbiochem 411492). For each case, IgG4-positive plasma cells/HPF were recorded in 10 random HPFs sampling superficial ampulla and duodenal papilla. The average number was computed for each case; sensitivity and specificity were calculated based on the averages.

Results: The average number of IgG4-positive cells in a high power field for the AIP cases range from 4.4 to 36.6, with a mean of 18.53 and median of 14.6. The average number of IgG4-positive cells in a high power field for the 9 non-AIP cases ranged from 1.3 to 16.4, with a mean of 5.38 and median of 2.6. Using the criterion that the presence of > 10 IgG-positive plasma cells /HPF supports AIP, our analysis reveals sensitivity = 67% and specificity =78%; positive predictive value =25%; negative predictive value= 88%.

	AIP1	AIP2	AIP3
Avg # of IgG4 + cells/hpf	4.4	36.6	14.6
Range of IgG4 + cells/hpf	1-13	12-55	3-36

Non-AIP1	Non-AIP2	Non-AIP3	Non-AIP4	Non-AIP5	Non-AIP6	Non-AIP7	Non-AIP8, Non-AIP9
1.3	1.3	16.4	2.3	1.7	2.6	11.6	7.7, 3.6
0-4	0-4	4-32	0-15	0-5	0-6	3-26	2-16, 0-9

Conclusions: The proposed threshold for diagnosing AIP (presence of >10 IgG4 positive plasma cells/HPF in duodenal ampullary mucosa) is not reliable for distinguishing between AIP and pancreatic adenocarcinoma. There is overlap in cases of AIP and pancreatic adenocarcinoma with false negative and false positive cases identified.

1479 The Over-Expression of Prion Protein Associated with Loss of SMAD4 in Pancreatic Ductal Adenocarcinoma

L Zhang, W Xin. Nanjing Gulou Hospital, Nanjing, Jiangsu, China; University Hospital Case Medical Center, Cleveland, OH; Case Western Reserve University, Cleveland, OH.

Background: Normal cellular prion protein (PrP) is a glycosyl-phosphatidylinositol anchored membrane protein. In our earlier study, we have detected that the over expression of PrP in about half of pancreatic ductal adenocarcinoma. However, we did not find genomic DNA or messenger RNA level changed, as well as genetic mutation. We concluded that the regulation of PrP expression was at post-transcriptional or translational level. SMAD4 (DPC4), which plays an important role in TGF-β signaling pathway, and the loss of expression has been found in 50-60% of the pancreatic ducal adenocarcinomas. In this study, we would like to explore the relationship between SMAd4 and PrP, and investigate the possible role of SMAD4 regulating PrP expression in pancreatic ductal adenocarcinomas.

Design: Sixty-seven consecutive cases of primary pancreatic ductal adenocarcinomas were selected. Forty three of these 67 carcinoma cases had regional lymph node metastasis. Immunohistochemical study was performed on tissue microarray slides using monoclonal antibodies specific for PrP and SMAD4, respectively.

Results: By immunohistochemistry, PrP expression was not detected in normal acinar, small and large non-neoplastic ductal epithelium in all cases. SMAD4 were detected in normal pancreatic tissue and pancreatitis. We found that PrP was over-expressed in 58.2% (39/67) of pancreatic carcinomas, and loss of SMAD4 was identified in 59.7% (40/67) of pancreatic carcinomas. The expression of PrP was 80.0% (32/40) in SMAD4 negative carcinomas, which was much higher than that was 25.9% (7/27) in SMAD4 positive ones (P<0.01). Nevertheless, the association of expression of PrP and loss of SMAD4 does not correlated with the tumor staging.

Table 1: The Expressions of PrP and SMAD4 in Pancreatic Ductal Adenocarcinomas

	PrP positive	PrP negative	Total
SMAD4 positive	32	8	40
SMAD4 negative	7	20	27
Total	39	28	67
Sensitiveity 80%, specificity 75%, P < 0.01			

Conclusions: Our data indicate that there is a higher rate of PrP protein over-expression in pancreatic ductal adenocarcinomas with loss of SMAD4. Therefore, the loss of SMAD4 might play an important role in regulating PrP expression, and it also suggests that PrP might involve in pancreatic carcinogenesis as a component of TGF-β signaling pathway.

1480 IgG4+ Plasma Cell Infiltrates in Liver Explants with Primary Sclerosing Cholangitis

L Zhang, J Lewis, SC Abraham, S Leung, C Rosen, J Poterrucha, TT Wu. Mayo Clinic, Rochester; MD Anderson Cancer Center, Houston.

Background: Sclerosing cholangitis can be primary (PSC) or secondary. One unusual cause of secondary sclersoing cholangitis is the newly-recognized entity of IgG4-related sclerosing disease. The prevalence and significance of IgG4+ plasma cells in patients who are clinically and radiologically classified as PSC, however, are unknown.

Design: We studied 99 consecutive liver transplants performed for clinical/radiologic diagnoses of PSC between 1996-2005. Periductal lymphoplasmacytic infiltrates in the explanted livers were scored as none, mild, moderate, or marked, and sections with the most prominent infiltrates were chosen for IgG4 immunohistochemistry (1:100; Zymed/Invitrogen). Corresponding cholecystectomy specimens (avavilable in 74 cases) were

also subjected to IgG4 immunostaining. IgG4 positivity (defined as >10 IgG4+ plasma cells/high power field) was correlated with clinical features (age, gender, presence of inflammatory bowel disease, PSC duration, PSC recurrence after transplant, and number of acute rejection episodes) and histologic findings in the liver explants (periductal fibrosis and degree of periductal lymphoplasmacytic inflammation).

Results: Twenty-three (23.2%) liver explants showed increased (>10/HPF) IgG4+ periductal plasma cell infiltration. Histologically, IgG4 positivity in the liver strongly correlated with moderate to marked periductal lymphoplasmacytic inflammation (p=0.007) but only loosely with the presence of increased IgG4+ plasma cells in the gallbladder (17.6% vs 5.3%, p=0.13). All cases showed dense periductal fibrosis; there was no storiform fibrosis (as often seen in IgG4-associated pancreatitis). Clinically, IgG4 positivity correlated with shorter PSC duration before transplant (5.3 ± 4.6 yrs vs 8.5 ± 6.2 yrs, p=0.03), but was not associated with age, gender, IBD, PSC recurrence, or rejection.

Conclusions: Nearly one quarter of explanted livers that carry a clinical diagnosis of PSC contain increased IgG4+ periductal plasma cells, a finding that correlates with more intense periductal inflammation. Whether these patients also have increased serum IgG4 levels and whether this is a distinct subtype of PSC or represents an early (more inflammatory phase) of "ordinary" PSC are questions that require further study. The shorter time to liver transplant in these patients could suggest either a more aggressive disease course of untreated IgG4+ sclerosing cholangitis, or simply an earlier phase of PSC.

1481 Frequent Aberrant Activation of the PI3K/Akt/mTOR Pathway in Pancreatic Endocrine Tumors

XP Zhou, WL Frankel, M Bloomston, OH Iwenofu, AM Bellizzi. Ohio State University, Columbus, OH.

Background: Mammalian target of rapamycin (mTOR), a serine-threonine kinase, functions in the regulation of apoptosis, proliferation, and cell growth. Signaling through the PI3K/Akt/mTOR pathway results in increased translation of key mRNAs governing cell cycle progression and metabolism. Aberrant activation of this pathway, either by signaling through growth factor receptors, activating mutations/amplification of kinases, or by loss of function of the tumor suppressor PTEN, has been described in a number of human cancers. Utilizing immunohistochemistry for PTEN, p-Akt, p-mTOR, and p-S6rp (a target of mTOR activation), we analyzed signaling through this cascade in a cohort of pancreatic endocrine tumors (PET).

Design: Tissue microarrays were constructed from formalin-fixed, paraffin-embedded blocks of 101 PET from our departmental archive and stained for PTEN, p-Akt, p-mTOR, and p-S6rp. Expression intensity was scored as 0 (absent), 1+ (modest), or 2+ (strong). Islets from 7 normal pancreata served as controls.

Results: The normal islets expressed PTEN (2+ in 4, 1+ in 3), with no demonstrable expression of p-Akt, p-mTOR, or p-S6rp. PTEN expression was detected in the majority of tumors (2+ in 77 and 1+ in 19). Twenty-three tumors showed modest (1+) p-Akt expression, which tended to inversely correlate with PTEN expression. Modest to high levels (1-2+) of p-mTOR expression were present in 79 tumors (2+ in 35, 1+ in 44), and modest to high levels of p-S6rp were detected in 37 (2+ in 8, 1+ in 29). Results are summarized in the table.

PI3K/Akt/mTOR Pathway Protein Expression

	Intensity	PTEN*	p-Akt*	p-mTOR*	p-S6rp*
PET	0	5	78	22	64
	1+	19	23	44	29
	2+	77	0	35	8
Islets	0	0	7	7	7
	1+	3	0	0	0
	2+	4	0	0	0

* data represents number of cases expressing the protein at a given intensity

Conclusions: Aberrant activation of the PI3K/Akt/mTOR pathway was detected in the majority of PET. In most of these cases this activation appears to be "downstream" (p-mTOR or p-S6rp immunoreactivity) and not attributable to PTEN loss/p-Akt activation. Given these findings, mTOR may represent a rational therapeutic target in PET.

Neuropathology

1482 Analysis of Natural Antisense Transcripts in Human beta-Site Amyloid Precursor Protein Cleaving Enzyme 1(*BACE1*)

C Arai, T Miura, K Kasai, H Nozaka, T Sato. Hirosaki University Graduate School of Health Sciences, Hirosaki, Aomori, Japan.

Background: Amyloid-beta (Abeta) is a pathologic hallmark of Alzheimer's disease (AD). BACE1 (beta-site APP cleaving enzyme1) is known as producing Abeta by processing the APP (amyloid precursor protein). BACE1 is a drug target for AD. Recently, natural antisense transcripts (NATs) are well known as functional RNA. If NATs possess overlap region in an opposite sense RNA, it is thought NATs have multiple functions, for example transcription or translation regulation, stabilization of sense-strand RNA, RNA editing, etc. But the functions of NATs have not been cleared in mammalian. Here, we identified some novel antisense-*BACE1* on the opposite strand of the *BACE1* loci, and investigated the interaction of the sense transcript and antisense transcripts of *BACE1*.

Design: We performed rapid amplification of cDNA end (RACE) and determined some novel natural antisense BACE1 in total RNA extracted from HEK293 cell line. Furthermore, to study the interaction of the sense and antisense RNA, HEK293 cells were transfected with siRNAs of *BACE1* and *AS-BACE1* including all splice variants to knockdown the expression of transcripts. The effect of the siRNAs on the expression of RNAs transcribed from the opposite strand was evaluated by the qRT-PCR.

Results: We identified 4 novel natural antisense transcripts. These all transcripts are spliced, and have poly (A) tail and conserved one exon against *BACE1* exon5. *AS-BACE1* has 135bp, 69bp and 36bp overlap regions against *BACE1* exon 5, 6 and 7, respectively. Interestingly, *AS4-BACE1* has long exon without splicing a part of intron. We suggested these transcripts have functions which regulate the *BACE1*. These novel transcripts were conserved one exon against *BACE1* exon5. Then, the expression of the *AS-BACE1* was suppressed by siRNA in order to analyze the role of AS in the regulation of *BACE1*. Though the knockdown of *BACE1* did not affect the expression of *AS-BACE1*, the expression of BACE1 was decreased by the knockdown of *AS-BACE1*. These results suggest that *AS-BACE1*is involved in the regulation of expression of the *BACE1*.

Conclusions: We identified 4 *AS-BACE1* which are spliced, have poly (A) tail, and conserved one exon against *BACE1* exon5. It is indicated that *AS-BACE1* equivalently expressed with *BACE1* and are concerned in the regulation of *BACE1*.

1483 Focal Myositis: A Clinicopathologic Study of 115 Cases

A Auerbach, JC Fanburg-Smith, EJ Rushing. The Armed Forces Institute of Pathology, Washington.

Background: Focal myositis (FM) is an uncommon inflammatory pseudotumor of skeletal muscle that may be confused with a variety of neoplastic and inflammatory diseases.

Design: 206 cases coded as "focal myositis" were culled from our files. Only cases with adequate material, a solitary lesion, and correct diagnosis were included. IHC was performed.

Results: 115 FM cases were included, with 61 males, 52 females, and 2 of unknown sex. Ages ranged 7 -94 years (mean 41, median 36 years). All but 12 patients were otherwise healthy, and all but 10 lacked antecedent trauma. All patients presented with an intramusclular mass. Lesional sizes ranged from 1 .0 to 20.0 cm (median 3.0 cm, mean 3.9 cm). These were mainly located in specific muscles of the lower extremities [vastus lateralis /groin (n=39), gastrocnemius (n=22)], followed by the trunk (abdominal wall n=12), neck (submental n=8) and upper extremity. Histologically, these were composed of variable myopathic (93%) and neurogenic (89%) changes, fibrosis, and inflammation (97%) occasionally accompanied by prominent eosinophils (n=20). IHC: Most cases had CD163 positive macrophages that were negative for S100 protein and CD1a and CD3 positive lymphocytes, negative for CD20, EBER, ALK-1, TIA1 and granzyme. MHC-1 and weak IgG4 was focally positive in skeletal muscle. Cases with severe inflammation had CD20 positive/ CD123 positive cells. S100 is strongest in skeletal muscle fibers with vacuolar change. Initial pathologic diagnostic considerations ranged from malignant rhabdomyosarcoma, leiomyosarcoma, liposarcoma, lymphoma to benign rhabdomyoma, intramuscular lipoma, fibromatosis, myositis ossificans, proliferative myositis, polymyositis, and inflammatory myofibroblastic tumor. Follow-up to date reveals spontaneous regression.

Conclusions: FM occurs as a mass in specific muscle groups of young adults of both sexes without significant trauma. It is a largely unrecognized specific histologic entity that can be easily mistaken for an inflammatory myopathy or dystrophy, alternate reactive or even a neoplastic process. These appear to be macrophage and T-cell rich lesions that change to B-cell and dendritic plasmacytoid cells when markedly inflamed, but do not seem to have a known viral or molecular etiology. IgG4 presence may explain fibrosis in these lesions; IgG4 associated entities often have a autoimmune etiology. Careful attention to reproducible clinicopathologic features can aid diagnosis and spare patients from excessive surgery or adverse therapy.

1484 Pax-2(-)/Inhibin(+) Immunoprofile in Hemangioblastoma: A Helpful Combination in the Differential Diagnosis with Metastatic Clear Cell Renal Cell Carcinoma to CNS

P Banerjee, R Albadine, R Sharma, P Burger, GJ Netto. Johns Hopkins, Baltimore.

Background: Hemangioblstomas, which account for up to 2.5% of all intracranial tumors, may occur sporadically or as a part of the multi-system genetic syndrome von Hippel-Lindau disease (vHL). Approximately, 25% of hemangioblastomas occur as a part of vHL, which is caused by the inherited mutation of the vHL gene on chromosome 3p25-26. Patients with vHL are also at increased risk of developing clear cell renal cell carcinoma (cRCC). Distinguishing hemangioblastomas from metastatic cRCC to the central nervous system could be at times challenging on routine H&E sections. We propose a combination of Pax2 and Inhibin immunohistochemistry panel as a helpful approach to distinguishing the two lesions.

Design: Nine hemangioblastomas were retrieved from our surgical pathology archives (2005-2006). All H&E sections reviewed by two pathologists on the study. Clinical information was gathered from electronic medical records. Representative paraffin embedded section from each case was selected for immunohistochemical analysis. Eight metastatic cRCC to CNS represented on a Metastatic RCC Tissue Microarray were also used. IHC was performed using monoclonal antibodies for Pax2 (Zymed) and Inhibin (Serotec).

Results: Hemangioblastoma: Four lesions were located within the spinal cord and 5 in posterior fossa. No documented history of von Hippel-Lindau disease was seen in any of the patients. Pax2(-)/Inhibin (+) profile was exhibited by all 9/9 (100%) examined hemangioblastomas. Inhibin staining was cytoplasmic in nature. Nuclear Pax2 staining was not present in any of the 9 lesions. **Metastatic cRCC to CNS:** 5/8(63%) lesions demonstarted a Pax2(+)/Inhibin (-) immunoprofile while the remaining 3(37%) lesions were Pax2(-)/Inhibin (-).

Conclusions: We suggest a panel of Pax2 and Inhibin as a useful adjunct in the differential diagnosis of hemangioblastoma vs metastatic cRCC. In our pilot group of cases, the immuoprofile of Pax2(-)/Inhibin(+) supported the diagnosis of hemangioblastoma with a sensitivity and a specificity of 100% . On the other hand, a Pax2(+)/Inhibin(-)profile supported the diagnosis of metastatic cRCC with a sensitivity of 63% and a specificity of 100%. An expanded group of lesions is being evaluated.